CELL SPECIFIC GUIDANCE OF NERVE REGENERATION THROUGH SUSTAINED GROWTH FACTOR RELEASE

by

PARISA LOTFI

Presented to the Faculty of the Graduate School of

The University of Texas at Arlington in Partial Fulfillment

of the Requirements

for the Degree of

DOCTOR OF PHILOSOPHY

THE UNIVERSITY OF TEXAS AT ARLINGTON

December 2011

ACKNOWLEDGEMENTS

This work which is a very small contribution to the challenging world of science is, hopefully, an opening to my further contribution to the humanity.

I would like to express my deepest gratitude to my advisor, Dr. Mario Romero-Ortega, for his excellent vision and patience. He is a mentor who has faith in his students and never belittles the power of encouragement. His seek for excellence, which sometimes might seem too meticulous for amateur scientists, instills and inspires a sense of attention to the details that is inevitable in science.

I would like to thank and acknowledge the time and support of my committee members in University of Texas Southwestern medical center and university of Texas at Arlington.

I would like to lovingly acknowledge my husband. Without him, I would not be able to endure the hardships of the personal life accompanied with tediousness of research. I am looking forward to our journey of life. Moreover; I would like to thank my parents for enkindling the first ignition of the light of knowledge and curiosity in my heart from childhood. I hope to be as good of a parent to my children as they were to me.

And at last I want to thank my colleagues and friends who enriched my life with many memorable moments and experiences.

November 21, 2011

ABSTRACT

CELL SPECIFIC GUIDANCE OF NERVE REGENERATION THROUGH SUSTAINED GROWTH FACTOR RELEASE

Parisa Lotfi, PhD

The University of Texas at Arlington, 2011

Supervising Professor: Mario Romero-Ortega

Regenerative peripheral nerve interfaces have been proposed as viable alternatives for the natural control of robotic prosthetic devices. However, sensory and motor axons at the neural interface are of mixed submodality types, which difficult the specific recording from motor axons and the eliciting of precise sensory modalities through selective stimulation. Here we evaluated the possibility of using type-specific neurotrophins to preferentially entice the regeneration of defined axonal populations from injured peripheral nerves. Segregation of mixed sensory fibers from dorsal root ganglion neurons was evaluated *in vivo* by compartmentalized diffusion delivery of nerve growth factor (NGF) and neurotrophin-3 (NT-3), to preferentially entice the growth of TrkA+ nociceptive and TrkC+ proprioceptive subsets of sensory neurons, respectively. A “Y”-shaped tubing was used to allow regeneration of the transected adult rat sciatic nerve into separate compartments filled with either NFG or NT-3. A significant increase in the number of CGRP+ pain fibers were attracted towards the sural nerve, while N-52+ large diameter axons were observed in the tibial and NT-3 compartments. Conversely, the preferential growth of pain fibers (CGRP+) and motor fibers (ChAT+) was evaluated using a polymeric sustained release method. Growth factor loaded PLGA microparticles created a

gradient for a longer time compared to when they used directly. Two specific growth factors for pain fibers (NGF) and motor neurons (Pleiotrophin factor; PTN) were encapsulated in microparticles and tested in a femoral nerve double crush injury model. The common femoral nerve bifurcates to two branches: saphenous branch (SB) and motor branch (MB). After injury in the common femoral nerve, the sensory and motor axonal fibers are mixed and lose their ability to innervate the proper target. We used PLGA encapsulated NGF and PTN to guide the axons to their respective target. The results of this study confirmed that more nociceptive fibers and motor axons were attracted to NGF and PTN, respectively. The experimental group treated with BSA (negative control) did not show any preferential growth in either of branches. This study demonstrates the guided enrichment of sensory and motor axons and, and supports the notion that neurotrophic factors can be used to segregate sensory and perhaps motor axons in separate peripheral interfaces.

In order to test if a growth factor gradient will enhance axonal guidance, we developed a method that consistent of coiling a polymeric fiber inside hydrogel microchannels. We used finite element analysis (FEA) to model drug delivery and to compare the diffusion dynamics between the non-gradients versus gradient model. This is needed both for the repair of sensory and motor branches and for the development of closed-loop peripheral neural interfaces. This strategy can be used to entice a specific sub-type of axons in a mixed population of nerves to the channels and eventually will guide them to the proper target.

Together the data indicates that modality specific growth factors can be used to enrich the motor and sensory axonal fibers guidance to the correct target. However; the separation of the different subtype of the axonal fibers was not completely achieved indicating that either more than one growth factor or a combination of neurotrophic and pleiotrophic factors is needed to separate the axonal fibers more precisely.

In addition, computer modeling and initial experiments indicate that gradient release of growth factor may help further in achieving enhanced selective nerve growth.

TABLE OF CONTENTS

LIST OF ILLUSTRATIONS

LIST OF TABLES

CHAPTER 1

INTRODUCTION

The complex mechanisms involved in axonal regeneration is result of the interaction of neurons with other supporting cells, as well as paracrine and extracellular molecules (Ozkaynak et al 2010). During development, the neuronal projections are guided to their targets through growth factors, which are specific for different cell types. The evidence that neurotrophic factors might be responsible for guiding the separate pathways of sensory and motor neurons was first provided by Ramon y Cajal(Cajal 1928). He showed that gamma motor axons depart from sensory fibers to innervate the muscle spindle. This phenomenon is now recognized as neural response to specific growth factors (Bloch et al 2001; Gallarda et al 2008).

The first nerve growth factor (NGF) was discovered in the 1950's by Rita Levi-Montalcini (Chaldakov 2011; Levi-Montalcini & Angeletti 1963) subsequently; others have been uncovered and together formed the neurotrophin family. Neurotrophins include NGF, brain derived neurotrophic factor (BDNF), neurotrohin-3 (NT-3), and neurotrophins 4-6 (Gotz et al 1994). In addition other neuron growth factors have been identified such as glial cell line-derived neurotrophic factor (GDNF), ciliary neurotrophic factor (CNTF) and fibroblast growth factor (FGF-2) (Boyd & Gordon 2001; 2003a; Sahenk et al 2008; Schmidt & Leach 2003; Toth et al 2002; Zhou & Snider 2006).

1.1 Nerve Growth Factors in PNS Development

The growth effect that neurotrophins convey on neurons is known to be mediated through binding to distinct Trk receptors A, B or C which bind specifically to NGF, BDNF, and NT-3 respectively (Boyd & Gordon 2001; 2003b; Ernsberger 2008; Wood et al 2010), and to p75 receptors not specifically (Friedman & Greene 1999; Yano & Chao 2000). Binding of the neurotrophins to their Trk receptors lead to their dimerization of the receptor and activation of

their intracellular kinase domain. Signal transduction initiated by phosphorylation of Trk kinase residue propagates intracellularly through the mitogen-activating protein kinase (MAPK) signaling cascade, ultimately activating ERK and modulating gene transcription (McInnes & Sykes 1997; Mocchetti & Brown 2008; Skaper 2008).

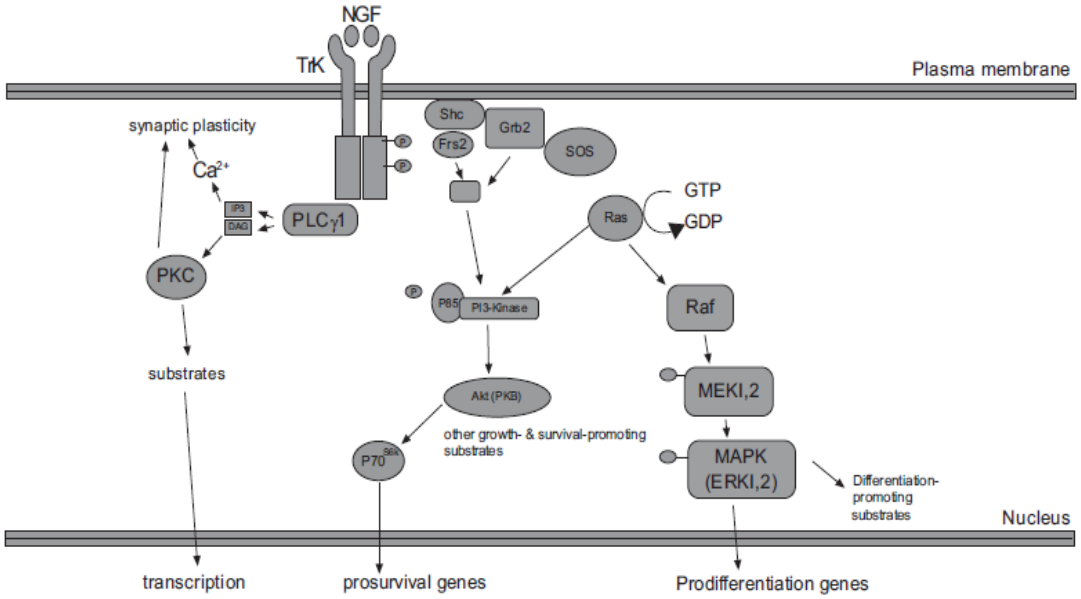

Figure 1.1 Signal transduction induced by neurotrophin factor (NGF) and its specific tyrosine kinase receptor (TrkA). Autophosphorylaton of the intracellular domain of the receptor initiates the MAPK pathway (Skaper et al 2008).

Neurotrophins are not only known to play critical roles during development of the nervous system, but also have proven beneficial in the repair of injured neurons both in the central nervous system and peripheral nerves.

1.2 PNS Injury and Spontaneous Regeneration

In the peripheral nervous system neuropathy could be acquired by inflammation, autoimmune diseases, trauma, local infection, application of the regional anesthesia, toxins, vascular and metabolic disorders or could be outcome of a preexisting genetic disorders such as neurofibrosarcoma (peripheral nerve sheath tumor) (Belmin & Valensi 1996; Jeng et al 2010; Rana & Masroor 2011; Rosenberg et al 2002).

In contrast to the CNS, peripheral nerve regenerates spontaneously. This ability proceeds through three main steps; i) cell body response, ii) Wallerian degeneration and iii) axonal regrowth.

Cell body response to direct injury and the cytokines secreted in the distal end by expressing immediate early genes due to the injury including; RNA production and protein synthesis such as peptides, cytokines, growth factors and receptor (Lundberg & Lerner 2002; Navarro & Udina 2009) increase to initiate axonal regeneration. During Wallerian degeneration, macrophages phagocyte cellular debri; including myelin; created at the injury site and distal to it (Rotshenker 2011). In parallel with Wallerian degeneration, axonal fibers regenerates sprouts with terminal growth cones designed to sample the environment actively responding to molecular cues, and ultimately guiding the regenerating axons toward the natural target, whether a gland, skin or muscle (Adelson et al 2004; Arvidsson & Johansson 1988; Fu & Gordon 1997; Lowrie 1999; Madison et al 2007; Robinson & Madison 2006; Terenghi 1995; 1999).

If nerve injury is too proximal or consists in nerve tissue loss, nerve regeneration proceeds with difficulties. In the first case, the time needed to regeneration may take weeks or months depending on the distance as axons are known to grow at a rate of 1-2 mm/day (Edstrom et al 1992; Sjoberg & Kanje 1990; Sjoberg et al 1988). During that time the distal muscles might go under hypotrophy and may not be available for reinnervation after nerve regeneration (Dadon-Nachum et al 2011; Wu et al 2011). If damage to the nerve resulted in tissue gaps, then autografts or tubularization techniques are needed to bridge the gap, which can also contribute to path-finding and targeting errors by the regenerating neurons (Dodla & Bellamkonda 2006; Li & Shi 2007; Tzou et al 2011; Yu & Bellamkonda 2003). These issues underlie the need of months and sometimes years to achieve nerve regeneration, and the fact that often times the recovery of function is only partial at best (Madison et al 2007).

1.3 Preferential Motor Reinnervation

Some studies on peripheral nerve regeneration have reported that motor axons preferentially regenerate into the distal motor branch. This phenomenon is known as "preferential motor reinnervation" (PMR) (Figure 1.2) (Brushart 1993; Hoke et al 2006). Currently, two different hypotheses have been proposed to explain this observation. One emphasizes on the apparent difference in Schwann cell composition in the sensory and motor nerves, as it has been shown that L2/HNK-1 or PSA-NCAM are expressed only in the motor fibers distal to the injury and thus maybe involved in preferential regeneration (Brushart 1991; Franz et al 2005; Hoke et al 2006; Martini et al 1994; Martini et al 1992). A contrasting hypothesis suggests that the relative level of trophic support provided by each branch determines if axons stay in that particular pathway (Robinson & Madison 2004; 2005). Support for this notion was provided by the higher number of motor axons regenerating to the cutaneous branch in a femoral nerve injury, when the muscle target was not accessible (Robinson & Madison 2004; 2005). Both of these studies agree in that preferential motor pathway seems to be sufficient in the young animals (3 weeks or younger) to guide modality specific axons accurately even in the absence of distal targets (Brushart 1993). Whereas this pathway seemed to be lost in the elder animals (Robinson & Madison 2006).

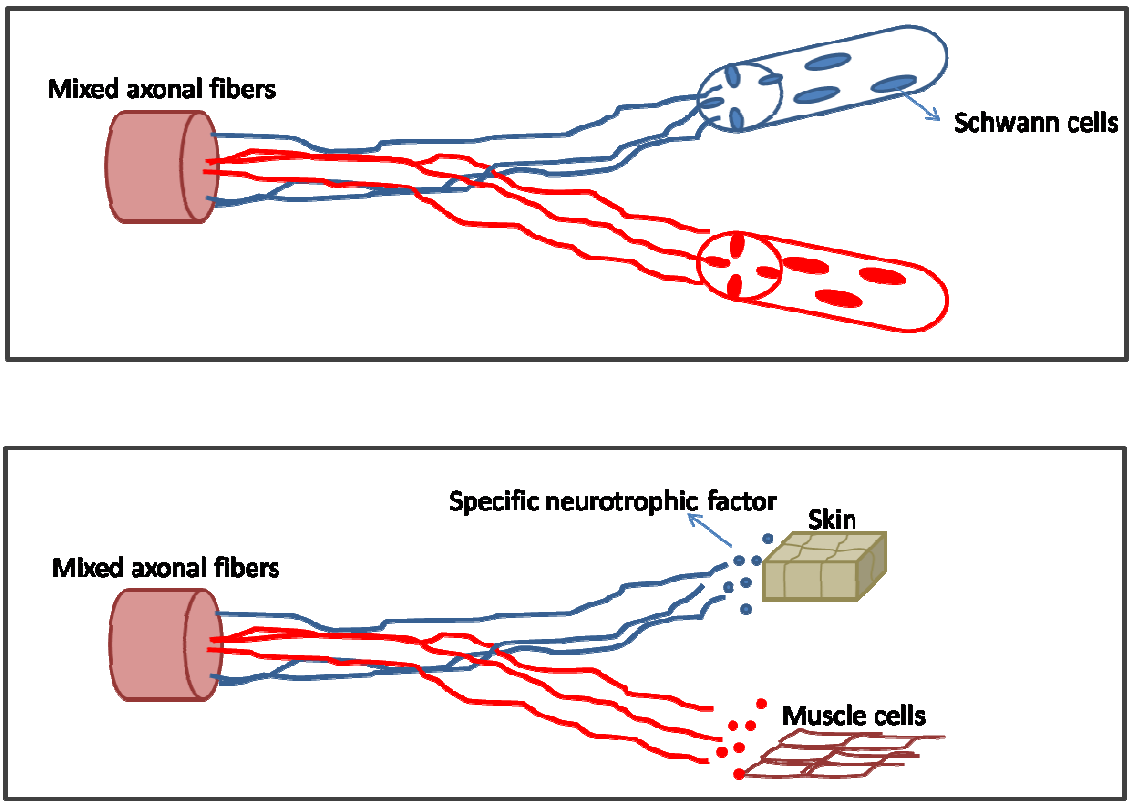

Figure 1.2 Schematic diagrams of the two main mechanisms describing the preferential motor reinnervation (PMR). First one suggests the existence of different Schwann cells types creating an inherent conduit for specific axonal subtypes (top). The second focuses on the importance of target enticing molecular cues in attracting some subtype of axons rather than the other (bottom).

1.4 Growth factors enticement in nerve regeneration

Many chemical stimuli are necessary for proper target innervations of the injured peripheral nerve, and growth factors play a very important role. This has been demonstrated by a number of studies showing that neuron growth can be harness though growth factors be provided to enhance and direct nerve regeneration in both central and peripheral nerves after injury (Boyd & Gordon 2003a; b; Romero et al 2001; Romero et al 2000). These studies have been successful in attracting specific subtypes of neurons using defined growth factors. For example; in the peripheral nerve, BDNF and glial-derived neurotrophic factors (GDNF), have been shown to specifically promote axonal regeneration of motor neurons (Boyd & Gordon 2003b), whereas NGF and NT-3 are known to regenerate calcitonin gene-related peptide

positive (CGRP+) pain and larger myelinated proprioceptive axonal fibers, respectively (Hu et al 2010). Similarly; some other studies in the central nervous system including previous experiments in our lab; have shown that exogenous supply of NGF can successfully entice and direct axonal regeneration of CGRP-positive pain axons in the brain (Curinga & Smith 2008) and spinal cord (Romero et al 2001; Romero et al 2000). Peripheral nerve fibers are comprised of several different subtypes, including sensory (nociceptive, proprioceptive and mechanoreceptor fibers) and motor fibers (alpha and gamma motor neurons). Although all these studies are successful in guiding one modality specific axonal fibers, the specific generation of two or more different axonal subtypes remains challenging.

1.5 Neurotrophin specificity: NGF and NT-3

NGF is a dimeric of two 26-kDa identical amino acids units bound through monovalent bonds. It plays important roles during development and regeneration of sensory neurons after injury. This neurotrophin factor binds specifically to the TrkA receptors. During developmental stages TrkA is expressed by neurons and muscle cells. However; in adults this receptor is only expressed by small diameter, CGRP+ fibers which are responsible for the perception of the pain (Chung et al 2007). It has also been shown that NGF expression is significantly up-regulated after injures in peripheral nerve fibers (Bloch et al 2001; Chung et al 2007). Together, these finding suggest that NGF acts as a very specific guidance cue for the regeneration of pain fibers.

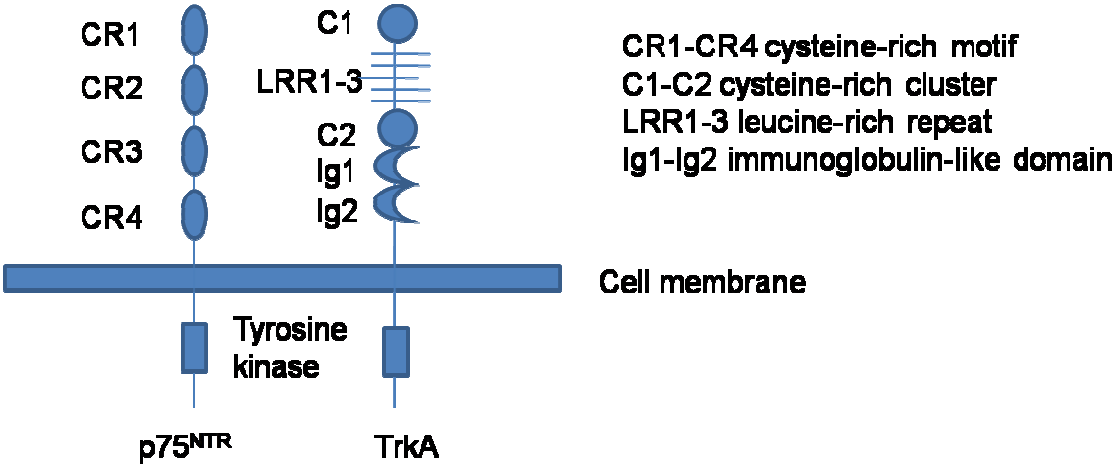

Figure 1.3 Neurotrophins receptors (like; TrkA) is a dimer with an extracellular domain and an intracellular tyrosine kinase domain. NGF binds with lower affinity to a co-receptor called $p75^{NTR}$.

In contrast, NT-3 the only growth factor that binds to the TrkC receptor and does so with high affinity while binding to TrkA and TrkB with lower affinity (Ilag et al 1994; McInnes & Sykes 1997; Skaper 2008; Urfer et al 1994). TrkC is expressed by skeletal muscle cells and mutation in TrkC receptors in mice have been shown to cause severe losses of proprioceptive fibers (Hu et al 2010; McInnes & Sykes 1997).

1.6 Pleiotrophin general growth effect: VEGF and PTN

Vascular Endothelial Growth factor (VEGF) is a 45-kDa glycoprotein involved primarily in endothelial cell proliferation and other recognized biological effects (Ladoux & Frelin 2000; Nomi et al 2006). VEGF acts through multiple receptors tyrosine kinase receptor VEGFR1 and VEGFR2 and neuropilin-1 co-receptor (Frelin et al 2000; Soker et al 1998b). VEGF receptor is a member of the platelet-derived growth factor. Like neurotrophin receptors, VEGF receptors have an intracellular tyrosine kinase domain which can be activated after dimerization initiated by receptor-ligand interaction (Neufeld et al 1999). VEGF is mainly upregulated due to hypoxia and a demand for vascularization (Shweiki et al 1992). Recently, VEGF has been demonstrated to have a trophic effect in neurons (Piltonen et al 2011).

Pleiotrophic factor (PTN) a 17 kDa growth factor is consistent of 168 amino acids, which is expressed in neuronal and several non-neuronal cells (macrophages, Schwann cells and endothelial cells) during different developmental stages and is highly up-regulated at birth (Blondet et al 2005; Yanagisawa et al 2010). In the peripheral nervous system, PNT is involved in survival and regeneration of motor neurons and their muscle targets (Jin et al 2009; Mi et al 2007; Yeh et al 1998; Zhang et al 1999). In addition, PTN seem to be highly expressed in motor neurons compared to sensory neurons (Jin et al 2009), which suggest that this growth factor may function as a guidance cue for motor axons.

1.7 General hypothesis

Errors in nerve regeneration path-finding result in poor functional recovery, based on the demonstrated role of individual growth factors on regeneration in defined neuronal populations, it is hypothesized that specific growth factors can be used to differentially guide the regenerated sensory and motor axons in a way that target reinnervation accuracy can be increased. Moreover, the ability of selectively guiding axon regeneration can contribute to the development of neuron-specific multi-electrode interfacing, a device which will likely improve the natural move and feel of prosthetic limbs.

The hypothesis was tested according to the following Specific Aims:

- *Specific aim I:* To test NGF and NT-3 effect to selectively attract NGF-responsive nociceptive axons and NT-3 responsive proprioceptive axons in sciatic nerve model (Chapter 2). We inspected the possibility of separating nociceptive and proprioceptive subtypes of sensory neurons in a sciatic model using NGF and NT-3 growth factors. This can be used to entice the regenerated axons into separate multielectrode compartments for selective recording/stimulation
- *Specific aim II:* Study segregation of the ChAT+ motor axons and CGRP+ pain fibers in a femoral nerve model using PTN and NGF growth factors (Chapter 3).

We examined the application of NGF and pleiotrophin (PTN) loaded PLGA microparticles in sustained delivery of growth factors to segregate nociceptive fibers from motor neurons in a femoral nerve injury model. The results of this study can guide axons to the correct path and ultimately the reinnervation of the correct target.

- *Specific aim III:* Fabrication of PLGA coiled fibers in order to facilitate delivery of growth factors in a gradient (Chapter 4). Here we developed a sustained method to deliver the growth factors in a gradient mimicking the natural phenomena of cell guidance.
- *Specific aim IV:* Examine the synergetic effects of pleiotrophic and neurotrophic factors on axonal growth *in vitro* (this part of study is included in the appendix A).
- *Specific aim V:* Investigate the application of the VEGF growth factor to entice endothelial cells sprouting from adult aorta explants to a 3-D multiluminal hydrogel scaffold (Appendix B). To combine cell specific nerve regeneration with increase and directed vascularization, we investigated the possibility of generating neo-vasculature sprouting from old and young existing blood vessel into 3-D multiluminal channels.

CHAPTER 2

PREFERENTIAL GUIDANCE OF NOCICEPTIVE AND PROPRIOCEPTIVE AXONS AFTER PERIPHERAL NERVE INJURY

2.1 Introduction

Advanced robotic prosthetic limbs designed with multiple degrees of freedom bear great promise as substitutes for the human arm/hand in amputees (Lin & Huang 1997; Matrone et al 2010; Miller et al 2008; Otr et al 2010; Velliste et al 2008). However, while thousands of touch-sensing receptors in the natural hand provide information about skin deformation and limb position, current hand prostheses lack such sensory feedback systems. Instead, users rely on unnatural vibrotactile and electrotactile sensors for surrogate feedback information, and operate the prosthetic limbs mostly under visual control (Marasco et al 2009; Micera & Navarro 2009; Phillips 1988).

Indwelling multi-electrode arrays (MEA) placed in the premotor cortex have been used successfully to record neural activity associated with motor intention in monkeys and humans, and to actuate robotic prosthesis (Hochberg et al 2006; Simeral et al). These findings have fueled interest in the possibility of developing a closed-loop cortical interface able to convey tactile and positional information to amputees by direct electrical micro-stimulation of the sensory cortex (Fitzsimmons et al 2007). However, since the topographic mapping in the somatosensory cortex is quite variable, and is unclear which neurons provide information during sensory submodality discrimination, this strategy may be limiting in conveying distinct sensations such as pain, touch, thermal, and limb/digit stretch. Furthermore, direct cortical stimulation lacks the benefit of signal integration and modulation from neural networks in the spinal cord and thalamus, known to provide critical context-dependent regulation of information and sensory discrimination (Brown et al 2004; Lee et al 2008; Rosenzweig et al 2010).

Alternatively, tactile and positional information detected from specialized neurons innervating the skin, muscle and tendons can be interfaced at the dorsal root ganglia (Gaunt et al 2009; Weber et al 2007) or in the transected peripheral nerve (Brill et al 2009; Dhillon et al 2004), and used for eliciting sensation in amputees (Dhillon & Horch 2005). However, modality specific neurons such as nociceptive and proprioceptive have intermixed perikarya in the dorsal root ganglia (DRG), and assorted axons in most peripheral nerves (Castro et al 2008). Thus, selective electrical stimulation is particularly challenging, and is further complicated by the fact that large myelinated axons (i.e., proprioceptive) are depolarized with smaller currents, while smaller diameter neurons (i.e., nociceptive) require larger stimuli. Thus, when stimulating the small caliber fibers in a nerve with assorted axon types, it is likely large-size axons will be non-specifically recruited, which will likely elicit either mixed sensations and/or involuntary motor movements (Grill et al 2009). Here we hypothesize that such limitation can be overcome if type-specific axons are specifically enticed to regenerate into separate compartments.

DRG neurons have been broadly classified based on cell body size, axonal diameter, conduction velocity, and the expression of either NGF, BDNF or NT-3 Trk receptors (Harper & Lawson 1985; Misko et al 1987; Oakley et al 1997), and further differentiated based on the expression of N-52 and CGRP, which are preferentially expressed in large and small-diameter nerve fibers, respectively (Goldstein et al 1991; Ho & O'Leary 2011; Zhang et al 1995). We and others have shown that exogenous expression of NGF can be used successfully to entice and direct axonal regeneration of CRGP-positive pain axons in the brain (Curinga & Smith 2008), spinal cord (Romero et al 2001; Romero et al 2000), and peripheral nerves (Hu et al 2010).

Previously our lab used a “Y” assay shaped polydimethylsiloxane (PDMS) template to demonstrated that mixed sensory fibers can be separated to compartmentalized chambers *in vitro* with the molecular guidance like NGF and NT-3 (Garde 2008). Briefly, dorsal root ganglia (Drgas & Blaszak) were obtained from neonate (P0-P3) rats. The animals were anesthetized by hypothermia and sacrificed. The spinal column was harvested into Hank’s buffered salt solution

(Gibco, Carlsbad, CA), and dorsal root ganglions were collected and cleaned from ventral roots using tungsten needles. Individual DRGs were placed in the main well of the choice assay and fixed in place using 50 µl of growth factor reduced ECM (Matrigel; BD Biosciences, San Jose, CA). After ECM polymerization for 30 min at 37^{o}C, the explants were cultured in neurobasal medium supplemented with L-glutamine, B-27 and penicillin/streptomycin (Gibco).

After two days in culture, pieces of gelfoam (3mm x 3mm) pre-soaked in saline (n=10; negative control), NGF (n=10; 100ng/ml, Sigma, St. Louis, MO) or NT-3 (n=12; 5ng/ml, Sigma, St. Louis, MO) was placed in the "target" wells. A piece of glass coverslip was then placed over the entire PDMS template with openings at the DRG and gelfoam ends. The coverslip served as a ceiling to the microchannels, prevented floating of the gelfoam and delaying neurotrophin dilution into the media (Figure 2a).

To demonstrate that the choice assay provides independent gradients of neurotrophins from the separate "target" compartments to the DRG, a piece of gelfoam with Cy2 (897 Da-green) and Cy3 (765 Da-red) dyes was placed in the two separate compartments and determine the fluorescence diffusion into the microfluidic channels at 4, 6, 8 and 12 hours. A Zeiss Pascal laser confocal microscope equipped with an environmental chamber was used to evaluate the optical densitometry of the Cy2 and Cy3 fluorescence over time, maintaining the cultures at 37^{o}C and 70% humidity. The diffusion rate was confirmed in separate experiments using Gelfoam loaded with bovine serum albumin (BSA) conjugated alexafluor-594 (66kDa), as its molecular weight approximates that of the neurotrophins (NGF=135 kDa and NT-3=27 kDa) used in this study. It was confirmed that the molecules diffused separately in each arm of the "Y" assay, providing a distinctive and measurable gradient for up to 8-12 hours (Figure 2.1b).

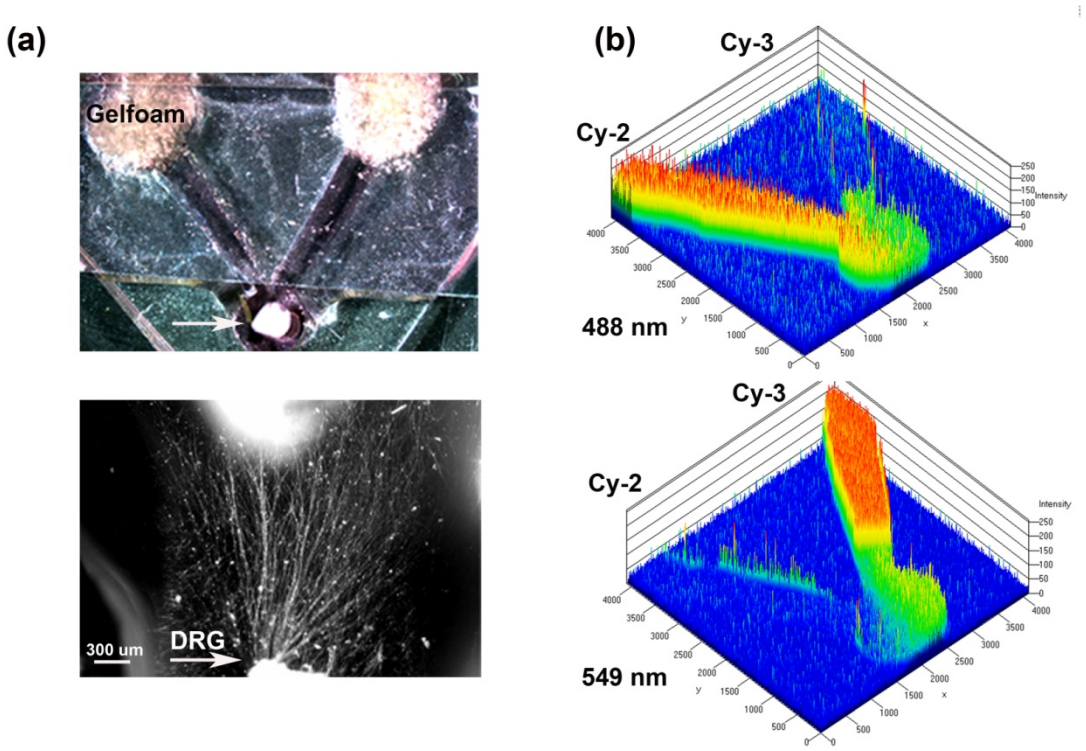

Figure 2.1 Y-shaped in vitro assay for axonal segregation. (a) Gelfoam-diffusion delivery of neurotrophins into the distal arms was used to differentially entice axonal outgrowth from neonatal DRGs. Bottom: Higher magnification shows axonal growth from the DRG (arrow) in the choice area. (b) Diffusion of green (Cy3) and red (Cy3) labeled antibodies, were imaged over time and quantified to demonstrate independent gradient formation (Garde 2008).

In absence of guidance cues, DRGs showed axonal growth of mixed axon morphologies (i.e., length or number of branches) into the arms of the Y assay (results not shown). In contrast, when NGF was delivery into both arms we observed that axons were long and lacked branches (Figure 2.2a left image). Conversely, when NT-3 was delivered into the microchannels the axons were shorter and with numerous branch collaterals (Figure 2.2a right image). We realized that long unbranched axons and short-branched axons are morphologically characteristic of the nociceptive and proprioceptive sensory neurons seeing in vitro (Romero et al 2007). Therefore, we questioned whether NGF and NT-3 if presented simultaneously in two separate microchannels would differentially entice the growth of distinct population of neurons. In those assays, axons growing from single DRGs towards the NGF-containing compartment

were long and relatively unbranched, while those attracted towards NT-3 were branched and shorter in length. Double immunolabeling for ß-tubulin (axonal marker) and CGRP (specific marker for nociceptive sensory axons), confirmed that CGRP+ pain/nociceptive fibers are predominantly attracted towards NGF, while those growing towards NT-3 were CGRP-/NF200+ axons (Figure2.2b).

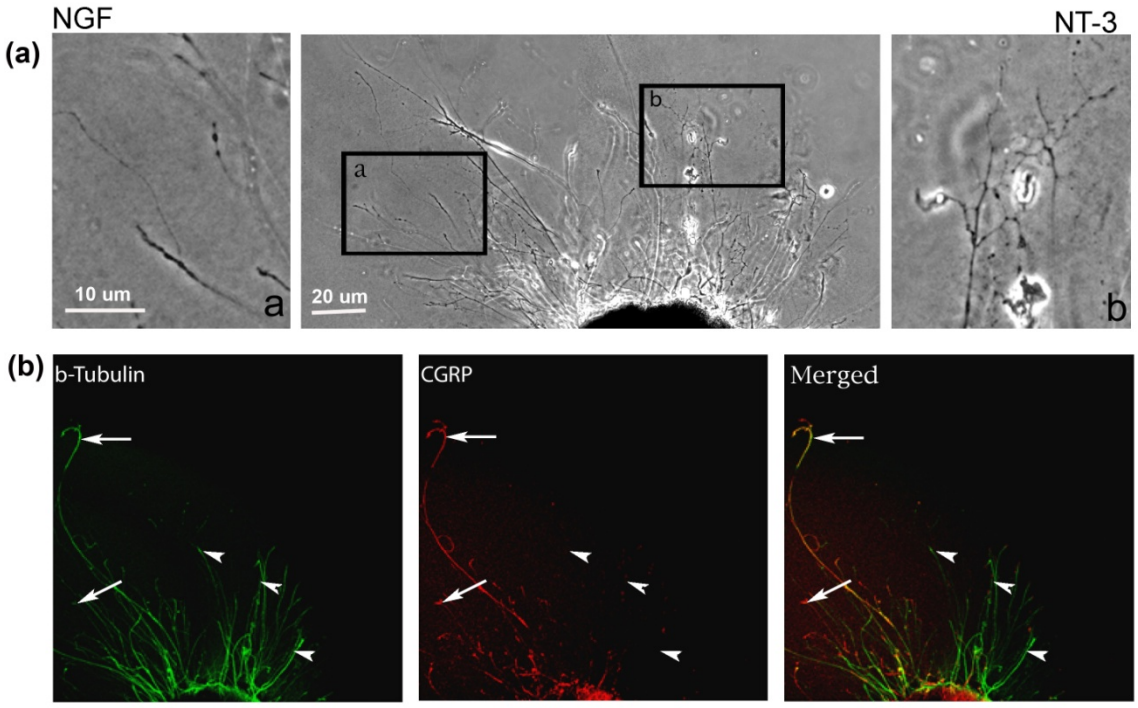

Figure 2.2 Differential axonal morphology of axons growing towards NGF or NT-3.(a) Mixed axon morphologies were observed in control DRGs. Magnified images of the area in boxes (in right and left) detail the morphological differences in the NGF and NT-3 treated groups. Axons growing towards NGF showed characteristic long and unbranched morphology. In contrast, those growing towards NT-3 were short and highly branched axons. (b) Visualization of ß-tubulin (green) and CGRP (red) demonstrated that axons growing towards NGF are CGRP positive (i.e., nociceptive, arrows), while those growing towards NT-3 are CGRP negative. Scale bar = A 50 µm (left) and 250 µm (center), B 500 µm (Garde 2008).

Quantitative analysis (Figure2.3) showed that axon length and branch number averaged 139.5 ± 17.85 µm, and 4.85 ± 0.82 respectively, in the saline treated groups. In contrast, the average axon length in the NGF channel (352.1 ± 40.24 µm) increase 2.5 fold ($p \leq 0.001$) compared to that in saline or NT-3 (115.8 ± 10.30 µm), whereas the number of branches

increased 3 fold in the NT-3 channels (15.75 ± 2.25; n=12; p ≤ 0.01), compared to saline or NT-3 treated (7 ± 0.95) groups. This study showed that compartmentalized diffusion of NGF and NT-3 can differentially entice and direct the regeneration CGRP+ nociceptive and N-52+ large diameter fibers, such as proprioceptive and mechanoceptive axons, into separate chambers. This notion is further supported by the observed morphological dimorphism observed in DRG axons growing into the NGF and NT-3 compartments, in which, similarly to that previously reported in vitro, NGF-dependent nociceptive neurons grow mostly long and unbranched axons, while NT-3 dependent proprioceptive neurons show increased axonal branching (Romero et al 2007).

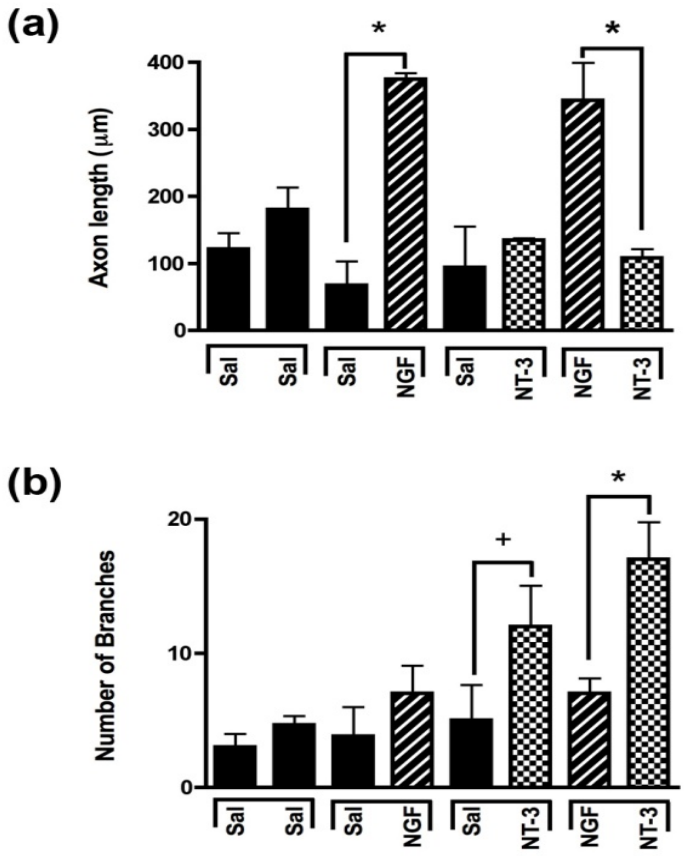

Figure 2.3 Selective neuron growth of DRG sensory axons by compartmentalized neurotrophin delivery. (a)NGF selectively induced the growth of longer axons compared to control and NT-3-treated groups. (b) NT-3 increased significantly the number of branches per axon compared to control and NGF. *= p< 0.001, + = p < 0.01. n =10-12 (Garde 2008).

These preliminary results confirmed our initial objective that different axonal modalities have different receptors and can be guided by specific molecular cues. Amit Chohuan in our laboratory also obtained preliminary evidence that **mixed axons from an amputated nerve can be segregated into separate regenerative compartments through neuron-type specific neurotrophins.** To fully test this possibility, I investigated the feasibility of using NGF and NT-3 to selectively attract TrkA nociceptive axons and TrkC proprioceptive axons *in vivo*.

2.2 Material and Methods

2.2.1 In vivo "Y"- shape nerve regeneration

To test if mixed axons in the transected peripheral nerve could be segregated into modality-specific compartments *in vivo*, we compared the segregation effect of natural distal targets such as the sural (primarily sensory) and tibial (mixed sensorimotor) nerves, distally connected to each arm of a Y-shaped tube, and compared it to that enticed by NGF and NT-3. The arm C of the tube was filled with collagen without growth factor, the arm B and A were filled with collagen and 100ng NGF/ml or 500ng NT-3/ml, respectively (Figure 2.4). The sciatic nerve in 32 rats was completely transected and repaired with either straight or Y-tubes with either segregated nerves or neurotrophins. Following a two-month survival the regenerated tissue was longitudinally sectioned and stained for specific markers

2.2.2 Immunocytochemical analysis

Animals were perfused with PBS-1% heparin, followed by 4% PFA. The regenerated nerve was harvested and processed for immunohistochemistry. Double labeling studies were done on longitudinally cut cryosections using the monoclonal N-52 clone of neurofilament 200 (N-52+) and CGRP (rabbit anti-CGRP, 1:2000; Chemicon, Temecula, CA). The tissue was then visualized using Cy2 Goat anti-Rabbit 1:250, Cy3 &Cy2 Goat anti-Mouse 1:500; Cy3 Goat anti-Rat 1:400 (Jackson labs, West Grove, PA). Sections mounted using Vectashield containing the nuclear label DAPI (Molecular Probes, Carlsbad, CA).

2.2.3 Image analysis and quantification

Three stacked images of the A, B and C arms (Figure 2.4b) were captured using confocal microscopy for each subject. Double-level standardized optical density threshold was applied to subtract the background and the saturated intensity values. A circle (fixed area 0.03mm^2) was placed over three randomly selected areas for fiber growth quantification. The area (in μm^2) of positively stained N-52+ axons and CGRP+ axons was measured in all three arms of the Y-shaped nerve regenerate.

2.2.4 Statistical analysis

The data is reported as the mean and the standard error of the mean (SEM). An unpaired Student's t-test was used to determine statistical differences. In multiple group comparisons, one-way ANOVA was used followed by Neuman-Keuls multiple comparison post hoc evaluation (Prism 4, GraphPad). P values ≤ 0.05 were considered significant.

2.3 Results

2.3.1 N-52-positive fibers are enriched by compartmentalized NT-3

. All implanted groups demonstrated axonal outgrowth in the common arm of the implants (Figure 2.4). Compared to simple tubularization nerve gap repair that mediate the regeneration of a single nerve cable (Figure 2.4a), Y-tubes containing collagen connected distally to sural and tibial nerves showed robust Y-shaped nerve regeneration (Figure 2.4b). Growth in those with collagen-only was minimal in absence of distal targets (Figure 2.4c), but was qualitatively enhanced if NGF and NT-3 were added in the Y- arms (Figure 2.4d).

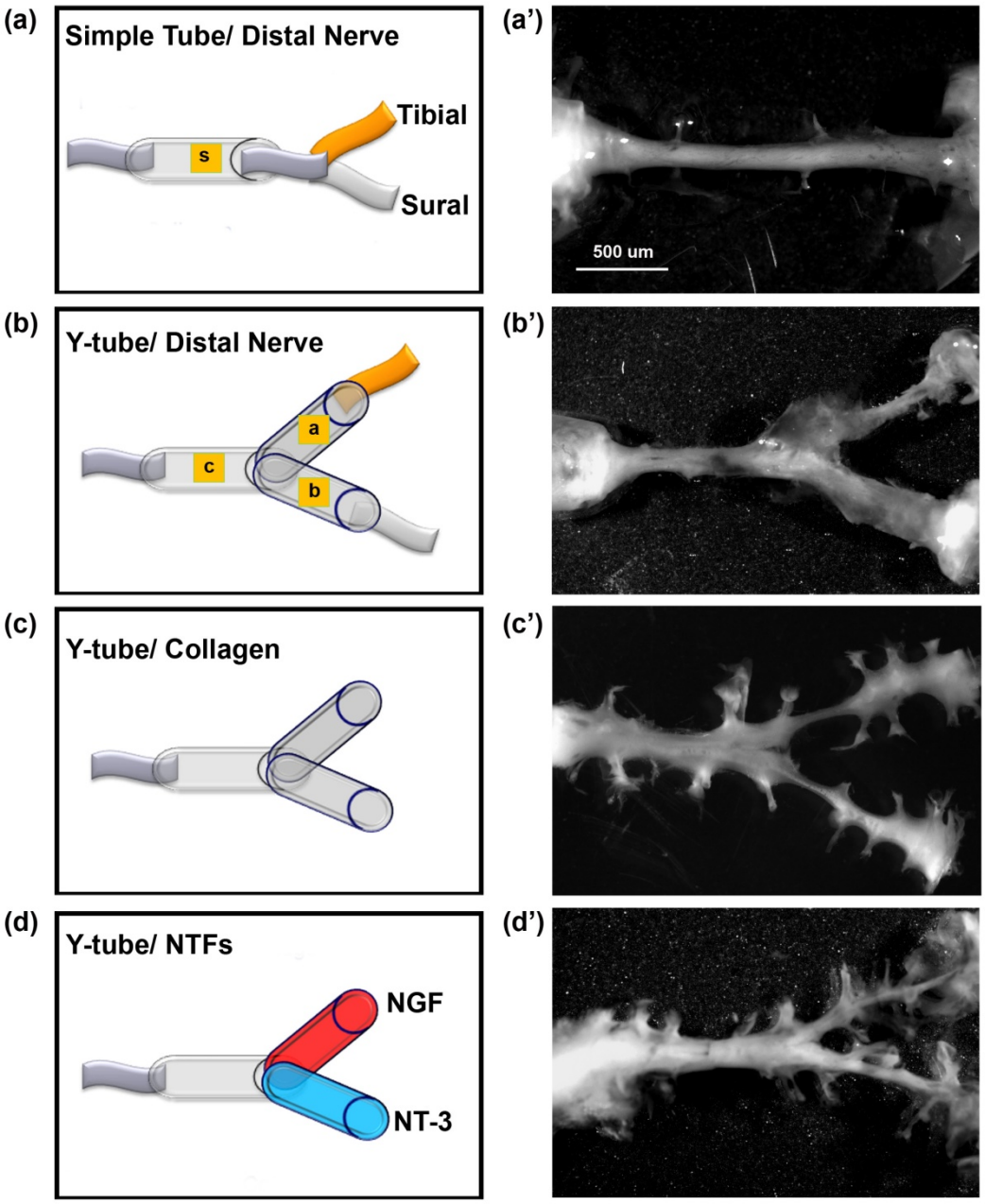

Figure 2.4 Guided peripheral nerve regeneration. (a-d) Schematic representation of the experimental groups tested in vivo. s= single tube, c= common arm, a and b= left and right arms of the Y-shaped tube. (a'-d') Photographs of regenerated nerves 60 days post tubularization. (a) Single nerve cable was observed in nerves repaired with straight tubes (a'), A Y-shaped nerve regenerate formed in the other groups. The regenerated tissue was thicker with the sural and tibial nerves attached distally (b'), dramatically reduced in absence of distal treatment (c'), and increased with neurotrophin delivery (d').

To determine the specific modality of the neurons that grew into the different “Y” chambers, we tried to retrograde label those axons using Flourogold as recently reported (Tansey et al 2011). However, the limited amount of tissue distal to the Y-arms caused cross-contamination during labeling. Alternatively, we resourced to markers specific for nociceptive fibers (CGRP+) and for large-diameter axons (N-52+). In DRG, sciatic nerve (Figure2.5) and spinal cord (not shown), CGRP labeled exclusively the TrkA pain fibers while N-52 stained large TrkC neurons and large diameter axons.

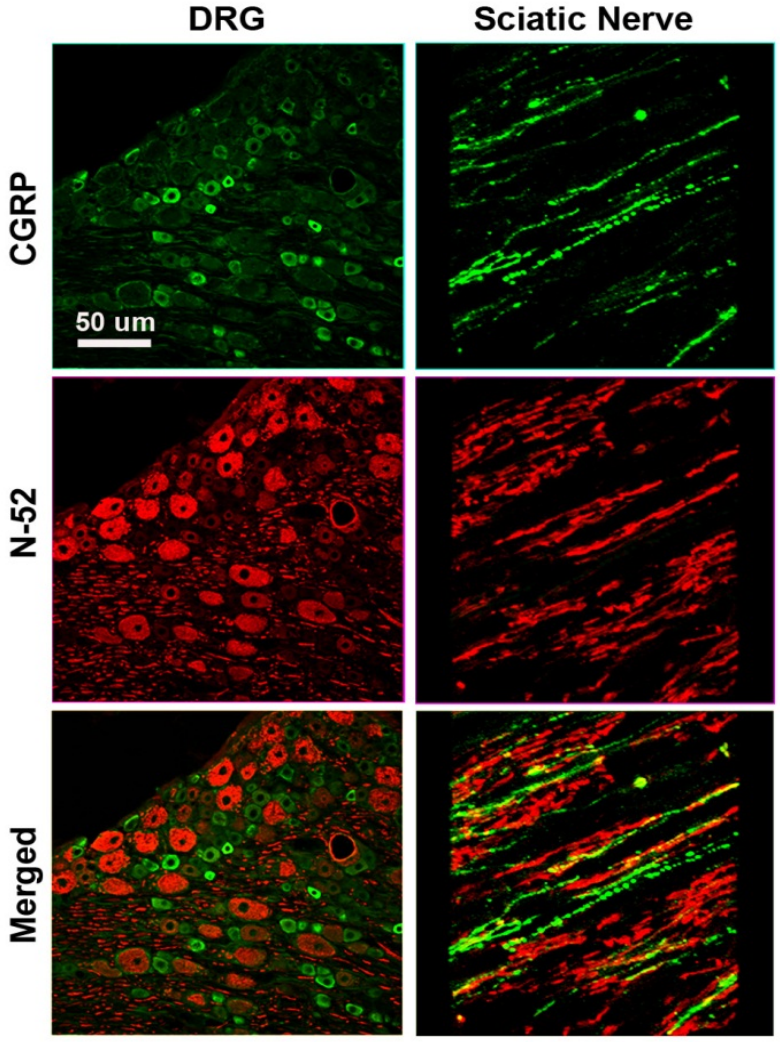

Figure 2.5 Differential labeling of large myelinated proprioceptive (N-52+; red), and small unmyelinated nociceptive (CGRP+ green) neurons in dorsal root ganglia (left) and sciatic nerve (right) in rat demonstrates the specificity of the markers as no overlap is apparent.

The staining did not overlap, thus labeling these two distinctive sub-populations of neurons in the experimental groups confirmed that the CGRP+ fibers were qualitatively more abundant in the arms of the Y-tube sutured distal to the sural nerve (Figure 2.6a), and N-52+ axons appeared to be more dense in the arm attached to the tibial nerve (Figure 2.6b). In those with NGF/NT-3, no differences were apparent with CGRP labeling, but seemed more abundant when labeled with N-52+ in the arm with NT-3 (Figure 2.6c).

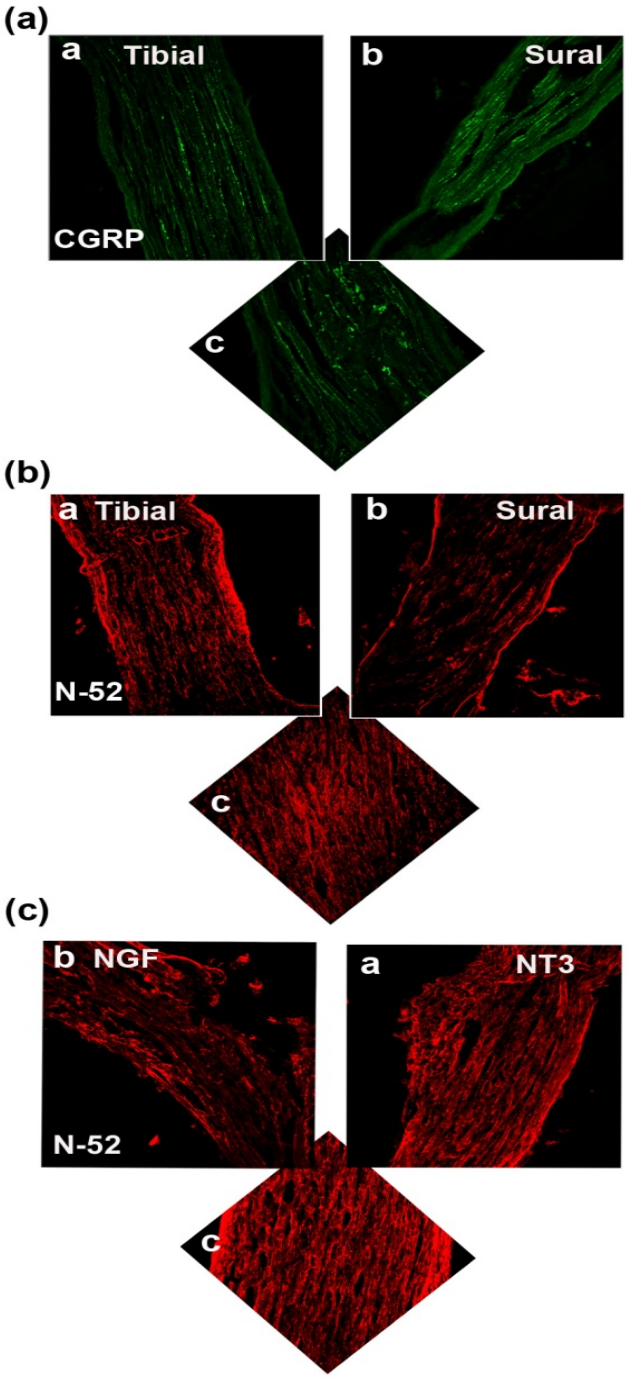

Figure 2.6 (a) In the “Y” shaped nerve regenerate, both axon types are present in the common arm, whereas those attached to the tibial nerve showed apparently less CGRP+ axons compared to those growing into the sural nerve compartment. (b) Conversely, N-52+ axons appear denser in the tibial compared to the sural compartments. (c) In the NT3 and NGF groups, N-52+ axons were more prevalent in the NT-3 arm.

Quantitative analysis using optical densitometry at the single tube (s), or the common (c) arm of the Y-tube, showed no significant differences between the treatment groups (Figure 2.7). In sharp contrast, the density of CGRP+ axons (Figure2.7a) was significantly increased in the compartment attached to the sural nerve ($p < 0.01$; 7528 ± 604.7 OD units), but not in that supplemented with NGF (1884 ± 504.8 OD units). Conversely, that of N-52+ was significantly increased ($p < 0.01$) in both the tibial (8718 ± 769.2 OD units) and NT-3 (9120 ± 1080 OD units) compartments (Figure 2.7b). We also noted significant increases ($p < 0.05$) in CGRP in the tibial (4894 ± 739.4 OD units) and of N-52 in the sural (9689 ± 676.3 OD units), compartments.

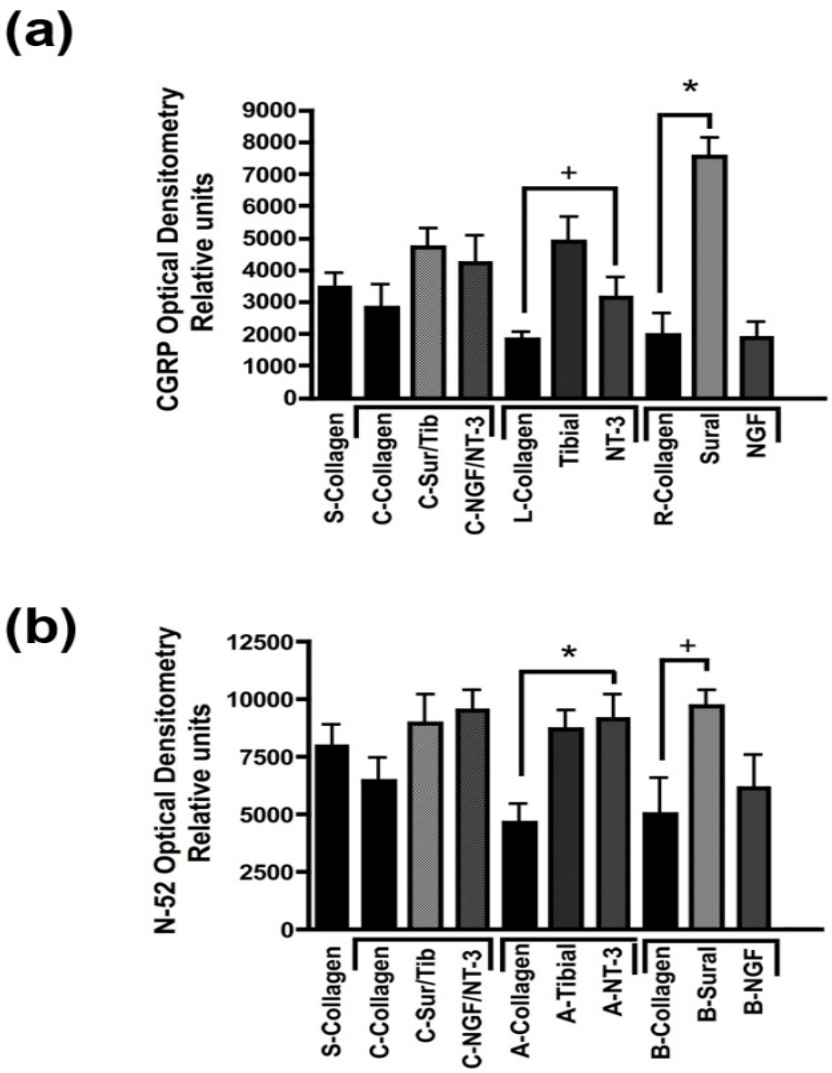

Figure 2.7 Optical densitometry of CGRP and N-52 axons. (a) Pain fibers (CGRP+) axons are grown in a significantly larger numbers in arms filled with NGF and tibial nerve compared to collagen or NT-3. (b) Large diameter axons were attracted towards the tibial and NT-3 channels, but also to the sural nerve compared to collagen controls. *= $p< 0.01$, + = $p < 0.05$.

Together, the data indicate that specific growth factor combinations can be used to guide the axonal growth of a mixed population in an amputated nerve and coerce specific types of regenerative fibers to grow into separate compartments.

2.4 Discussion

2.4.1 Sensitivity of the neural interfaces can be increased by attracting specific axons to the recording sites

The transected peripheral nerve provides an optimal site for the neural interfacing as movement commands can be recorded from motor axons, and electrical stimulation of sensory fibers can convey natural sensation to the user of advanced robotic prosthetic devices. Stimulation of sensory axons conveys sensory feedback with natural integration and modulation at the spinal cord, brain stem and thalamus prior to reaching the sensory cortex. Furthermore, neuron-specific stimulation will be able to convey precise sub-modality sensory information such as pain, temperature and limb stretching.

Peripheral nerve interfacing has been accomplished either through extraneural (i.e., cuff electrodes;(Leventhal & Durand 2004) or intraneural electrodes. Indwelling interfaces like the longitudinally implanted intrafascicular electrodes (LIFEs; (Lefurge et al 1991) have been used successfully to record motor signals from the peripheral nerve, and through stimulation, used to convey sensation in long-term amputee human volunteers (Dhillon et al 2004);(Benvenuto et al 2010). However, indwelling electrodes like LIFE provide limited long-term efficacy due to the progressive reduction in the number of active sites over time, poor bio-abio interface, tissue damage and loss of recording activity due to electrode insulation as a result of tissue scar formation (Biran et al 2005; 2007; Leung et al 2008; Williams et al 2007).

Regenerative sieve electrodes were proposed more than three decades ago as a viable alternative to interface motor and sensory nerve axons (Mannard et al 1974);(Dario et al 1998; Edell et al 1982). Sieve electrodes have been shown to obtain neural recordings after long-term (i.e., 2-6 months) implantation (Klinge et al 2001); (Lago et al 2007); (Panetsos et al 2008), and we recently obtained long-lasting single and multiunit recordings using a non-obstructive regenerative multielectrode interface placed between the transected ends of an end-to-end repaired nerve, and after interfacing the nerve 5-6 months after injury despite absent connections to their normal target muscles(Garde et al 2009). Here we tested the possibility to

use neurotrophins to guide the regenerative process of the transected peripheral nerve and segregate the growing axons into modality-specific compartments.

Previous reports have shown that incorporation of growth factors into neural interface electrodes can increase the sensitivity of the neural interfaces by attracting axons to the recording sites. Indeed, several growth factors and adhesion molecules have been incorporated to conductive substrates. NGF has been attached to polypyrrole(Gomez & Schmidt 2007), or combined with laminin and applied to polymer polyethylene dioxythiophene(Green et al 2009) and brain-derived neurotrophic factor (BDNF)and NGF have been entrapped in hydrogels polymerized over the electrodes or in nanopore membranes (Jun et al 2008; Lopez et al 2006; Winter et al 2007).

This study showed that NT-3 can mimic the specific enticement of N-52+ axons observed in chambers in which the tibial mixed sensory-motor nerve was sutured distally. Conversely, the sural sensory nerve was able to attract a larger population of CGRP-positive axons towards that compartment. However, we were unable to replicate such effect when NGF release was compartmentalized. Since we used a larger concentration of NGF (100 ng/ml) compared to that of NT-3 (5 ng/ml), it is possible that a lower NGF concentration is needed for an optimal axonal enticement, and future studies will be required to optimize the concentration and nature of the signaling cues needed to achieve maximal and more selective segregation.

The data demonstrates the guided enrichment of nociceptive axons in this particular regenerative chamber, and supports the notion that neurotrophic factors can be used directly as a means to enrich sensory and perhaps motor axons into an electrode interface. To test this possibility, future experiments will test the ability of glial-derived neurotrophin factor and BNDF, known to stimulate the regeneration of motor neurons (Boyd & Gordon 2003a; Jubran & Widenfalk 2003), to segregate motor from sensory fibers.

Our laboratory recently reported the use of an 18-electrode regenerative multielectrode interface that was able to record multiunit activity in both acute and chronically damaged

peripheral nerves (Garde et al 2009). Regenerative interfaces such as REMI are unique since axonal growth can potentially be guided specifically to compartmentalized electrodes using neuron- specific growth factors. These results shows that in addition to the general chemoattractive nature of the neurotrophins, neuron-specific molecular guidance cues can be used to separate the regeneration of specific types of neurons.

My results suggests that in addition to the general chemoattractive nature of the neurotrophins, neuron-specific molecular guidance cues can be used to separate the regeneration of specific types of axons, ultimately enticing them into separate multielectrode compartments for selective recording/stimulation (see model in Figure2.8). Achieving a greater concentration of axons from a particular neural subtype is expected to provide a more sophisticated and selective peripheral neuro-interface. The selective regeneration of subtypes of neurons into specific target chambers would be better suited to achieve selective stimulation of a neuron subtype, compared to the penetration electrodes that are in contact with mixed axons from different neuron types; as this would minimize the possibility of unintentionally neural activation. Ultimately, such an arrangement would reduce the burden of data extraction from mixed signals from electrodes embedded in a mixed neuron population, and achieve selective recording and stimulation of the regenerative peripheral neurointerfaces, which in turn can be valuable in order to achieve more precise control of the robotic prosthetic hand.

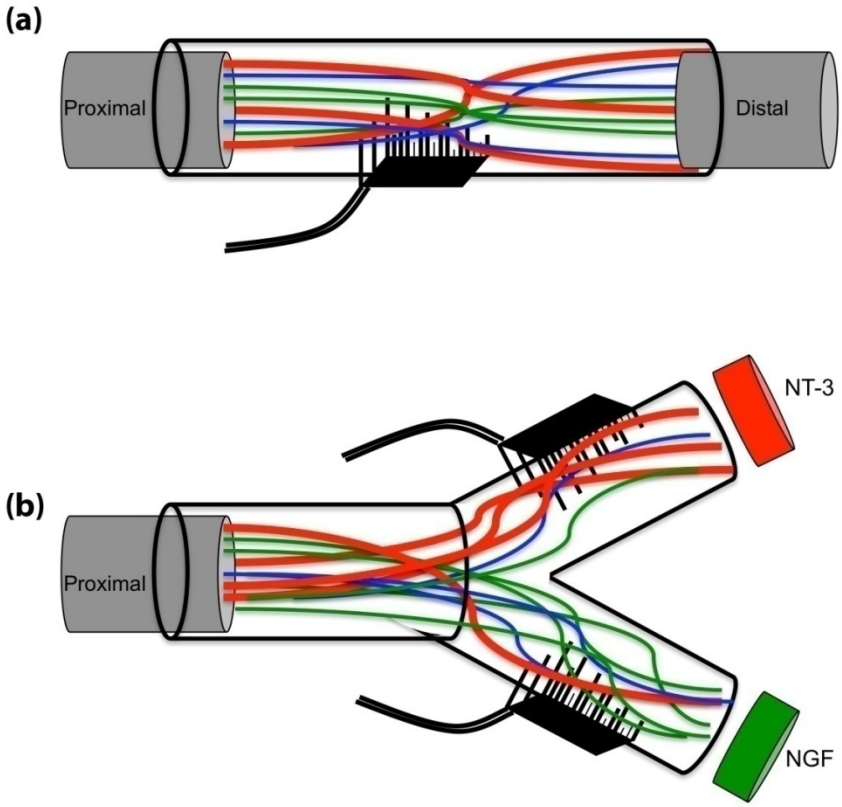

Figure 2.8.Schematic demonstration of multielectrode compartments. (a) Mixed nature of regenerative nerve in the absence of any molecular cues. (b) Specific growth factors attract a subtype of neurons to the modality-specific compartment.

CHAPTER 3

MODALITY SPECIFIC GUIDANCE OF SENSORY AND MOTOR AXONAL FIBERS IN FEMURAL NERVE MODEL USING PLGA LOADED GROWTH FACTOR

3.1 Introduction

The peripheral nervous system is capable of spontaneous regeneration after injury. However; complete recovery is impaired due to lack of integrating sensory feedback to efferent motor pathway (Gallarda et al 2008).Regenerative electrodes have been demonstrated to be a viable alternative to interface motor and sensory peripheral nerve fibers (Klinge et al 2001; Lago et al 2007; Panetsos et al 2008). Recently our lab reported the recording of multiunit activity in both acute and chronically damaged peripheral nerves with non-obstructive regenerative multielectrode interfaces (Garde et al 2009). Though, the mixed nature of axonal regeneration complicates the interpretation of the nature of the recording signals, and the stimulation strategy that might be used to convey modality-specific sensation through such regenerative interfaces.

During peripheral nerve development, motor and different subtypes of sensory neurons naturally segregate from other subtypes and establish distinct trajectories to distal target zones. Sensory-motor heterotypic neuron segregation is known to be due in part to repulsive interactions of EphA3/EphA4 receptor tyrosine kinases in motor, and ephrin-A ligands in sensory, in proximal fibers (Gallarda et al 2008). Moreover, some labs have reported the exigency of some molecular cues in organs, like muscle and skin that guide regenerating axons towards specific distal targets (Masuda et al 2009; Oakley et al 1997; Wenner & Frank 1995). These molecular cues can be used to manipulate axonal guidance (Flanagan 2006; Moises et al 2007; Tannemaat et al 2008; Walker et al 2008).

Manipulations of guidance molecules in adult mammalians after injury have been used to control detrimental effects of axon sprouting and target regenerating axons (Curinga & Smith

2008; Flanagan 2006; Madison et al 2007; Moises et al 2007; Tannemaat et al 2008; Winter et al 2007). Some molecular cues such as the neurotrophins promote neuronal survival, shape neuronal morphology and guide a preferential neuronal subtype (Flanagan 2006; Moises et al 2007; Tannemaat et al 2008; Walker et al 2008). Neurotrophin receptors are located on the surface of axons and dendrites and must convey their signal retrogradely to the nucleus to influence transcription of target genes (Flanagan 2006; Moises et al 2007). These receptors which guide the extending axons toward the distal target during the development stage continue to be functional in adulthood (Josephson et al 2001). Thus, it is not illogic to speculate that application of different growth factors can guide different axonal types.

The application of growth factors on regeneration of some of modality-specific fibers have been demonstrated with some other labs(Curinga & Smith 2008; Flanagan 2006; Gallarda et al 2008; Lerma et al 2008; Madison et al 2007; Masuda et al 2009; Moises et al 2007; Oakley et al 1997; Porter et al 1995; Shen et al 2004; Tang et al 1992; Tannemaat et al 2008; Walker et al 2008; Winter et al 2007). It is known that NGF, NT-3, GDNF induces neuritis outgrowth and axon guidance of sensory neurons (Lerma et al 2008) and that their absence results in drastic motor-sensory miswiring (Flanagan 2006; Moises et al 2007; Tannemaat et al 2008; Walker et al 2008). Specifically, TrkA nociceptive neurons depend on NGF for survival and axonal growth(Hu et al 2010; Oakley et al 1997). Among all growth factors, PTN is the only one that is expressed higher in motor neuron rather than sensory neurons (Jin et al 2009). PTN is highly expressed in denervated muscle and some type of Schwann cells (Jin et al 2009). There are evidences on this growth factor initiating axonal growth of motor neurons in peripheral as well as central nervous system (Jin et al 2009; Mi et al 2007).

Here, it is **hypothesized that mixed axons form a regenerated nerve can be enticed to grow preferentially crossing the lesion towards the specific target using neuron-type specific growth factors.** Such segregated neural fibers would predictably increase the probability of specifically recording from motor neurons and stimulating a sub-type of sensory

axons in an advanced neural interface devices. To test this possibility, we investigated the feasibility of using two specific growth factorsnerve growth factor (NGF) and pleiotrophin factor (PTN) to promote segregated regeneration of pain and motor fibers.

3.2 Material and Methods

3.2.1 BSA, NGF and PTN microparticle fabrication

Polylactic-co-glycolic acid (PLGA) microparticles were synthesized using the double emulsion (water-in-oil-in-water) evaporation method (Rocha et al 2008). PLGA (Lakeshore Biomaterials, Birmingham, AL) was dissolved in dichloromethane (DCM; Sigma-Aldrich, St. Louis, MO) at a concentration of 200 mg/ml; mixed with aqueous solutions of PTN (10µg/ml; PeproTech Inc., Rocky Hill, NJ), NGF (10µg/ml; Invitrogen, Carlsbad, CA) or BSA (20mg/ ml; Sigma-Aldrich, St. Louis, MO), and sonicated. This solution was then added to polyvinyl alcohol. The mixture was stirred to evaporate the DCM and centrifuged at 4000 rpm for 15 min to pellet the particles. The particles were resuspended in 10ml PBS and freeze dried for storage. The morphology of the particles was evaluated using a scanning electron microscope (Hitachi S-3000N Variable Pressure SEM), and the size distribution was ascertained with the particle size analyzer (Zeta Pals, Zeta Potential Analyzer).

3.2.2 Consistancy of the microparticle shape, size and release profile

Double emulsion method (W/O/W) is the most common approach for making microparticles. Using organic solvent (which can be toxic) and the broad size distribution are its main disadvantages. A volume of 20 ul of microparticle was placed on a glass cover slip. Then was allowed to dry out in an oven ovrnight at 37^{o}C. The dried microparticle mounted cover slip was put in a high-vaccum sputter coating device (CrC-100 sputtering system; Torr international Inc, New Windsor, NY) to cover the non-conductive PLGA polymer with a thin layer of Ag (Argentum, silver). The Scanning Electron Microscopy (SEM) images of micropariclе loaded BSA, NGF and PTN were taken in high pressure using a variable SEM machine (Hitachi S-3000N; Hitachi High Technology America Inc, Pleasonton, CA). These images showed that

there is a wide variety in diametere of microparticles but there was a consistancy when the fabrication was repeated and different growth factors were used (Figure 3.1).

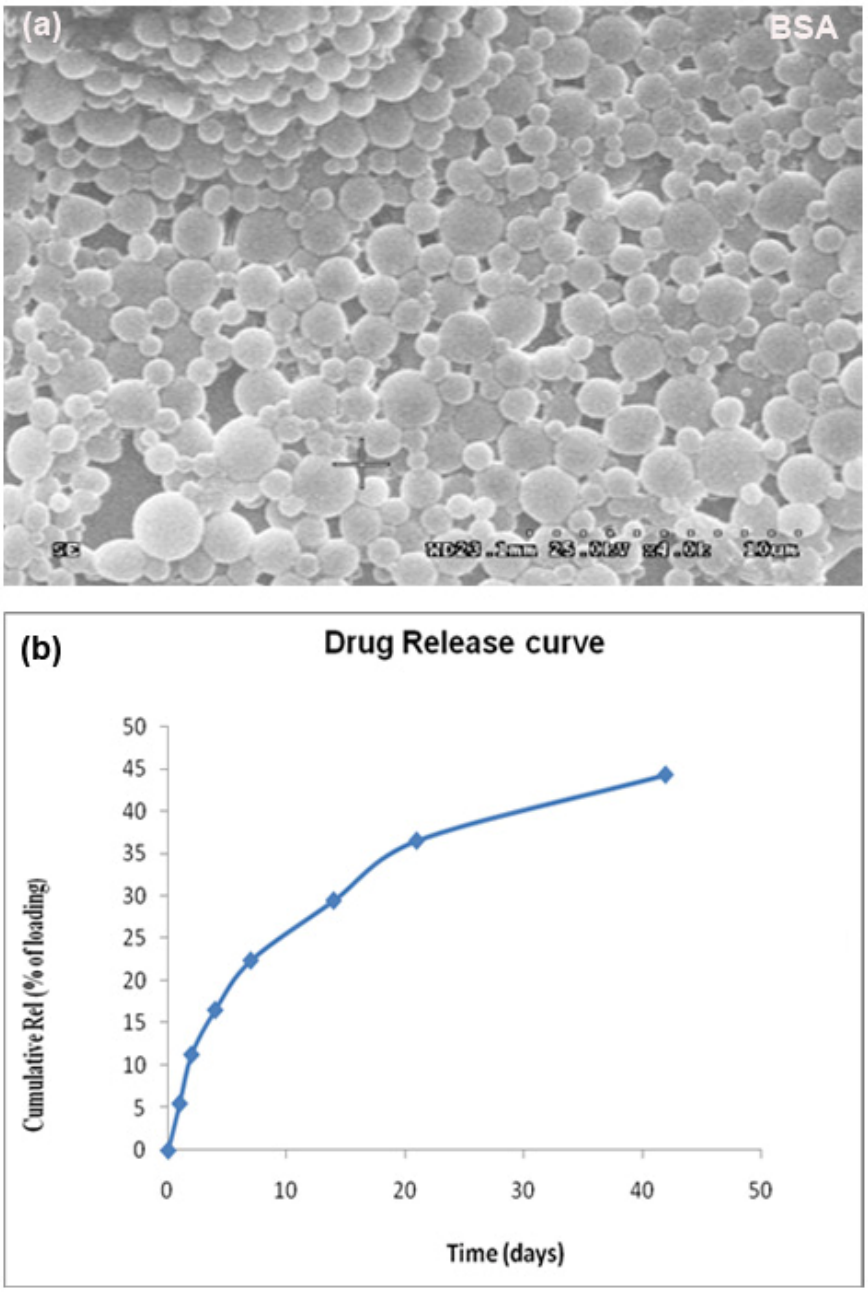

Figure 3.1 Characterization of the PLGA-BSA microparticles (a) SEM image of the microparticles showed the spherical morphology of the microparticles. (b) BSA assay of the PLGA-BSA microparticles showed that less than 50% of the BSA enccapsulated was released over 40 days.

3.2.3 Morphology, size, release profile and biological activity of the microparticles

The morphology of the particles was evaluated using a scanning electron microscope (Hitachi S-3000N Variable Pressure SEM), and the size distribution was measured with the particle size analyzer (Zeta Pals, Zeta Potential Analyzer). PTN or NGF release in PBS was evaluated at 37℃ in a shaker incubator at several time points (1, 2, 4, 8, 24, 38, 96 hrs, and weekly thereafter for 4 weeks) using ELISA (Invitrogen, Carlsbad, CA). PLGA microparticles-loaded with BSA were used as controls and their release measured by standard protein assay methods (BCA Assay, Thermo Scientific, Rockford, IL) and 562 nm spectrophotometry.

To confirm the biological activity of the PTN and NGF loaded microparticles, cortical tissure of deeply anaesthetized neonate mice (postnatal day 3) (CharlesRivers, Wilmington, MA) were collected under sterile conditions and kept in cold Hank's balanced solution (HBSS; Hyclone,Waltham, MA) supplemented with 1% penicillin/streptomycin. The collected cortical tissues were transferred to a solution containing 0.25 % trypsin diluted in L-15 was added to the pellet and kept at 37^{o}C for 30 minutes. Afterwards, a flamed tip glass was used to triturate the DRGs. After dissociation, cells are precipitated by centrifuging at 1200 gs (rcf) for 5 minutes. Cells were seeded in 8 chamber slide plates (Lab-Tek^{TM}, Thermoscientific, Rochester, NY) and kept in Neurobasal medium complemented with 1% B-27 and L-glutamine and penicillin / streptomycin (Gibco, Carlsbad, CA). All the cell cultures were kept in normal condition at37^{o}C and 5% CO_2. PLGA-PTN microparticles (3 mg) or PLGA-NGF microparticles (12 mg) or BSA encapsulated PLGA microparticles (control; 4 mg) were added to cell culture media for 3 days. Cells were fixed and immunohistochemically stained to be visualized using confocal fluorescent microscope.

3.2.4 Quantification of the axonal length and cell surface area

Axonal length and cell surface area were measured in ImageJ using the images of the stained cell culture wells with β-tubulin. Average and standard deviation of the length of the

axonal fibers and surface of the soma were calculated in experimental groups (NGF and PTN) compared to control (BSA).

3.2.5 Assessment of sustained release by measuring fluorescent intensity of Cy2-microparticles compared to Cy2 antibody

A block of 1.5 % agarose was made in 4 chamber slide plates (Lab-Tek^{TM}, Thermoscientific, Rochester, NY). Using a small biopsy punch (2 mm), a circle was created in one side of the agarose block and the agarose inside the circle of removed to create a well. Using a marker, 1, 2, 3, 4, 5, 6 and 7 mm distant from the created well was marked on the back of the glass slide (Figure 4.1). 0.4 ug of the Cy2-IgGantibody or 8 mg of the PLGA loaded Cy2 microparticle was placed in the well created by 1.5 % agarose. At different time points (1 hour, 24 hours, 3 days and 7 days) using fluorescent microscopy diffusion of the dye in the agarose block was visualized. Later, using optical densitometry, the images taken at different time points were quantified.

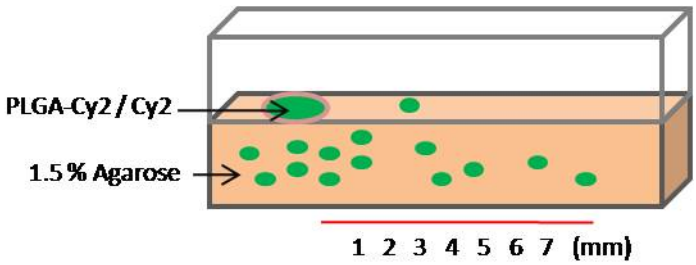

Figure 3.2 Schematic demonstration of the experimental design for the measurement of the diffusion in Cy2 particles compared to Cy2 dye in 1.5% agarose.

3.2.6 Rat femoral nerve model

Deeply anesthesized animal using an intraperitoneal (IP) injection of pentobarbital (25 mg/ Kg), underwent the double crush injury in the common femoral nerve. Breifly, common femoral nerve was exposed and braches were identified (Hu et al 2010). A double crush injury was created in the common femoral branch 5 mm proximal to the bifurcation. The femoral nerve is absolutely crucial to segregation because proximally (at the site of injury in the common

arm) both cutanous and muscle Schwann cell tubes intermingle and distally it bifurcates to the terminal cutanous and muscle branches (Redett et al 2005). Thirty-two rats were categorized in 4 different experimental groups (n=8): i) BSA-BSA, ii) NGF-BSA, iii) PTN-BSA and iv) NGF-PTN (Figure 3.3). They were double crush injured in common femoral 5 mm proximal to their bifurcations to motor branch (MB) and saphanous branch (sensory branch; SB) (Hu et al 2010). Then, another small incision was created in the distal sides of SB and MB to make the epineurium penetrable to the PLGA microparticles (Figure 3.4). This incision was covered according to the experimental group of the animals (Figure 3.3) with a mixture of 1x=11mg, 5x=56mg and 10x=112mg of NGF loaded PLGA-microparticle or 1x=1.5mg, 5x=12mg and 10x=24mg of PTN loaded PLGA-microparticle with 10 ul of fibrin sealant (Baxter, Deerfield, IL), respectively. The quantity of the microparticle mixed with fibrin glue was measured based on the release profile prior to surgery.

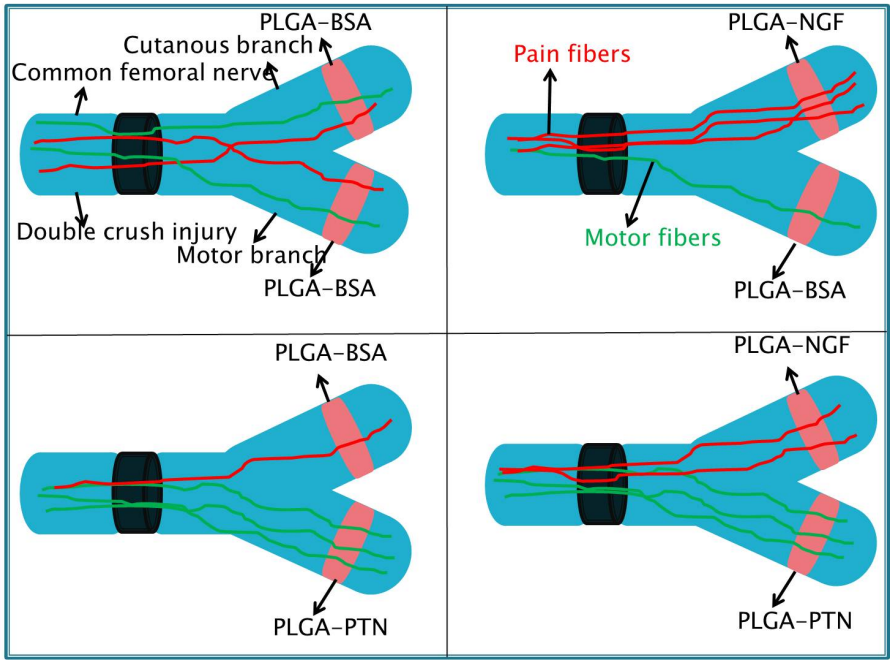

Figure 3.3 Experimental design of the in vivo femoral model. Four different experimental groups (n=8) were treated either with growth factors or with BSA (negative control). More pain fibers were expected to be enticed to NGF in sensory branches. However, number of motor fibers are predicted to be higher in motor branches when they were treated with PTN.

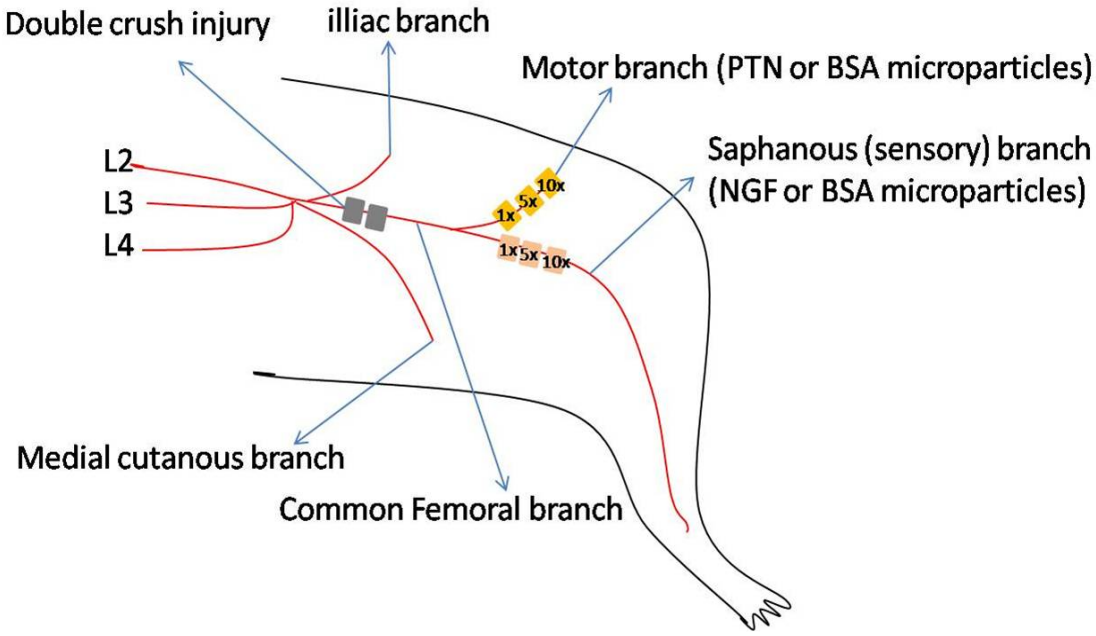

Figure 3.4 Schematic illustration of the femural nerve model in rat. The sensory and motor branches were double crushed and then later treted with NGF and PTN, respectively. A double crush injury in the common femural branch was created 5 mm proximal to bifurcation.

3.2.7 Staining and imaging

For *in vitro* biological activity studies, digital images of 20x magnifications were obtained using a confocal microscope (Zeiss LSM 510 Meta). The length of axons and surface area of soma were quantified in each experimental group to calculate mean axonal length and cell surface area of cell soma. For in vivo segregation studies, two stacked images of the SB and MB branches were captured at 40x magnification using confocal microscopy for each subject. Double-level standardized optical density threshold was applied to subtract the background and the saturated intensity values. All the areas of the longitudinally sectioned explants viewed in the images were selected for fiber growth quantification. The area (in μm^2) of positively stained ChAT+ axons and CGRP+ axons was measured in regenerated branches of the femoral nerve.

3.2.8 Functional recovery and muscle weight

Rats were walked prior to injury and 4 weeks after injury on a narrow beam. They were recorded from back while walking and snapshots of the still frame of the video were compared

characterize the functional recovery of the axonal fibers in different experimental groups. A difference was observed between the way animal lifted its injured (right) and uninjured (left) leg. The angle between the ankle and floor in the left leg (angle α in Figure 3.13) was compared with the same angle in the right leg (angle β in Fgiure 3.13) The difference between these two angles was measured as an indicator to determine the extent of the recovery in each animal (α-β in Figure 3.13).

Animals were perfused with 4% PFA and the quadriceps muscle of the injured and uninjured side was collected weighted to compare the muscle weight loss induced by the nerve injury.

3.2.9 Statistical analysis

The data is reported as the mean and the standard error of the mean (SEM). An unpaired Student's t-test was used to determine statistical differences. In multiple group comparisons, one-way ANOVA was used followed by Neuman-Keuls multiple comparison post hoc evaluation (Prism 4, GraphPad). P values ≤ 0.05 were considered significant

3.3 Results

3.3.1 PLGA Microparticles sustained release in the hydrogel

Quantitative analysis of the fluorescent intensity data collected from PLGA-Cy2 and Cy2 antibody loaded in cut wells in agarose blocks showed that the microparticles diffused in the agarose slowere. The study of the diffusion profile of the Cy2 and PLGA-Cy2 confirmed that the Cy2 released from microparticles diffuse slower in its environment and therefore, creates a gradient. Moreover, it showed that there is a delay in the diffusion of Cy2 released from the microparticle (1hour and 24 hours) compared to the experiment when Cy2 antibody was added directly. However, the gradient created with microparticles remains longer throughout the the study (7 days) compared to antibody itself (Figure 3.5). This makes the microparticle a great vehicle for the growth factor delivery in a gradient manner.

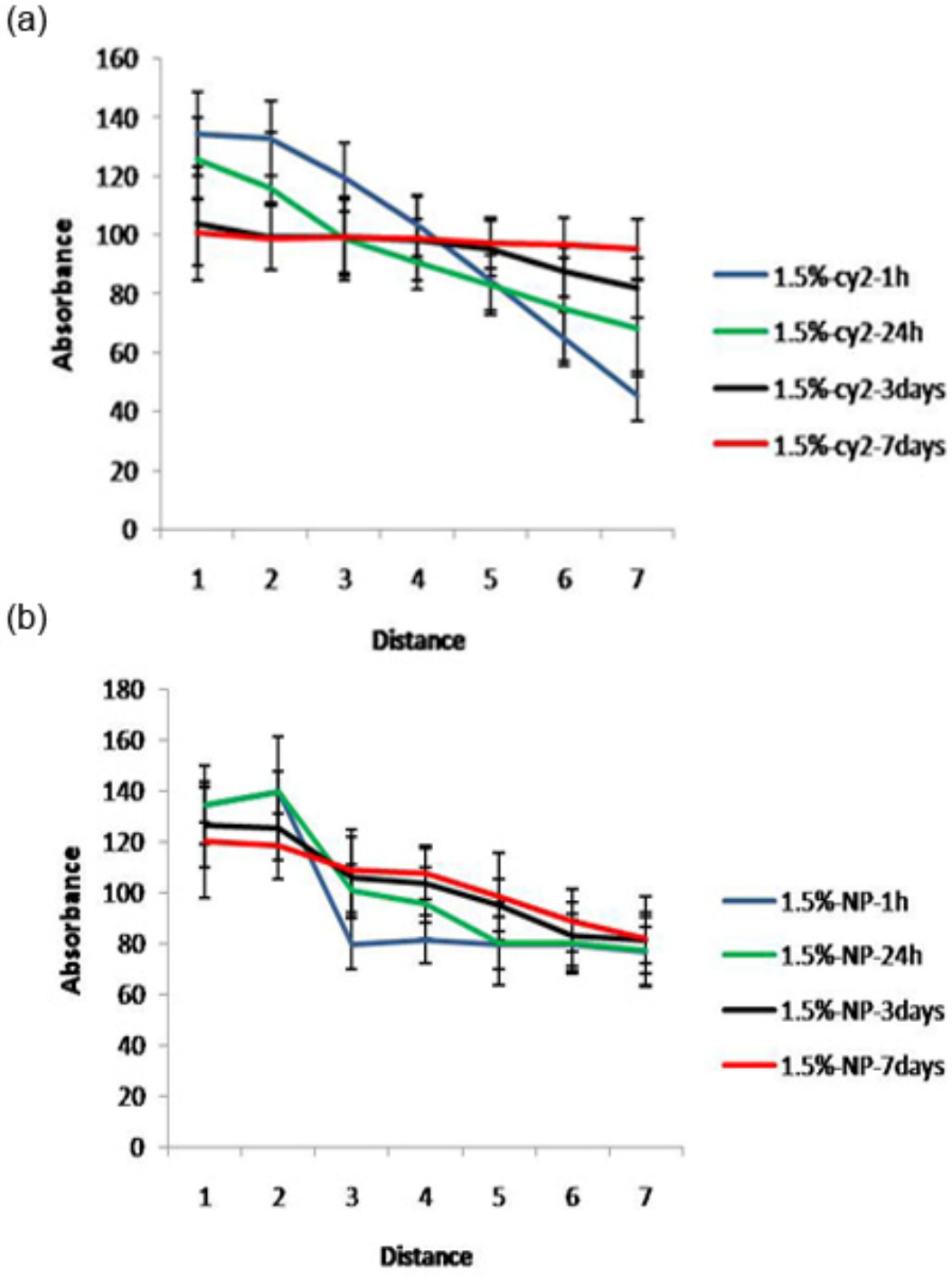

Figure 3.5 Measuring gradient established with microparticles using optical densitometry. (a) The gradient created with Cy2 antibody did not last more than 24 hours whereas (b) microparticles tend to release slower and for longer period of time (at least 7 days). (n=3)

3.3.2 PLGA-NGF/PTN microparticles

Particle size analysis using Zeta Potential Analyzer (ZetaPlus; Brookhaven Instrument Co. ; Holtsville, NY). The results of the size analysis showed that there are two different size distribution; 50-70% of the particles were smaller than 500 nm and 20-30 % of the particles were bigger than 2000 nm in diameter in all the groups (NGF and PTN loaded microparticles) (Figure 4.5b and 4.6b). This confirms the reproducibility of the microparticles using the double emolsion method. To confirm that the encapsulation of protein with PLGA polymer did not defect their biological activity, a NGF and PTN ELISA was done. Lyophilized microparticle were weighted and 1 mg of microparticle was collected and dissolved in 1 ml of PBS in a 1.5 ml conical tube. The tubes kept in a shaker incubator at 37^{o}C for 28 days. Samples were centrifuged at different time points and the supernatant was collected and replaced with fresh PBS. The collected supernatants were kept frozen in -20^{o}C upon usage. The results of the ELISA shows that there is a burst release of protein and by day 5 about 40-55 % of the growth factor was released. Later, It reaches its plateau and by the end of study 50- 70 % of the total NGF and PTN loaded was released, respectively (Figure 3.6c and 3.7c).

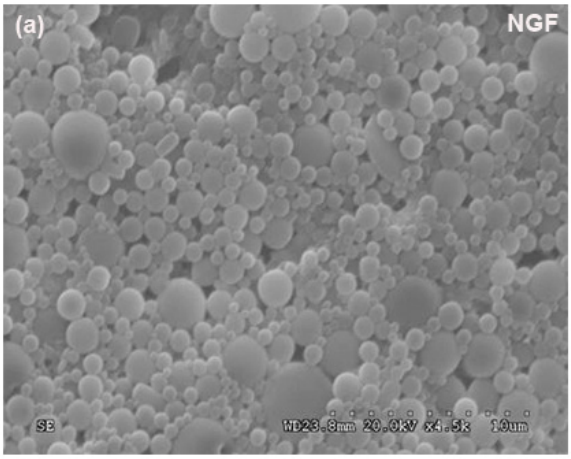

(b)

Sample ID	PLGA-NGF-080409 (Combined)
Operator ID	Parisa
Elapsed Time	00:09:00
Mean Diam.	1614.9 nm
Rel. Var.	0.673
Skew	0.324

d(nm)	G(d)	C(d)	d(nm)	G(d)	C(d)	d(nm)	G(d)	C(d)
276.6	0	0	763.5	0	56	2107.6	0	56
303.4	0	0	837.4	0	56	2311.5	0	56
332.7	0	0	918.3	0	56	2535.0	8	59
364.9	2	1	1007.2	0	56	2780.1	25	67
400.1	9	4	1104.5	0	56	3048.9	55	85
438.8	58	22	1211.4	0	56	3343.8	35	96
481.3	100	55	1328.5	0	56	3667.1	12	100
527.8	6	56	1457.0	0	56	4021.7	1	100
578.9	0	56	1597.8	0	56	4410.6	0	100
634.8	0	56	1752.4	0	56	4837.1	0	100
696.2	0	56	1921.8	0	56	5304.9	0	100

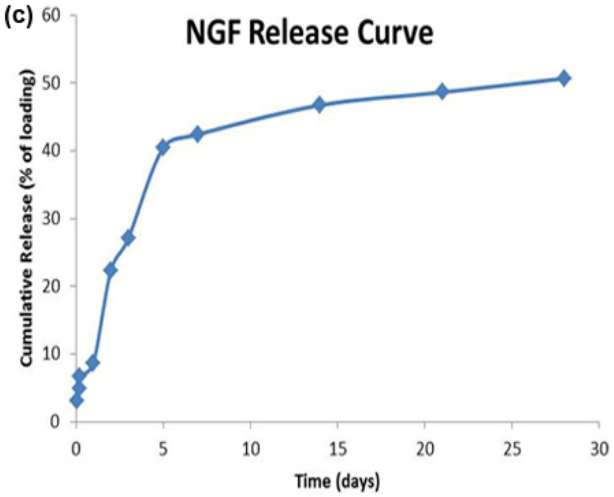

Figure 3.6 Characterization of PLGA-NGF microparticles (a) SEM image of the microparticles showed the spherical morphology of the microparticles. (b) Size analysis of the micrparticles showed that 55 % of PLGA-NGF microparticles had diameter of 480 nm or smaller. (c) The release profile of the PLGA-NGF microparticles showed that about 50 % of the loaded NGF was released in 28 days of the study.

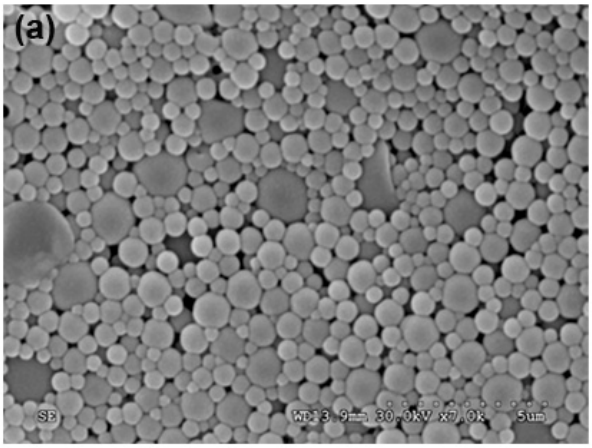

(b)

Sample ID	PLGA-PTN-080409 (Combined)
Operator ID	Abdul
Elapsed Time	00:09:00
Mean Diam.	946.6 nm
Rel. Var.	0.976
Skew	1.466

d(nm)	G(d)	C(d)	d(nm)	G(d)	C(d)	d(nm)	G(d)	C(d)
280.1	0	0	722.7	0	78	1864.4	0	78
305.3	0	0	787.7	0	78	2032.2	0	78
332.8	0	0	858.6	0	78	2215.0	0	78
362.7	1	1	935.8	0	78	2414.3	13	86
395.4	5	3	1020.0	0	78	2631.6	10	92
430.9	24	17	1111.8	0	78	2868.3	7	96
469.7	100	74	1211.8	0	78	3126.4	5	99
512.0	7	78	1320.9	0	78	3407.8	2	100
558.1	0	78	1439.7	0	78	3714.4	0	100
608.3	0	78	1569.3	0	78	4048.6	0	100
663.0	0	78	1710.5	0	78	4412.9	0	100

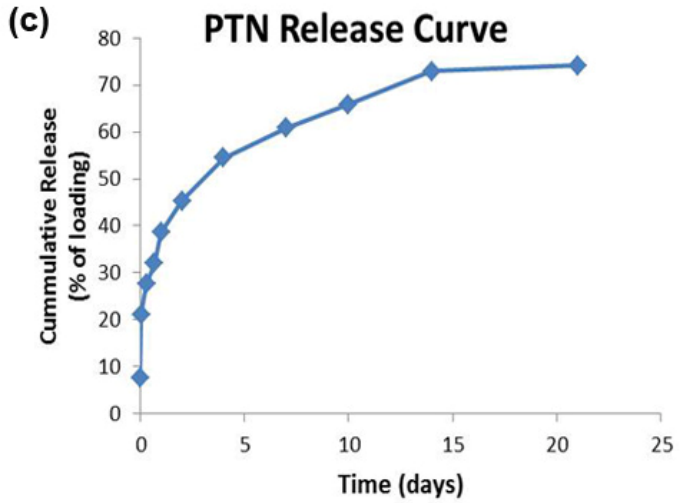

Figure 3.7 Characterization of PLGA-PTN microparticles (a) SEM image of the microparticles showed the spherical morphology of the microparticles. (b) Size analysis of the micrparticles showed that 74 % of microparticles had diameter of 469 nm or smaller. (c) The release profile of the PLGA-PTN microparticles showed that about 75 % of the loaded PTN was released in 28 days of the study.

3.3.3 Cortical neurons cell culture had longer axons and bigger cell somas when treated with microparticle loaded growth factor comapred to control (BSA)

We tested the biological activity of the microparticle loaded BSA, NGF and PTN in the cell cultures of cortical neurons (Figure 3.8 a-c). Micropartilces loaded proteins were added to the dissociated cell culture of the cortical neurons. Cell cultures were given neurobasal medium and kept in incubator at 37C and 5 % CO2 for 3 days. After 3 days, cell cultures were fixed with

4 % paraformaldehyde (PFA) and stained with β-tubulin (mouse anti- β-tub, 1:500; Sigma, St. Louis, MO). The stained cell cultures were visualized with confocal microscope and axonal length and soma surface were measured using ImageJ to obtain the average and standard deviation (Figure 3.9).

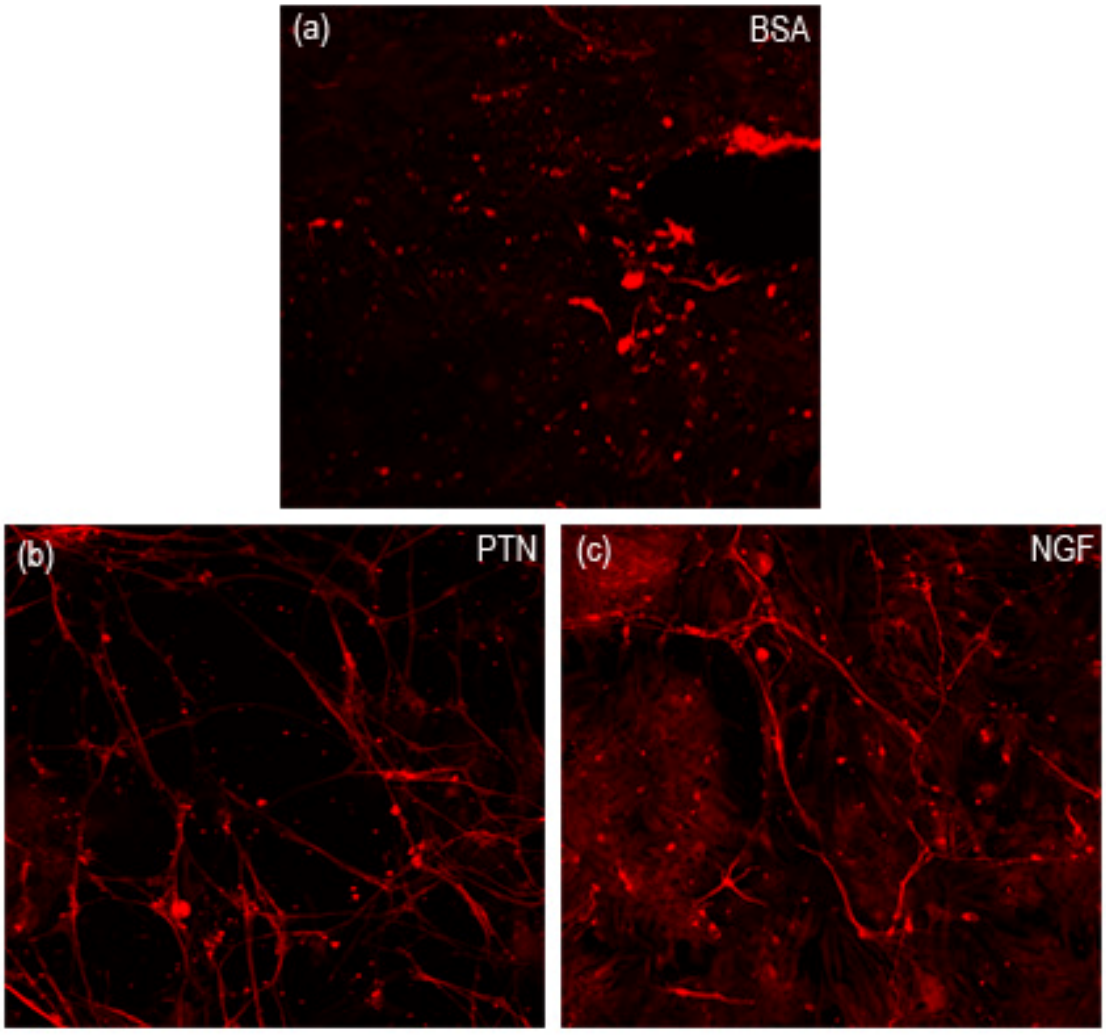

Figure 3.8 Dissociated cortical axons growing in the media containing PLGA-BSA, PLGA-PTN or PLGA-NGF. (a) Neurons growing in PLGA-BSA microparticle containing medium had very short axons. (b and c) In contrast, those growing in PLGA-PTN containing media and PLGA-NGF containing media had longer axons. The cell viability was higher in the presence of growth factors compared to control (BSA).

Quantitative analysis of the images showed that neurons treated with both of the growth facotors (NGF and PTN) had longer axonal fibers and bigger somas (Figure 3.9). The statistical analysis ($p<0.001$; $n=15$) between average length of axons in the experimental groups (NGF; 164.07 ± 36.18 µm or PTN; 217.4 ± 72.296) showed siginificant increase of the measured facotr compared to control (BSA; 53.2 ± 17.94 µm) (Figure 3.9a). Also, the average of the surface of the soma in the cell cultures treated with (NGF; 192.66 ± 57.77 μm^2 or PTN; 307.8 ± 74.53 μm^2) were significantly larger compared to control (BSA; 45.266 ± 24.81 μm^2). The longer axon and bigger cell soma confirms that cortical neurons responded to the treatment with growth factors. This confirms that the PLGA-NGF/PTN microparticles were biologically active and the released growth factors were not denatured.

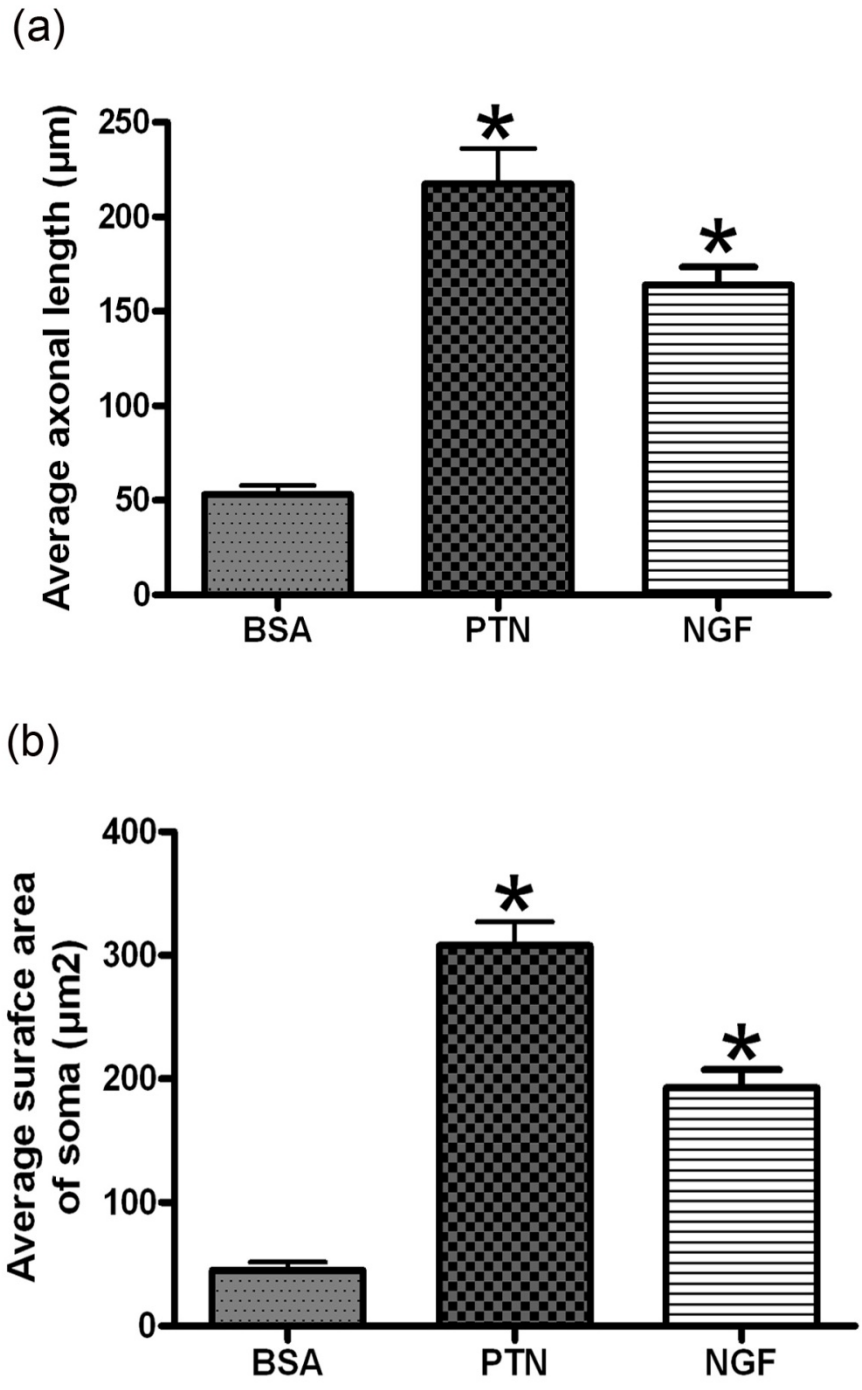

Figure 3.9 Dissociated cortical neurons growth in response to growth factors. (a)Neurons had longer axons in cell cultures containing growth factors compared to control. (b) Cell body surface was larger in cultures with growth factor compared to control. *= p< 0.001. n = 4.

3.3.4 PLGA-Cy2 microparticels traced the axonal fibers in femoral nerve

The epineurium around the nerve fibers is made of irregular dense connective tissue. This sheath which is an extension of the meniges is reponsible for the protection and integrity og the peripheral nerve. It is believed that epineurium acts as a diffusion barrier in peripheral nervous system ((Lehmann 1953; Sunderland 1965). To penetrate this protecion sheath and to confirm that the small incision created in the distal site of the biforcation in each of the branches is enough to permit the diffusion and uptake of the proteins by axonal fibers, the femoral model was tested with PLGA-Cy2 microparticles.

Rat femural nerve was exposed and the common femural branch and the saphanous and motor branch was identified as previously described in the publication (Hu et al 2010). A small incision was created in the saphanous branch to make the epineurium penetrable, using a cold forceps. Cy2 microparicles (0.01 mg) was mixed with 10 ul of fibrin sealant to place the microparticles on the site of incision. The viscose mixture of the microparticles in fibrin sealant was placed on the site and was wrapped like a sheath around the injury. The animal was sutured back and kept for 24 hours.

The animal was sacrificed and perfused and the saphanous nerve was harvested proximal and distal to the site of the injury. The nerve explant was embedded in a water soluble frozen embedding media (Tissue-Tek® O.C.T ; Sakura Finetek USA Inc., Torrance, CA) and sections. Sections were mounted on glass slide and visualized using a confocal microscope. The site of the incision and the contiguous area were fluorescent (Figure 3.10a and 3.10b). The area that was not in close proximity of the injury site did not show any fluorescent (Figure 3.10c). Moreover, the PLGA loade Cy2 microparticles were not autofluorescent when we changed the filter to Cy3 (Figure 3.10d). This results proved that our particles are uptaken with the axonal fibers as early as 24 hours post injury and injection. Therefore, the incision made in the epineurium created an area for the diffusion of the microparticles. This was confirmed by the uptake of the microparticles with the axons in the proximity of the incision. This results also

were confirmed with images taken father from the incision site or with different fluorescent filter from the site. The fluorescent visualized in the images were emanated by the microparticles and was not the effect of background.

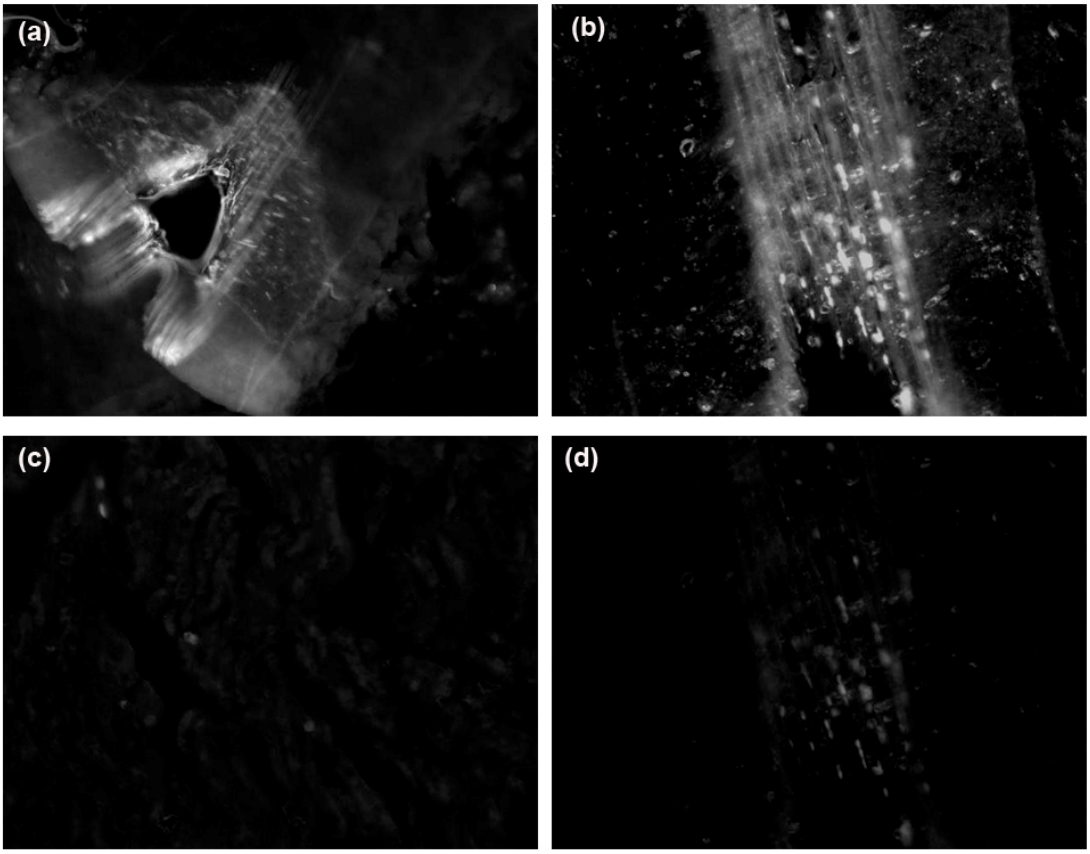

Figure 3.10 Microparticle loaded Cy2 covered the double crush injury site. (a) The released Cy2 was uptaken in 24 hours by axonal fibers in the site of injury and (b) its proximity. Whereas, (c) the axonal fibers far from the site of injury were not showing any fluorescent. (d) The same site of injury was visualized with a different fluorescnet filter (Cy3). This confirms the uptake of the Cy2 by axonal fibers at the cite of incision. The fluorescent light is emanated from the Cy2 microparticles and is not an effect of background.

3.3.5 More CGRP+ and ChAT+ axonal fibers are attracted to the NGF and PTN respectively

To test if mixed axons in the crush injured peripheral nerve could be segregated into modality-specific compartments *in vivo*; we compared the segregation effects PLGA-microparticle loaded NGF and PTN to that enticed to BSA (control). The femoral nerve in 32

rats was crushed and repaired with either NGF-microparticles (saphenous (SB)) or PTN-microparticles (motor branch (MB)). BSA-microparticles were used as control to evaluate the modality-specific guidance of axonal fibers without any exogenous molecular cues (Figure 3.10).

Double immunolabeling for choline acetyl transferase (ChAT; Specific marker for motor axons) and CGRP (specific marker for nociceptive sensory axons), confirmed that ChAT+ (motor fibers) and CGRP+ (pain fibers) are specific and do not overlap (Figure 3.11). Moreover, it confirmed that more numbers of motor fibers and sensory fibers were attracted to the branches repaired with PTN-microparticles and NGF-microparticles, respectively (Figure 3.11).

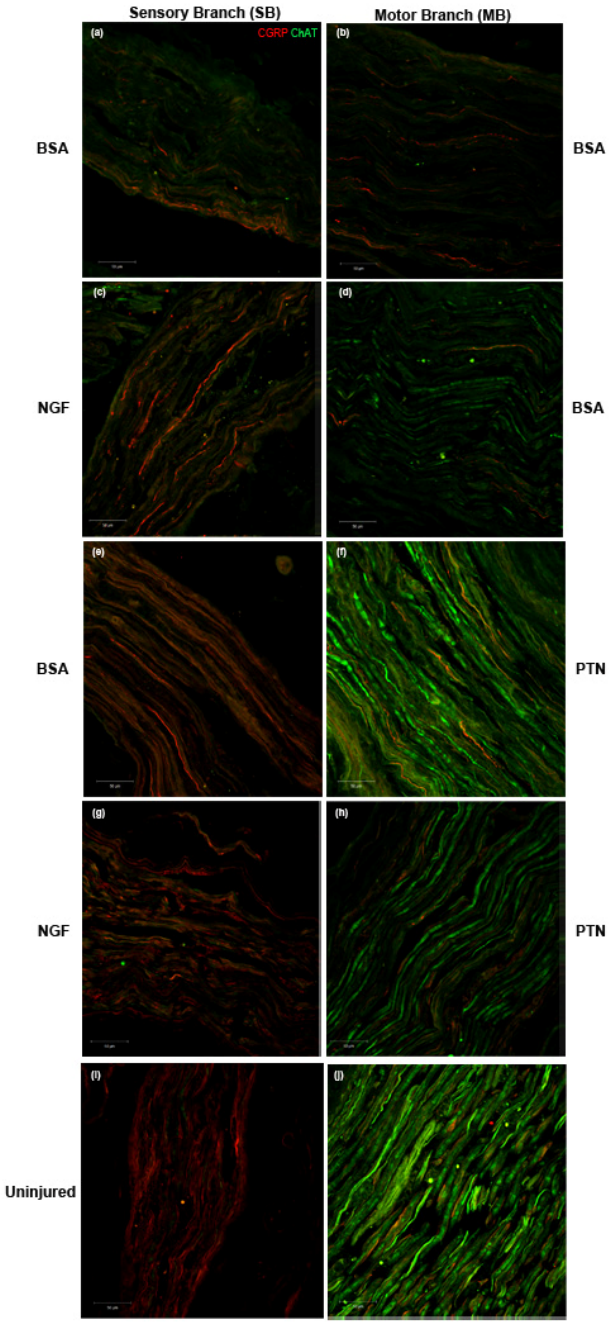

Figure 3.11 Differential labeling of large myelinated motor neurons (ChAT+; green), and small unmyelinated nociceptive (CGRP+; red) in femoral nerve in rat. There was not a distinctive growth of any subtype of axons in either of the branches in BSA-BSA group (negative control; a-b). There was more CGRP+ (pain fibers) in sensory branch of both NGF-BSA and NGF-PTN groups (c and g). Conversely, there was more motor neuron (ChAT+) in the motor branch of the PTN-BSA and NGF-PTN group (f and h). Density of pain fibers in sensory branch and motor axons in motor branch in NGF-PTN (g and h) was similar to uninjured animals (positive control; i and j).

Quantitative analysis using optical densitometry showed no significant differences in number of axons growing in both branches in control (BSA-BSA) (Figure 3.12) between the treatment groups. In sharp contrast, the density of CGRP+ axons in sensory branches (Figure 4.12a) were significantly increased in the animals treated only with NGF-BSA ($p < 0.001$; 737± 101) and group treated with NGF-PTN (459 ± 69 OD units). Moreover, that of ChAT+ was significantly increased ($p < 0.001$) in both group treated with PTN-BSA (745 ± 46 OD units) and NGF-PTN (690 ± 67 OD units) (Figure 3.12b). We also noted significant increases in CGRP+ ($p< 0.05$; 580 ± 29 OD units) fibers in motor branches treated with PTN compared to control. Interestingly, ChAT+ fibers in the motor branch of the NGF-PTN were not significantly different from uninjured (positive control). Comparing the results of the BSA/PTN and NGF/PTN showed that more ChAT+ fibers were attracted to the sensory branch in latter group compared to former. That is correlated with a reduction in the number of ChAT+ fibers regenerated in motor branch in NGF/PTN group.

(a)

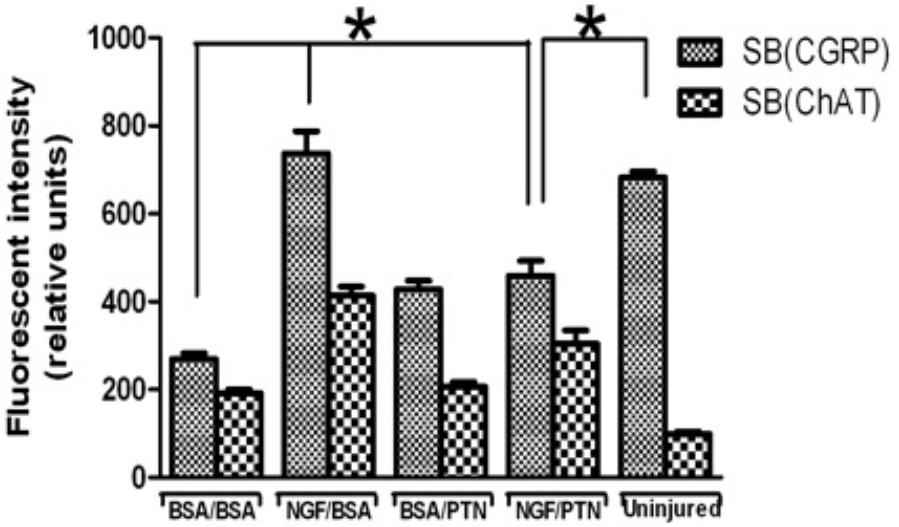

(b)

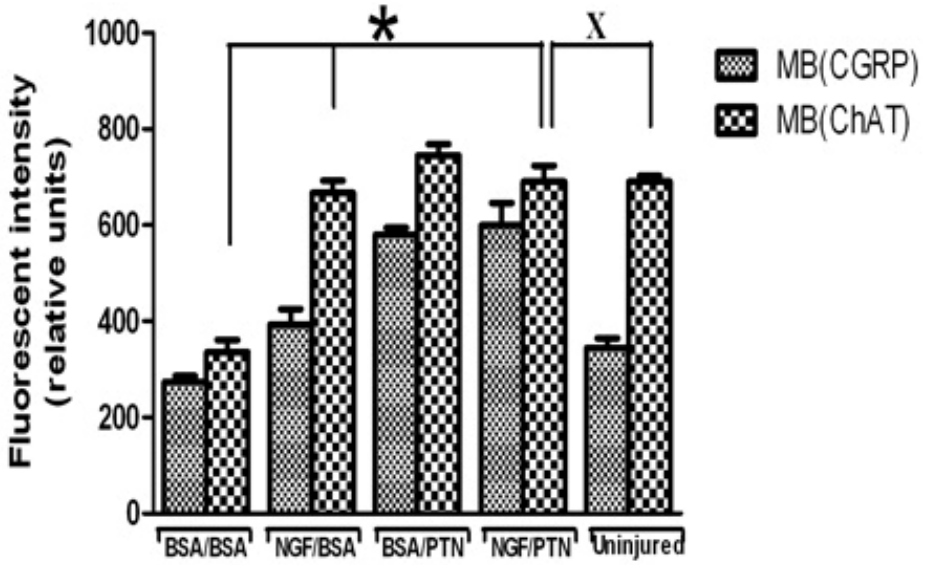

Figure 3.12 Optical densitometry of CGRP+ and ChAT+ axons. (a) Pain fibers (CGRP+) axons are grown in a significantly larger numbers in branches treated with PLGA-NGF compared to PLGA-BSA. (b) Motor neurons (ChAT+) were attracted towards the branches treated with PLGA-PTN compared to PLGA-BSA or PLGA-NGF. The axonal density in the motor branch of the animals treated with NGF-PTN were similar to uninjured (positive control) *= p< 0.001, x= not significantly different.

3.3.6 The angle of the ankle in experimental groups with reference to the ground

Femural nerve injury model is the most recommended model for the peripheral nerve segregation. However, most of the behavior studies of the recovery patterns are done in Sciatic injury model. Therofere, we had to do several different common studies like “cat walk” and “narrow beam walk” to notice if there is any difference between the uninjured group and different groups of the injured model. Video-taping the 5 groups of the animals; i) BSA-BSA (negative control), ii) NGF-BSA, iii) PTN-BSA, iv) NGF-PTN and v) Uninjured groups (positive control). The still frames of the movie showed a clear difference in the way that the animals lifted their legs. To quantify this observation, the difference between the angles of the left (uninjured nerve) and right (injured nerve) ankles with reference to the ground was measured. In the uninjured (normal) animals these two angles were almost 90^{o} and they were not a significantly different ($p< 0.001$; 1.047 ± 0.895 degree). Conversely, in experimental groups the walking pattern was distorted and animals showed a difference in the angle they were lifting up their right (injured) and left (uninjured) leg (Figure 3.13). Quantitative analysis of the angle measure in the left leg (uninured) and right leg (injured) between different experimental groups showed a significant difference (Figure 3.14a). The BSA-BSA group ($p < 0.001$; 35.167 ± 2.585 degree) had the biggest average of the measured angle difference. Whereas, the NGF-PTN group ($p< 0.001$; 0.681 ± 0.469 degree) had the smallest value and was very similar to and not significantly different from the average of the differece of the angles measured in uninjured animals ($p < 0.05$; 1.048 ± 0.895) (Figure 3.14a).

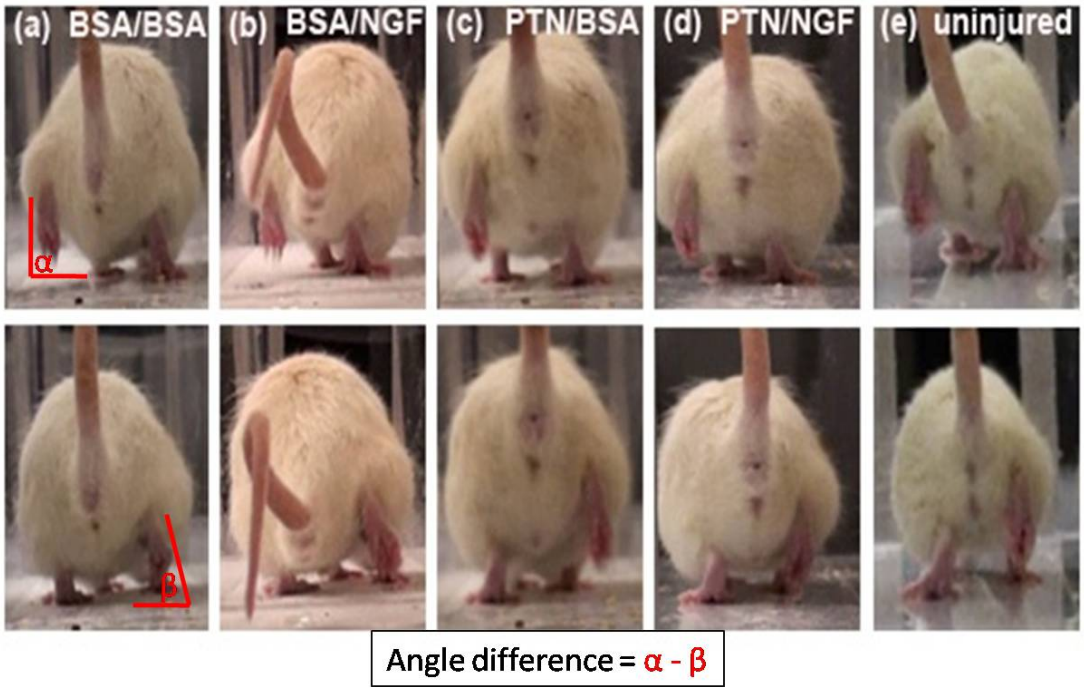

Figure 3.13 Functional recovery evaluation in the rat femural double crush injury model. (a) The angle of the lifted ankle between left (uninjured) and right leg was different. The injured leg was twisted laterally. (b) The same pattern was observed when the sensory branch was treated with NGF. (c) The injured leg was more similar to the uninjured when the motor branch was treated with PTN. (d) The animals showed more similar patterns in their walking behavior when treated with NGF and PTN for sensory and motor recovery. This was very similar to the normal walking in uninjured animal (e).

3.3.7 Muscle weight

Some studies have shown a strong correlation between peripheral nerve injury and its innervated muscle atrophy (Dadon-Nachum et al 2011; Wu et al 2011). Therefore, muscle mass was used as a powerful indicator of the functional recovery, particularly recovery of the motor fibers. The motor branch of the femoral nerve innervates the quadriceps muscle. The quadriceps muscle in 16 injured animals in 4 experimental groups (n=5) and 4 uninjured ones were collected. The water excess was removed using a Kim-wipe and immediately weighted. Statistical analysis between 5 groups: i) BSA-BSA(negative control), ii) NGF-BSA, iii) PTN-BSA, iv) NGF-PTN) and v) uninjured one (positive control) demonstrated a significant difference between experimental groups compared to control (Figure 3.14b). The muscle weight in PTN-

BSA ($p < 0.05$; 2.012 ± 0.023 g) and PTN-NGF ($p < 0.05$; 1.955 ± 0.165 g) groups were significantly higher compared to control ($p < 0.05$ 1.19 ± 0.16 g). Unexpectedly, there was a significant difference between NGF-BSA ($p < 0.05$; 1.711 ± 0.163 g) compared to BSA-BSA (negative control).

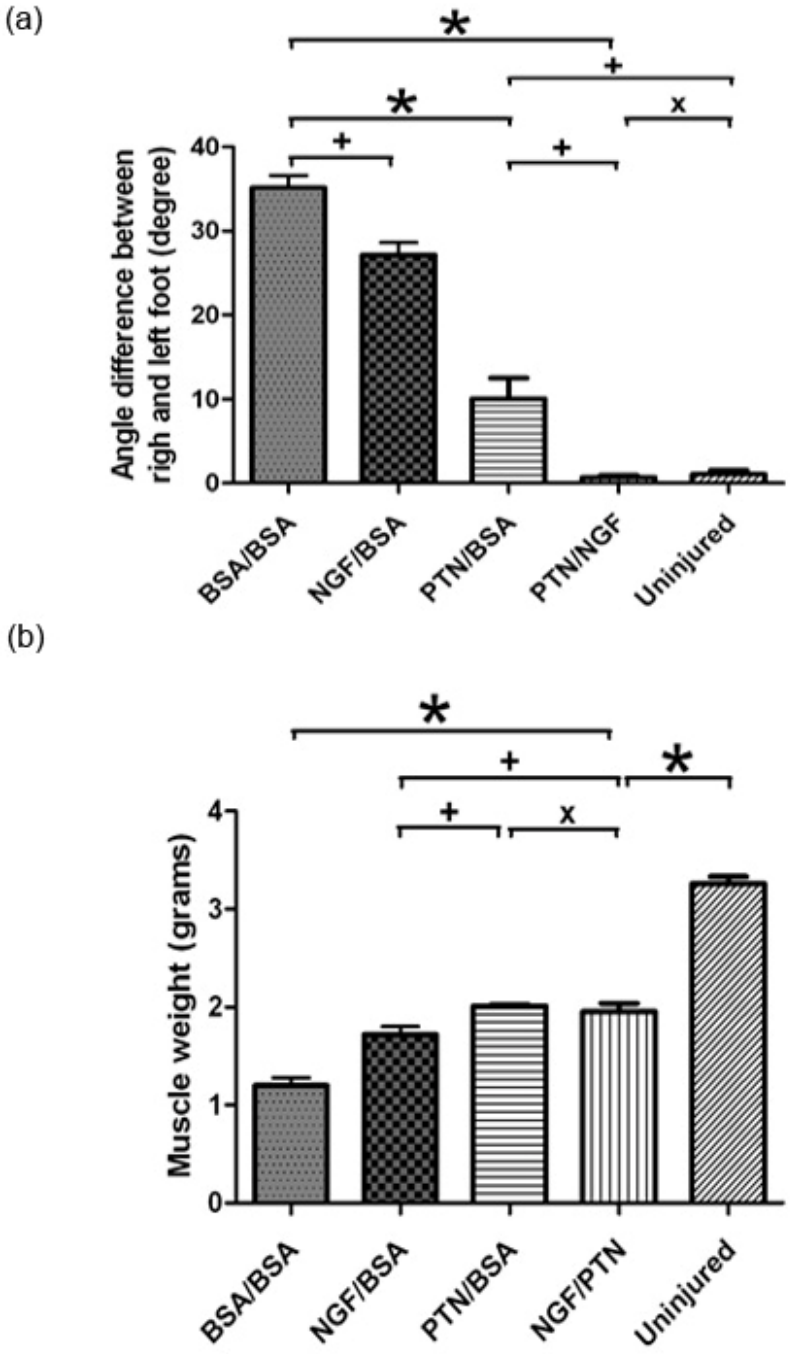

Figure 3.14 (a) Quantitative analysis of the angle between left (uninjured) and right (injured ankle). (b) Muscle weight comparison between uninjured, experimental groups and control (BSA/BSA) showed a significant difference between groups. (* $p<0.005$, + $p<0.05$, x not significant; n=5).

3.4 Discussion

Specific molecular cues such as neurotrophins and pleiotrophins are known to be involved in the precise targeting of the axonal fibers.(Kolodkin & Tessier-Lavigne 2011). Some of these factors influence neural adhesion and neural growth by making changes in cell-cell and cell-substrate interaction(Cheng et al 2003; Freier et al 2005; Haipeng et al 2000; Mingyu et al 2004). Whereas others affect the axonal guidance possible by cellular signaling cascades from neural transmitters, hormones and repulsive or attractive signals from filopodial and lamellar protrusions (Kolodkin & Tessier-Lavigne 2011; Mueller 1999; Seeger & Beattie 1999; Tessier-Lavigne & Goodman 1996; Zheng et al 1996a).

The key to axonal guidance by molecular cues lies in their ability to transduce the extracellular signals to interacellular changes. Growth factors tend to be able to make changes in intracellular expression of cytoskeletal molecules(Kolodkin & Tessier-Lavigne 2011). Some studies have simply shown the ability of these molecules in regeneration and guidance of cell neurites (Cao & Shoichet 2003; Raivich & Kreutzberg 1987); While others have confirmed the diverse morphological and functional response of different axonal subtypes to specific growth factors (Hari et al 2004). The members of the neurotrophin family growth factors bind to specific tyrosine kinase receptors (Averill et al 1995; Jubran & Widenfalk 2003; Michael et al 1997; Nagy & Hunt 1982; 1983). After binding to their specific Trk receptor the signals are internalized and retrogradely transported to the neuronal soma where the Erk and PI-3 kinase signaling cascades are activated, mediating axonal growth and cell survival respectively.(Averill et al 1995; Jubran & Widenfalk 2003; Michael et al 1997; Nagy & Hunt 1982; 1983; Terenghi 1999). NGF preferentially binds to TrkA receptors present on sympathetic neurons and some of sensory neurons of the dorsal root ganglion (DRG) (Jelsma & Aguayo 1994; Josephson et al 2001). TrkA+ neurons are small diameter neurons with unmyelinated axons that mediate pain perception and express calcitonin gene-related peptide (CGRP) (Josephson et al 2001; Piotrowicz & Shoichet 2006). PTN has been shown to interact with tyrosine phosphataseζ

(PTPζ), N-Syndecan and anaplastic lymphoma kinase (ALK) (Maeda et al 1996; Raulo et al 1994; Stoica et al 2001). Although the detailed mechanism of the PTN is yet to be discovered, there are some evidences confirming the interaction of the PTN with ALK receptor in neuronal regeneration (Yanagisawa et al 2010).

This study showed that, it might be possible to segregate or appropriately guide the regenerating axons from transected nerve by exogenously providing essential neurotrophic factors. The specific growth factors; NGF and PTN; can significantly guide more number of nociceptive and motor fibers to the target. NGF not only attracts more pain fibers but also act as a repellent for the motor fibers. This was confirmed by the results of the comparison of the muscle weight. Repelling of the motor fibers and guiding them to the motor branch in the animals treated with NGF might be an explanation to the higher muscle weight in this group compared to the control. On the other hand, PTN tends to attract some of the CGRP+ fibers (proprioceptive fibers) which might be due to its pleiopotency. It also showed that the growth factor enticed regenerated fibers can improve more functional recovery in the treated animals. The angle of the ankle in the NGF/PTN group was almost identical to the uninjured animal. Conversely, the ankle was twisted more laterally in the control (BSA/BSA) compared to the groups that were treated with PTN in motor branch. Moreover, muscle weight has been used as an indicator of the proper target innervations in motor fibers. There was a significant difference in the weight of the quadriceps muscle among the experimental groups. Quadriceps muscles are innervated with the motor branch of the femoral nerve. Finally, it showed that sustained release techniques of the drug delivery can be used to deliver the minimal effective amount of the growth factor locally to the site of injury. This can be used as a more reliable and less hazardous method for the growth factor delivery where molecular cues are needed to provide guidance for nerve regeneration. This study was an attempt to sort regenerating axons to increase specificity of recording/stimulation in regenerative interface.

CHAPTER 4

A METHOD TO ACHIEVE PROGRAMMABLE GRADIENTS OF DRUG DELIVERY

4.1 Introduction

Axons in developmental stages are guided to their target by a combination of attractive and repulsive signals from immobilized and diffusible molecular cues (Cajal 1928; Deuchar 1970; Sun et al 2000; Walsh & Doherty 1997). Growth cone is the most active part of the neurons and it is believed to guide axons by sampling their environment (Goodman 1996; Mueller 1999; Seeger & Beattie 1999; Zheng et al 1996b). Furthermore; some have reported that during developmental stages axons not only distinguish between cells and molecules in their microenvironment but also they have specific orientations toward the gradient of molecular cues (Bonhoeffer & Huf 1982; Cao & Shoichet 2003). Many researchers studying the topographic growth of axonal regeneration during these stages agree on the fact that establishment of the gradient causes the axonal guidance. To investigate these phenomena many have established some *in vitro* models (Bonhoeffer & Huf 1982; Cao & Shoichet 2003; Gierer 1981). These models are very helpful in describing the mechanism and cell-cell or cell-ECM interaction in a molecular level and they mimic the in vivo in many aspects. However; they are unable to explain when this gradient appears and how long it lasts. Moreover; one might hypothesis that loss of gradient after developmental stage might be the reason for lack of sense of direction in axonal fiber after injury. However; there are not many studies investigating these facts *in vivo* due to the lack of a precise, programmable model of gradient.

In nerve regeneration, the major factor of functional recovery after lesions is the accurate regeneration of axons to their original target. Unfortunately, regenerating axons are often misrouted to wrong end-organs (Madison et al 2007). To alleviate this problem, axons have been guided by neurotrophic factors, polypeptide adhesive molecules, cytokines, and

signals from such as those from Schwann cells. During development, guidance molecules play a key role in the formation of complex circuits required for neural functions (Curinga & Smith 2008; (Juttner & Rathjen 2005; Ponimaskin et al 2008). Neurons guide their axonal fibers into long distance targets areas where they can form synapses with selected target cells (Schmid et al 2006). It has been shown that growth cones will navigate over long distance if i) concentration of the growth factor is not too high to saturate the cell membrane receptors and ii) concentration gradient is steep enough for axons to detect the target (Cao & Shoichet 2001).

4.1.1 Different approaches to create gradient

Application of microfluidic channels and injection of viral vectors are among some of the methods for establishment of gradient (Dodla & Bellamkonda 2006; Kong et al 2011; Ziemba et al 2008). Some of these methods are only applicable for short-term studies *in vitro* (microfluidic channels) (Kong et al 2011). Whereas, others involve risks associated with the injection of the carrier (adenovirus injection) (Ziemba et al 2008). These studies propose a safety feature is introduced by creating replication-incompetent viruses (Ziemba et al 2008; (Fallaux et al 1999). Although, encouraging results are achieved, two main concerns are still remained: the severe immune response to viral vectors which needed to be treated with immunosuppressant drugs and generation of replication-competent viruses. Production of the replication-competent virus is unpredictable and difficult to control (Ginsberg 1996)Fallaux et al 1999; (Schaack 2005). Therefore; there is not a safe systematic sustain-release method available to study and deliver the optimized concentration and steepness of the gradient *in vitro* and in *vivo*.

Fabrication of drug delivery vehicles using biocompatible polymers is a safe way to avoid complications associated with administration of viral vectors. However; they often time create a linear and transient concentration (Figure 4.1a). We and others have used PLGA microparticles in multiluminal channels for the sustained release of the VEGF growth factors (Dawood et al 2011; Dawood 2011). However such method provides a linear GF concentration (Figure 4.1b). In order to establish a sustained gradient we designed the use of PLA fibers,

which when coiled around the microchannels offer a growth factor concentration which changed according to the number of coils. We reasoned that coiled fibers can be wrapped around the lumen of microchannels to provide a defined GF gradient in the lumen (Figure 4.1b).

(a). Short term drug delivery: Fabrication of the microchannels would provide a better control over the limited intended volume. However, the concentration is not sustainable.

(b). Long term drug delivery: Biodegradable microparticles will provide a sustained release of the chemicals (e.g. growth factors) in the optimal concentration in the desirable volume. This design lacks gradient.

(c). Long term drug delivery with a sustained gradient. Invention of the biodegradable coiled fiber to create a gradient will create a controlled release of the chemicals (e.g. growth factors) in an adjustable gradient manner .

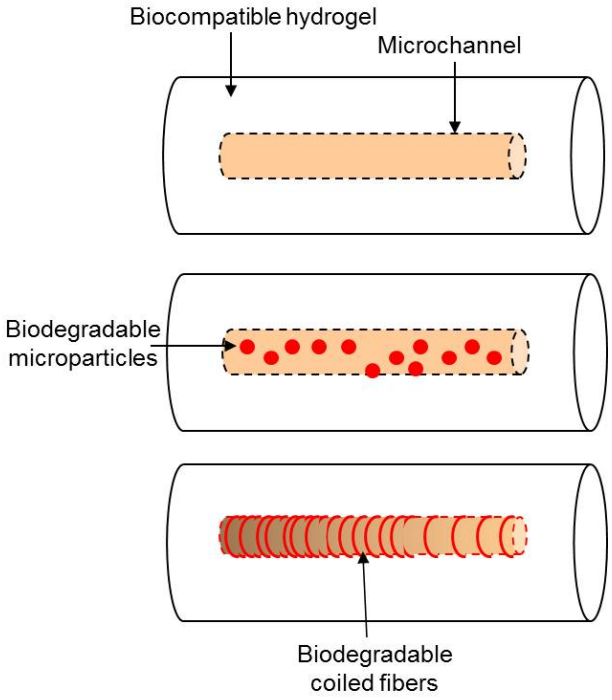

Figure 4.1 Schematic diagram of different approached to create a consistent concentration for in vivo purposes. A) Application of a microchannel embedded in a surrounding hydrogel with higher diffusion coefficient than the filling hydrogel will create a limited volume with the optimal concentration. B) Biodegradable microparticle loaded with chemical (e.g. growth factor) will provide a sustainable concentration over a long time. C) Coiled fibers will create a controllable gradient that can be adjusted by changing number of helical turns, the lateral distance between each turns and length of the channel.

4.2 Material and methods

4.2.1 Multiluminal NGF gradient modeling

Growth factor release from PLGA coils was modeled in two configurations (isotropic and anisotropic) of a multimedium model solved using finite element analysis. The model was implemented in COMSOL Multi physics using a 2.4 GHz Intel® Core™2 Quad processor computer and consisted in turns with a diameter of 250 micrometers and thickness of 1

micrometer distributed inside a cylinder with a diameter of 250 micrometers and a length of 1 centimeter. The release profile from the loaded PLGA coils was modeled using a modified version of Korsmeyer-Peppas equation for the release from a degradable polymer. The initial condition of the coil was taken as a uniform load of 1 microgram. The simulations were run for a period of 28 days.

4.2.2 Fabrication of coiled PLGA fibers

Poly-lactic-co-glycolic acid (85:15, 135,000 MW) coiled fibers were fabricated using wet-spinning. Briefly, a solution 20 wt.%PLGA was dissolved in dichloromethane (DCM; Sigma-Aldrich, St. Louis, MO) and was allowed for complete dissolution. The polymer solution was loaded into a glass syringe (gas-tight syringe; Hamilton, Reno,NV) and placed in a syringe pump (Harward Apparatus, Holliston, MA) as is described in other publications (Nelson et al 2003). Polymer solution was injected to the coagulation bath containing isopropanol to form the fiber. Pre-washed mylar substrates was used as collecting spool. With many spinning parameters possible, the spinning solution injection rate and the fiber collection speed was controlled at 1.8ml/h and 8.5m/min, respectively to achieve 30 um diameter fibers. PLGA solution formulations containing the nerve growth factor (NGF; 5µg/ml; Invitrogen, Carlsbad, CA) or BSA (20mg/ ml; Sigma-Aldrich, St. Louis, MO)or cyanine dye-3 (cy3; 5µg/ml; Jackson ImmunoResearch Lab, Inc., West Grove, PA) were prepared by adding the required amount of growth factor. Whenever necessary, PEG was added in the spinning formulation to preserve the bioactivity of the growth factor. Manufactured fibers were wound around a glass column and were dried out over night to let the the DCM.

The PLGA fibers were wrapped around the core titanium fiber 80 times. The total length of the titanium fiber (1 cm) was divided to 3 areas; proximal, middle and distal. In the anisotropic configuration, 40, 25 and 15 turns were placed in the proximal, middle and distal area, respectively, Whereas, in the isotropic configuration the total 80 turns were distributed homogenously in all 3 areas.

4.2.3 Fabrication of growth factor loaded coils

PLGA fibers were coiled around titanium fibers (d=250 um) and were kept in 4^{o} C before use. Later, they were immersed in NGF growth factor solutions (1mg /ml) overnight. Then they were casted in a TMM device as it is described in Chapter 3, Figure 3.1a (Dawood et al 2011). PLGA fibers loaded with BSA were used as controls.

4.2.4 Hydrogel embedded coiled fiber and loading PC-12 cells

Pheochromocytoma cells (PC-12 cells) were loaded in a novel rectangular frame (12.5mm X 36mm) used for casting agarose gels with a method described previously (Dawood et al 2011). The casting device was made of dental cement and used to guide multiple titanium fibers (0.25 mm X 17 mm; SmallParts, Logansport, IN).Titanium fibers wound growth factor coils were positioned through perforations at both ends of the device. Under sterile conditions, the casting device was placed over a glass slide in a cell culture dish and a 1.5% ultrapure agarose (Sigma-Aldrich, St. Louis, MO) solution was applied to cover the fibers and allowed to polymerize. PC12 cells ($1X10^{6}$ ml) were suspended in growth factor-reduced Matrigel (3.5 mg/ml, BD Biosciences, San Jose, CA). The negative pressure generated during removal of the titanium fibers from the solidified gel, drew the PC12 cells/ECM mix into the lumen of the casted hydrogel microchannels. Matrigel will allow the PC12 cells to grow inside the channels. The growth factor coiled fibers were intact in the lumen and in approximate contact of PC12 cells. The cell cultures were fed with RPMI-1640 medium (Sigma, St. Louis, MO) and kept in the incubator at 37ºC and 5% CO_2 for 72 hours.

4.2.5 Staining and visualization

For visualization of differentiated PC12 cells in the microchannels the gels were fixed in 4% paraformaldehyde (PFA) and processed for immunofluorescence. After rinsing the gels with a blocking solution (0.1% Triton-PBS/ 1% normal serum), the samples were incubated with Oregon Green Phalloidin and TO-PRO 3 Iodide (Invitrogen, Carlsbad, CA) as cytoskeletal and

nuclear labels, respectively. The staining was evaluated using a Zeiss confocal microscope (Zeiss Axioplan 2 LSM 510 META).

4.2.6 Image analysis and quantification

The staining was evaluated and analyzed using regular and fluorescent microscopy and z-stack 3D image reconstruction of the microvascular network in the multi-luminal hydrogels. Quantification of the length of PC-12 cells processes in 3 different coil density (none, low and high) was achieved using the Axiovision LE software (CarlZeiss, Axiocam, version 4.7.2) and Zeiss LSM Image Browser (version 4.2.0.12).

4.2.7 Statistical analysis

All data values were expressed as mean ± standard error of the mean. The data was analyzed by parametric student t-test or by non-parametric student-t test followed by Mann Whitney post hoc evaluation using the Prism 4 software (GraphPad Software Inc.). Values with $p \leq 0.05$ were considered to be statistically significant.

4.3 Results

4.3.1 Mathematical modeling of coiled fiber NGF gradient delivery

In our mathematical model the filling conduit was considered to have the diffusion coefficient of the agarose gel. The diameter of the channels was considered to be 250 um. The results of the mathematical analysis showed that the isotropic coiled fiber created a homogenous concentration in the channels which stayed for 28 days (Figure 4.2). The both ends of the conduite were considered to be open. Therefore, in the proximal and distal end a decrease in the concentration of the growth factor was observed due to the diffusion flux out of the lumen. Howeve, the change in the concnetration of the proximal and distal ends compared to the middle was minimal (less than 15 % of the concentration in the middle) and the conduite structure tend to preserve the homogenous concentration. The anisotropic configurations of the coiled fiber created a gradient as early as 5 days and tend to keep the gradient for long time (at least 28 days) (Figure 4.3). The out flux of the growth factor from the distal and proximal ends

did not affect the establishment of the gradient. The steepness of the gradient stayed the same throughout the study (from day 5 to day 28).

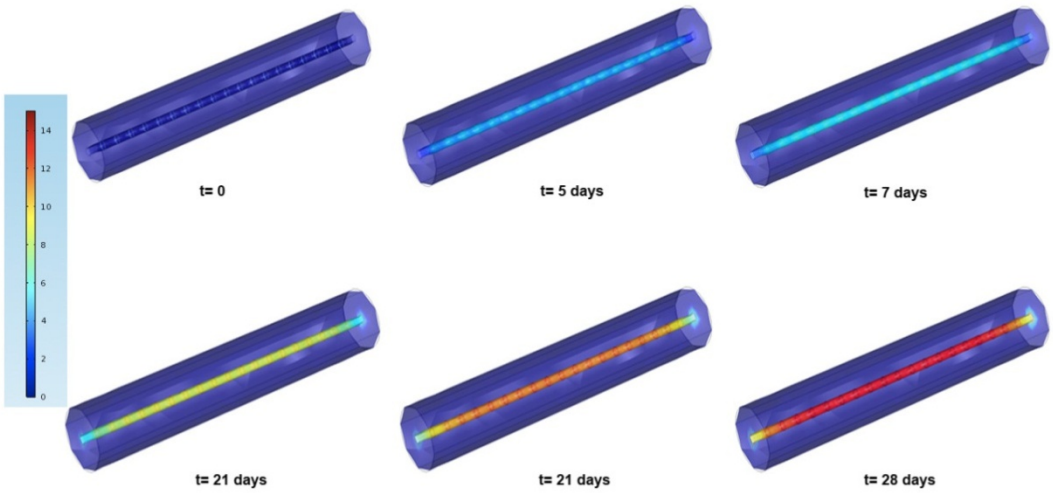

Figure 4.2 Snap-shots of the mathematical speculation of the isotropic desing of the coiled fiber. The homogenious distribution of the gradient in the isotropic desing will remain for at least 28 days in the microchannels.

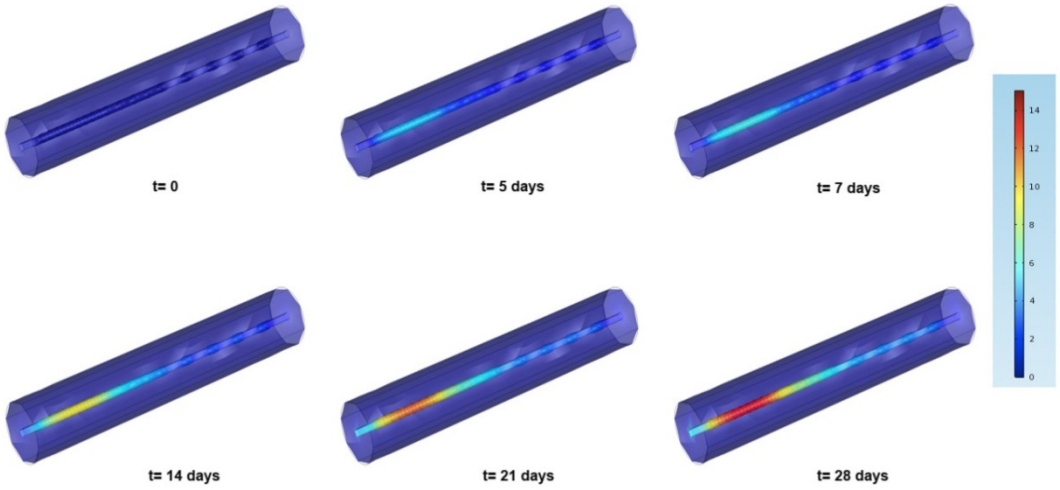

Figure 4.3 The images of the predicted concentration distribution in the microchannels using Comsol confirms the establishment of the a sustained gradient at least for 28 days in the anisotropic.

4.3.2 Establishment of gradient

To test our model Cy3 loaded PLGA coiled fibres were imaged using light microscopy and fluorescent microscopy to demonstrate that the coil has a gradient nature (Figure 4.4a) and they maintain their structure even after pulling out the fabrication metal fibre (Figure 4.4b). Magnified images of the same fibre in the low and high concentrated areas clearly confirmed the significant difference in the number of turns and the fluorescent light emanated from fibres in these two areas (Figure 4.4c).

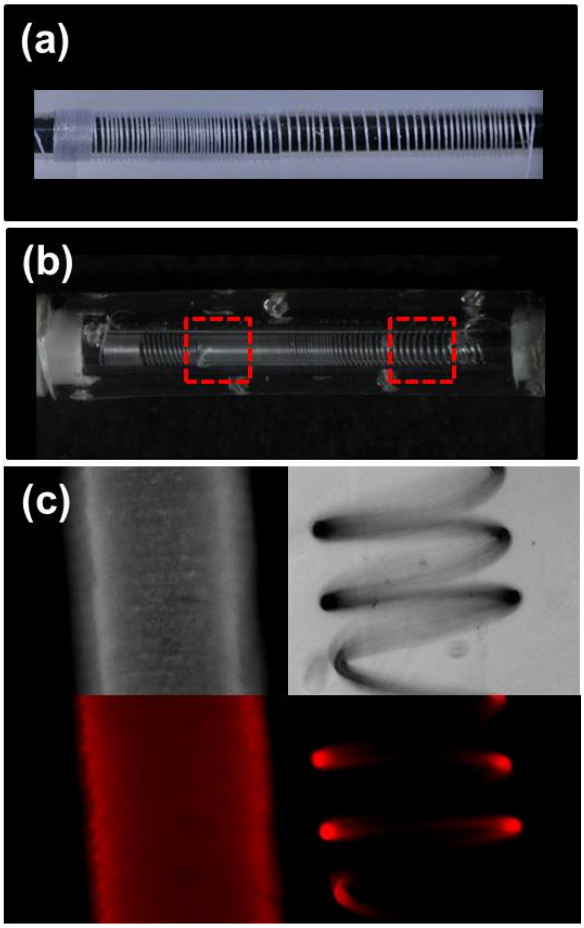

Figure 4.4 Coiled fibers loaded with fluorescent dye (Cy3) to demonstrate the establishment of the gradient. A) Image of the wound coil around the fabrication fiber. B) The coiled PLGA fiber can be placed in a nerve conduit. C) Higher magnification of the areas in box. The Cy3-PLGA coiled fibers are imaged the high density (left) and low density (right) areas.

4.3.3 Evaluation of biological activity of NGF loaded coiled fiber

Fabrication of the fibers requires harsh chemical perocedures such as application of organic solvents (dichroromethane). To confirm that growth factors (proteins) were preserved throughout the process of the fabrication of the coils, NGF loaded coiled fibers were tested in the presence of PC12 cells (Figure 4.5). PC12 is cell lines that have receptors to differentiate in the presence of the nerve growth factor (NGF); therefore they are proper cell line to test the biological activity of the loaded growth factor. Cells/ ECM suspension were loaded in the cell well (Figure 4.5a) of the casting device and were pulled inside the lumen by the negative pressure created by retreiving the titanium fiber out of the lumen as described earlier in a publication by our lab (Dawood et al 2011). Cells seeded inside the lumen were fixed in 24 hours with 4% paraformaldehyde (PFA) and stained with Oregon Green Phalloidin and TO-PRO 3 Iodide (Invitrogen, Carlsbad, CA) to visualize the as cytoskeletal and nuclear labels, respectively (Figure 4.5).To facilitate the penetration of staining dyes, the gels were placed in a cell culture plate while the solution was stirred over night at 4ºC using a magnetic plate and stir bar.

Images of the cells inside the lumen looked spherical and showed no processes (Figure 4.5b) in the area that there was no NGF loaded coil (Square B in Figure 4.5a). Whereas, cells seeded in the areas with NGF loaded coiled fibers (Square C and D in Figure 4.5a) were completely differentiated and had long processes (Figure 4.5c and 4.5d). Interestingly, these processes were longer in the area with higher density of coil (Figure 4.5c and 4.5d). This confirmed that areas with higher numbers of turns will release more NGF and therefore has higher concentration of the growth factor.

To quantify the visualized images, length of all the processes equal or longer than the cell body was measured. The quantitative analysis of the data showed a significant difference between the lengths of the cells processes (Figure 4.6) in the three areas depicted in the Figure 4.5a. P value equal or less than 0.05 was considered significant.

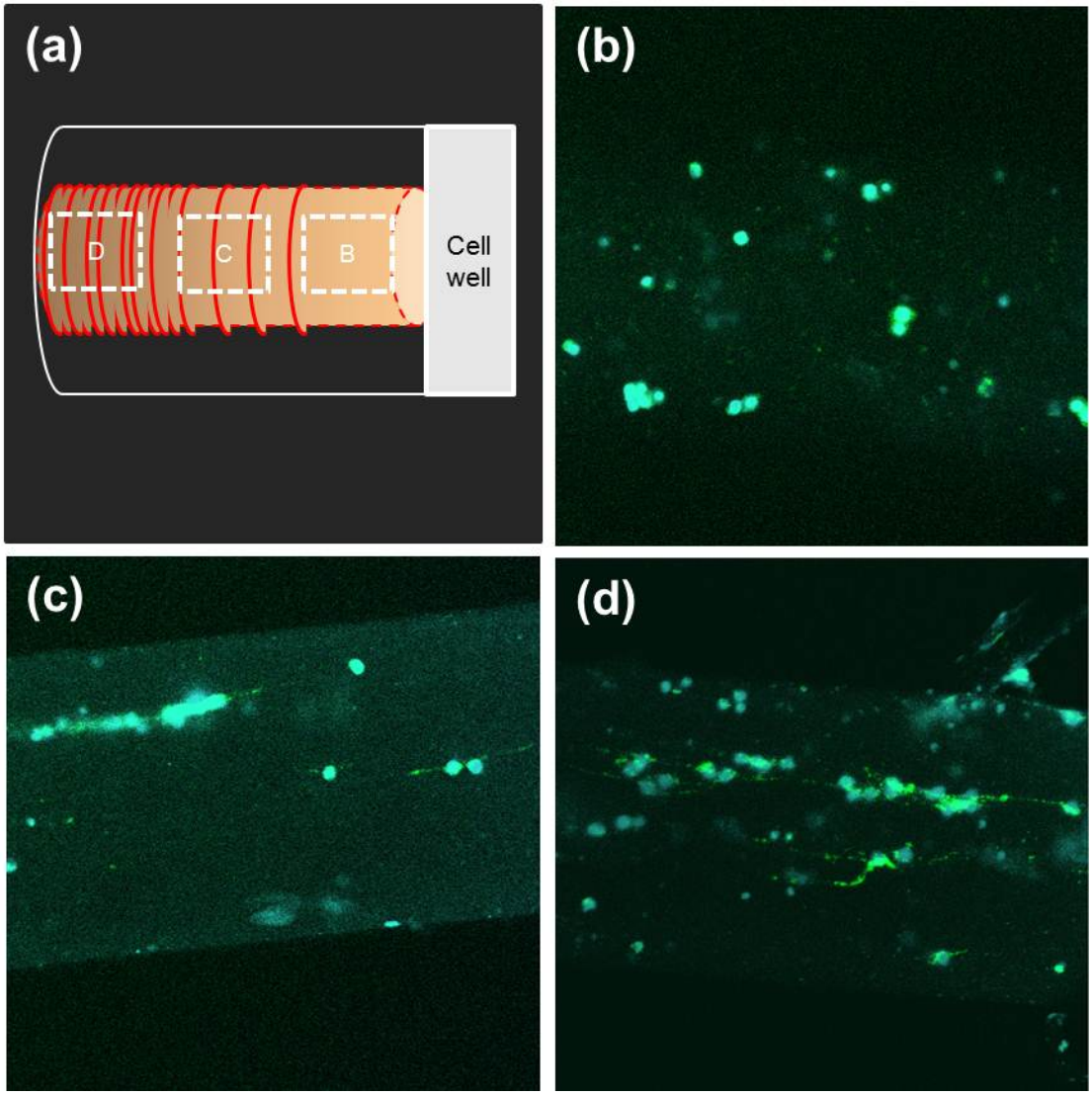

Figure 4.5 Bioactivity of the PC12 cells in NGF loaded coiled fiber channel. A) Schematic diagram of the design of the experiment. NGF loaded coil fiber was placed in a nerve conduit (as shown in the image 3 B). PC12 cells were loaded inside the channel. B) PC12 cells located distally from the coil (Box B in image A) did not show any processes 72 hours after being seeded. C) PC12 cells located in the middle of the coil (Box C in image A) differentiated and had some processes in 24 hours. D) PC12 cells located in the high density area of the channels with the most number of NGF loaded coil turns (Box D in image A). After 72 hours cells were differentiated and have long processes.

The PC12 cells processes length was measured in none, low and high concentration area (Figure 4.6). The average length of the processes was significantly higher in proximal ($p<0.002$;

n=6; 71.33 ± 12.17 µm) area and middle (35.66 ± 12.69 µm) compared to distal (1.4 ± 1.14 µm)

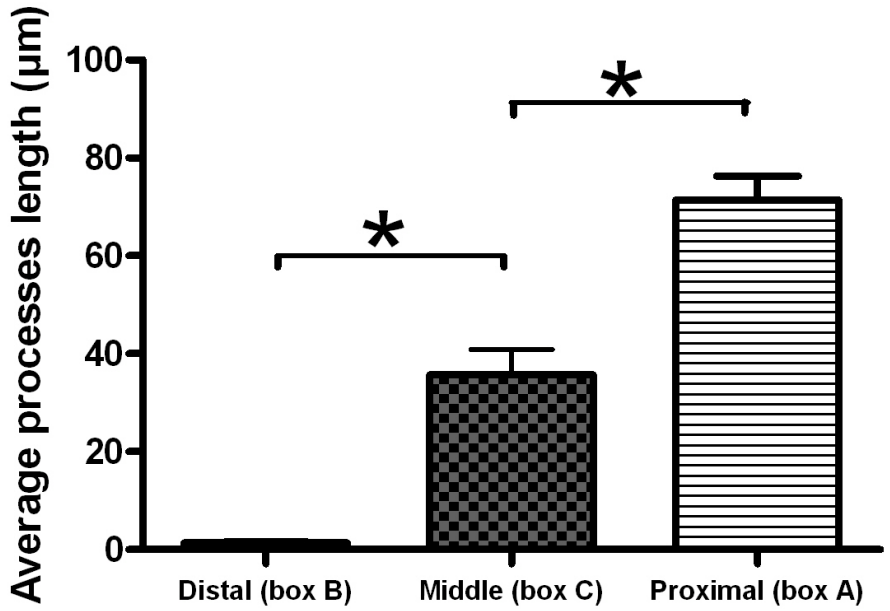

Figure 4.6 Bioactivity of the PC12 cells in NGF loaded coiled fiber channel and gradient establishment were determined by measuring cells processes in area without any NGF (distal ;box B), in the area with low density of NGF loaded coiled fibers (middle; box C) and the area with high density of NGF loaded coiled fibers (proximal; box D). Cells were imaged 72 hours after seeding and processes length was measured using ImageJ. There was a significant difference in the length of the cell processes in the different areas (* $p<0.005$ n=6).

4.4 Discussion

During development or after injury, neurons extend their axonal processes to their respective targets following a gradient of growth factors secreted by the targets (Berke & Keshishian 2011; Hale et al 2010; Tessier-Lavigne & Goodman 1996).

Recently, it has been demonstrated that an anisotropic design of the hydrogel scaffold can direct axons in long gap injuries compared to its isotropic equivalent (Dodla & Bellamkonda 2006). However; the components of the gradient in this study; are distributed inside the lumen and that might hurdle the axonal regeneration. Here, we developed a method to create a programmable gradient. The gradient is accomplished by the number of turns around a fiber.

The fibers do not block the conduit designed for the axons path. Moreover; the number of turns in each area can be programmed to create the proper steepness. This can be easily confirmed with the mathematical modeling. Additionally, this design can be easily translated to an *in vivo* implantable nerve conduit. Our findings demonstrated that the growth factor released from the fibers is biologically active and is not denatured in the process of fabrication.

This experiment needs to be investigated further to find the proper steepness of each growth factor and possibly combination of several growth factors *in vitro*. Besides; the findings of this experiment need to be investigated and confirmed in an *in vivo model*. This design can provide a novel method for establishment of gradient in vivo.

In addition to stimulation of axonal growth across a gap, there is also a need to separate specific modalities of axons into distinct compartments. This is needed both for the repair of sensory and motor branches and for the development of closed-loop peripheral neural interfaces. Application of different growth factors loaded coils in different channels will be facilitated with coiled fibers (Figure 4.7). This strategy will entice a specific sub-type of axons in a mixed population of nerves to the channels and eventually will guide them to the proper target (Figure 4.7).

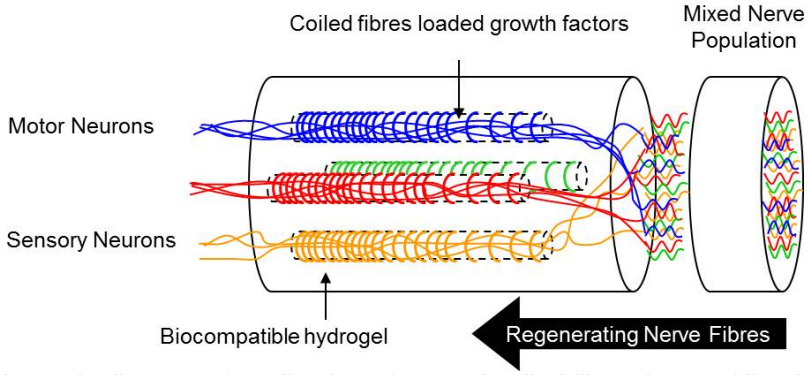

Figure 4.7 Schematic diagram of application of several coiled fibers in a multiluminal conduit to guide axons with different modality. Modality specific axonal guidance is one of the several applications of the establishment of the gradient. Each channel contains a helically wound fiber that contains a specific molecular cues (specifically neurotrophin or pleiotrophin) known to entice growth of a specific type of neurons (nerve cells). Release of the chemical guidance cues will create a gradient in the channels inside the coiled fibers. The gradient can be controlled by the fiber architecture (e.g. total number of helix turns, lateral distance of each turn from its adjacent ones and number of helix in distance unit).

The nerve guidance conduit can be completed applying different strategies like; using coils with different steepness to acquire optimal gradient for multiple growth factor/ drug (Figure 4.8), fabricating a multi-stranded coiled polymer with different polymers (e.g. using different PLA/PGA ration) in order to deliver multiple factors/ drugs at different rates, manufacturing a multi-stranded coil using same polymer but different fiber diameters, developing a coaxial fiber and finally utilizing electrically conducting strands within the coil.

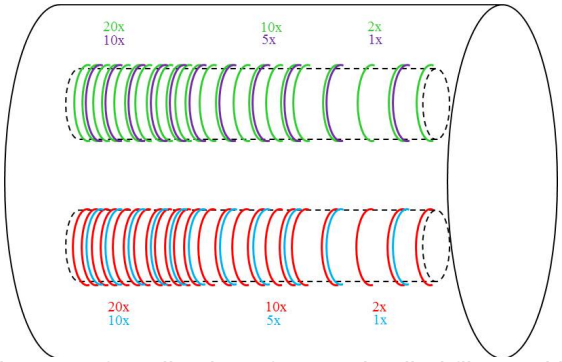

Figure 4.8 Schematic diagram of application of several coiled fibers with different gradient in a multiluminal conduit to guide axons and other type of cells. This will allow us to guide different cell types to the conduit with their optimal concentration gradient.

APPENDIX A

SYNERGISTIC EFFECTS OF NEUROTROPHIC AND PLEIOTROPHIC GROWTH FACTORS IN AXONAL REGENERATION

Introduction

Spontaneous axonal regeneration is absent in the adult central nervous system. The use of neurotrophic factors such as Brain-derived neurotrophic factor (BDNF), Glial cell line-derived neurotrophic factor (GDNF), Nerve growth factor (NGF), and Neurotrophin-3 (NT-3) have all shown good results in axonal regeneration. Recently, growth factors that stimulate multiple cell types such as Pleiotrophin/heparin binding growth factor-8 (PTN) have also demonstrated to induce neurotrophic effects. Brain-derived neurotrophic factor's ability to regenerate axons, motor and sensory, is mediated by two receptors: tropomyosin-related kinase B (TrkB) and p75 neurotrophin receptor ($p75^{NTR}$) (Boyd & Gordon 2001; 2002; Friedman & Greene 1999; Gavazzi et al 1999; Henderson et al 1993; Henderson et al 1994; Kimpinski et al 1997; Lindsay 1988; LoPresti & Scott 1994; Oppenheim et al 1995; Segal 2003; Sendtner et al 1992; Yan et al 1992; Yan et al 1995; Yano & Chao 2000; Zurn et al 1994). TrkB receptors can be found predominately on myelinated mechanoreceptor axons and α-motor neurons (Bloch et al 2001; Koliatsos et al 1993; Snider & Wright 1996). Conversely, the $p75^{NTR}$ receptor can be found in all types of sensory neurons (Bloch et al 2001). Glial cell line-derived neurotrophic factor regenerate axons, motor and sensory, via the receptor complex GDNF-family receptor α-1 (GFR α-1) and the signal-transducing tyrosine kinase subunit Ret (Baloh et al 2000; Gavazzi et al 1999; Henderson et al 1993; Kimpinski et al 1997; Lindsay 1988; LoPresti & Scott 1994; Oppenheim et al 1995; Saarma & Sariola 1999; Sendtner et al 1992; Yan et al 1992; Yan et al 1995; Zurn et al 1994). This complex can be found primarily in γ-motor neurons and a subpopulation of sensory neurons in the DRG (Airaksinen et al 1999; Shneider et al 2009). Nerve growth factor acts on sensory axons through the tyrosine kinase receptor TrkA, found predominately on unmyelinated nociceptive axons (Jenq & Coggeshall 1985). Neurotrophin-3 binds TrkC receptors found predominately on myelinated proprioceptive axons (Snider & Wright 1996). Pleiotrophin has been found to play a significant role in embryogenesis and is highly expressed in the developing nervous system (Bloch et al 1992; Muramatsu 2002;

Vanderwinden et al 1992). The three receptors found to interact with this growth factor have been found to be protein tyrosine phosphatase ζ (PTPζ), N-syndecan, and anaplastic lymphoma kinase (ALK) (Maeda et al 1996; Raulo et al 1994; Stoica et al 2001). Out of these three receptors it is believed that ALK is the key receptor responsible for neuritogenesis using the glycogen synthase kinase 3β/β-catenin/growth-associated protein-43 pathway (Yanagisawa et al 2010).

Table A.1 Summary of the neurotrophic and pleiotrophic factors tested in this study and their associated specific tyrosine kinase receptor and their trophic effects on different subtypes of neurons.

Growth factor	Specific receptor	Function
NGF	TrkA	Nociceptive fibers fibers
NT-3	TrkC	Proprioceptive fibers
PTN	ALK, PTPζ and N-syndecan	Motor neurons and some other cell types.

Whether these factors have different stimulatory or synergetic effects is currently unknown. However, if each growth factor targets a different sub-type of neurons, it can be concluded that the combination of the growth factors increase the number and sub-type of the axons. Some studies have shown that increased number of sprouted axons from explants enhances the chance of reaching the correct target (Morris et al 1972). Therefore; synergistic effects of the growth factors can be used to improve the innervations of the correct target if used *in vivo*. Here we evaluated the possibility of **achieving a synergistic growth effect in neurons when exposed to multiple neurotrophins or a combination of neurotrophins and pleiotrophic growth factors.**

Materials and Methods

Tissue Preparation

Postnatal (P3) mice were anesthetized hypothermically. Each pup was dissected and their dorsal root ganglions (DRG) were collected, dissections were performed in cold D1SGH. DRG explants were placed in separate chamber of a Lab-Tek® Chambered Slide coated with laminin

the night before. Each explant was held in place by a drop of extra cellular matrix (ECM) and placed in an incubator set at 5 % CO_2 and 37^o C for 5 minutes to allow for polymerization. After the ECM polymerized and adhered the explants to the slides each chamber was filled with minimum essential medium (MEM) and allowed grow in the incubator for 24 hours.

At the end of the incubation period each chamber with their perspective explants MEM solution was replaced by a new MEM solution containing different combinations of growth factors, the different group are shown in table 2.

Table A.2 Different combinations of growth factors applied to dorsal root ganglia explants.

Dorsal Root Ganglia
Pure MEM
100 ng/ml PTN
100 ng/ml NGF
2 ng/ml NT3
100 ng/ml of PTN and 2 ng/ml NT3
100 ng/ml of PTN and 100 ng/ml of NGF
100 ng/ml of PTN and 100 ng/ml of NGF and 2 ng/ml of NT-3

The concentration of each growth factor used agreed with their physiological level described by other researchers. Explants were allowed to incubate with new media for an additional 48 hours.

Immunocytochemistry and Microscopy

Each chamber was washed and phosphate buffered saline (PBS), Triton and normal donkey serum before they were incubated with the primary antibodies overnight at 4^{o}C. Then, they were stained with goat anti-β-tubulin in order to identify the axons from each explant.

Methods of visualization and Quantification

All the explants were imaged after staining. The partial images of the total axonal growth were mosaicked to create a full image of the experiment. Details of the preparation of the images and quantifications are as following:

1. *DRG Explant Pictures*

   DRG explant pictures were obtained through confocal laser scanning microscopy after staining with β-tubulin and TO-PRO-3. Entire DRG explant pictures were taken using the Plan-Neofluar 10x/0.3 objective lens to produce 1303.0µm x 1303.0µm images in Carl Zeiss Image Browser v4.2. The images produced were then sectioned into quadrants. In the quadrant with the most growth, pictures were taken using the Plan-Apochromat 20x/0.75 objective lens to produce 651.5µm x 651.5µm images.

2. *Picture Assembly*

   Zeiss LSM Image Browser v4.2 was used to scale the DRG explant quadrant images in increments of 20µm. The scaled images were imported to Adobe Photoshop Elements v8.0. For each set of DRG explant images, the explant body was made the primary layer. Images of the extending axons were made into secondary, tertiary, quaternary, etc. layers until the entire quadrant was imported. The layers were then stacked so that all the DRG quadrant explant images formed a single image of the explant and axons extending from it. To avoid incorrect positioning, the opacity feature in Adobe

Photoshop was used to stack each picture and at least five axon branching points per image were checked to insure correct location.

3. *Average Axonal Length and Longest Axon Length*

   For each assembled quadrant picture in Adobe Photoshop Elements, the edge of the explant body was outlined using the six pixel diameter brush tool. Extending axons were then traced from the outlined edge to the axon end and measured with the 20µm increment scale. This was repeated for twenty-five different axons and the mean value found. The longest axon was then traced and measured.

4. *Number of Projecting Axons*

   Images of the complete DRG explants, taken with the Neofluar 10x/0.3 objective lens, were imported into Zeiss LSM Image Browser v4.2. For each explant, the overlay function was used to trace the axons projecting from the explant body and the total number was recorded. The entire process was repeated three times per explant image and the mean value of projecting axons calculated.

5. *Number of Branches from a single Axon*

   Quadrant images of the DRG explants for NT3 and NGF had their axons traced with the six pixel diameter brush tool. Twenty- five axons per image were selected and number of branches extending from each axon was found. The mean value for branches per axon per image was then calculated.

6. *Glial Cell Count and Average Glial Distance*

   Glial cells were quantified from the quadrant pictures assembled in Adobe Photoshop Elements. A green overlay was used to count the stained glial cells three times. The average glial cell distance was calculated by the same technique that was used for average axonal length quantification; however, the measurements were made for the farthest glial cell on an axon rather than the axon end.

7. *Axonal Density*

Axonal Density was calculated with ImageJ 1.42q software. The freehand selection and picture analysis functions were used to calculate the area of axons per image (A_{axon}), the area of the DRG explant body (A_{body}), and the area of the total image (A_{total}). The axonal density was determined by: $(A_{axon})/(A_{total} – A_{body})$ (Shah et al. 2004).

Data Analysis

Each explant's total number of projecting axon was counted to get total number of axons. Eight of the most prominent axons from each explant was measured and averaged to show the average of the longest axons. The distance that glial cells and fibroblast travelled out of the explants was measured using a ruler. Statistical analysis of the data was done by Student's t-test and one way ANOVA. Values with $P<0.001$ were considered significant.

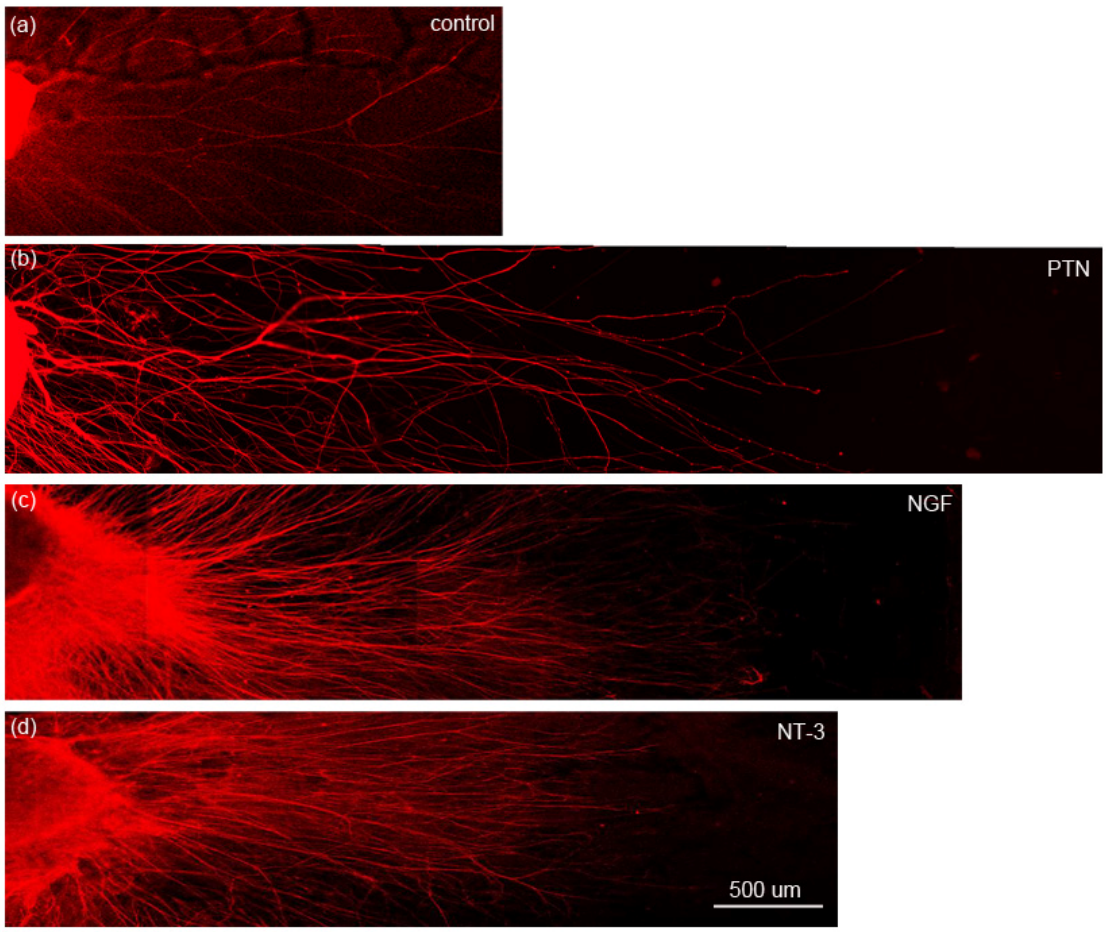

Figure A.1 Visualization of the DRGs growth with different growth factors compared to control. Axonal fibers were stained with β-tubulin (marker for axons cytoskeleton). (a) Without any growth factor less number of axons sprouted from the explants and the axonal fibers were shorter compared to when they were treated with pleiotrophic factor (b) or neurotrophic factors (c and d)

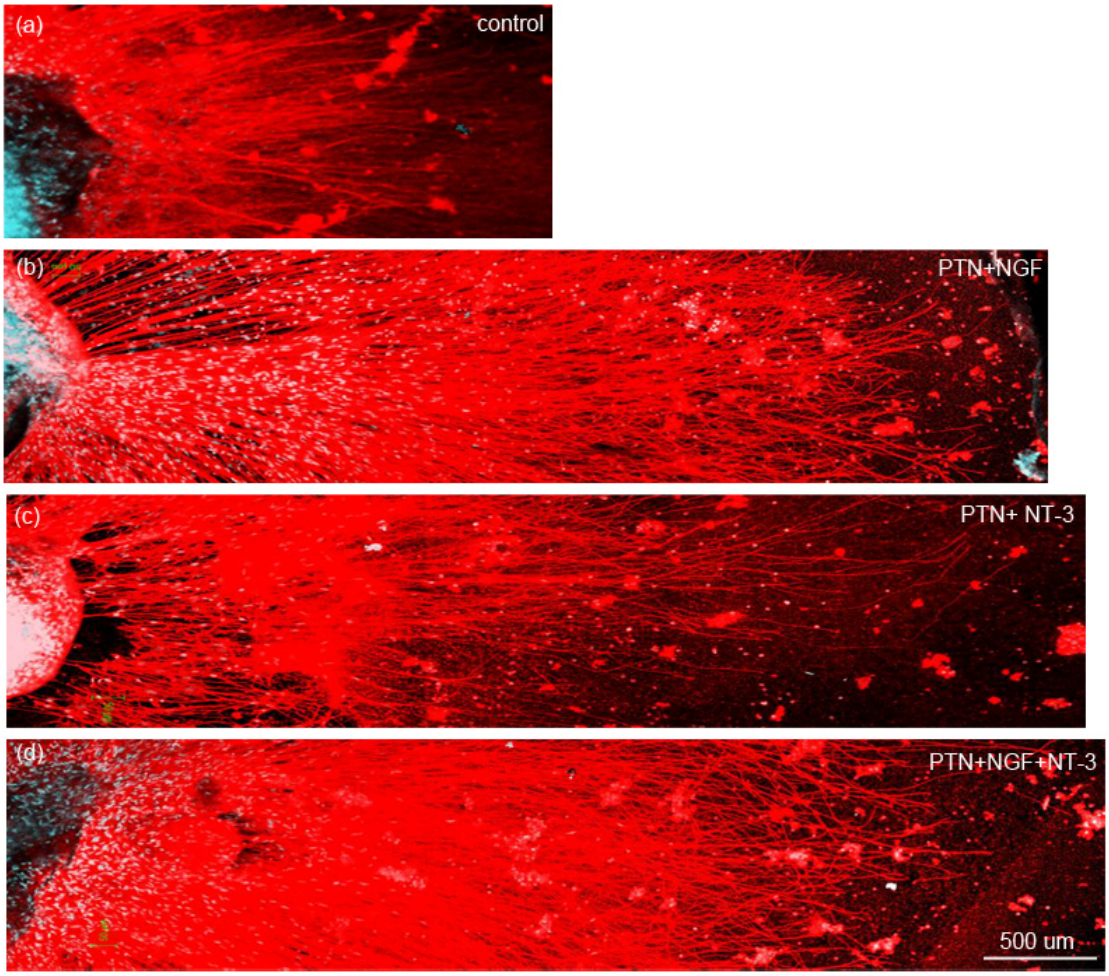

Figure A.2 Visualization of the DRGs growth with different combination of pleiotrophic factor with neurotrophic factors. Axonal fibers were stained with β-tubulin (marker for axons cytoskeleton). (a) Without any growth factor less number of axons sprouted from the explants and the axonal fibers were shorter compared to (b) PTN+NGF and (c) PTN+NT-3 and (c) PTN+NGF+NT-3

Combined growth factors resulted in increased axons density and glial migration.

The efficacy of growth factors, alone or in combination, were assessed by comparing their effects on DRGs. The number of axons projecting out of the explants treated with a single neurotrophic factor (NGF or NT-3) or pleiotrophic factor (PTN) is 8 times more than control (no growth factor). PTN+NGF+GDNF combination had the most projecting axons. The number of projections was two times more in PTN+NGF and PTN+NT-3. This was at least 3 times more

when explants were treated with PTN+NGF+NT-3 compared to when they were only treated with one of the growth factors.

Average of the distance travelled by glial cells was significantly higher (almost 5 times) in the PTN+NGF group compared to control (no treatment). This number was higher in the other experimental groups (PTN+NT-3 or PTN+NT-3+NGF). However, PTN+NGF had the highest number among all the experimental groups.

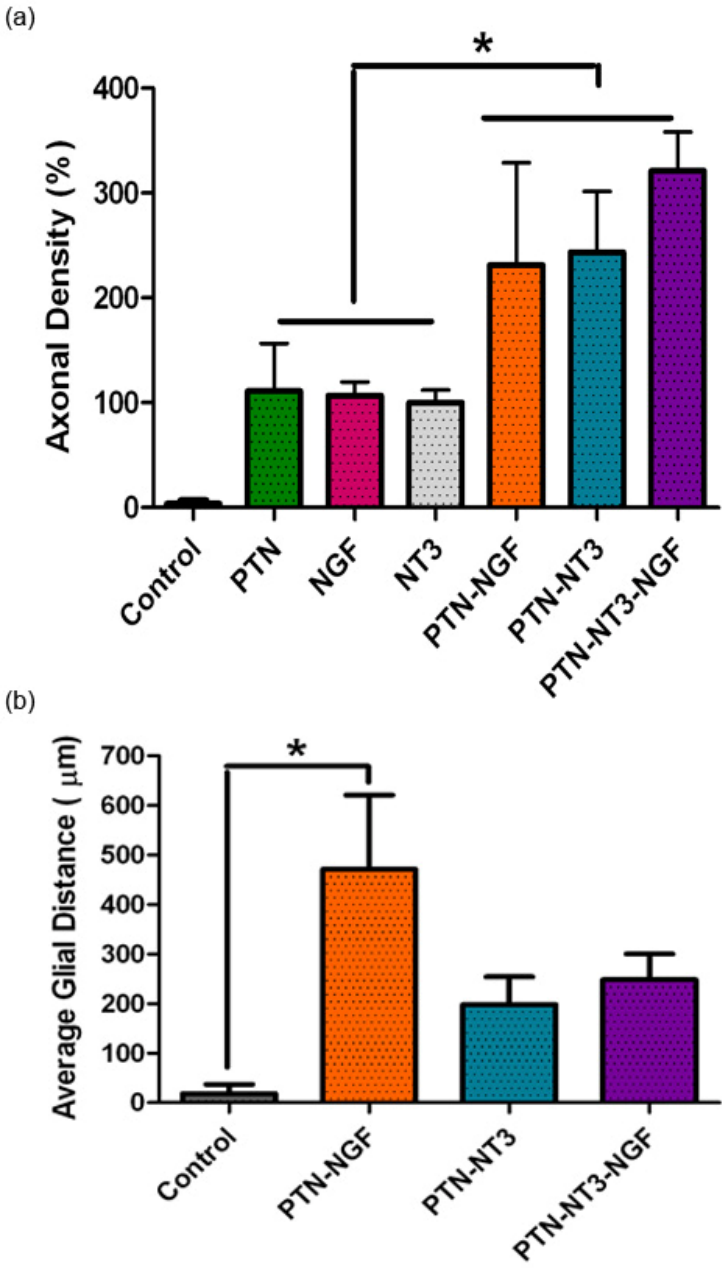

Figure A.3 Quantitative analysis of the (a) axonal density and (b) average of the distance that glial cells travelled out of the explants showed that all the combinatorial groups enticed more axons out of the explants compared to control ($p<0.05$; $n=4$-6). PTN+NGF had more number of glial cells farther from the explants.

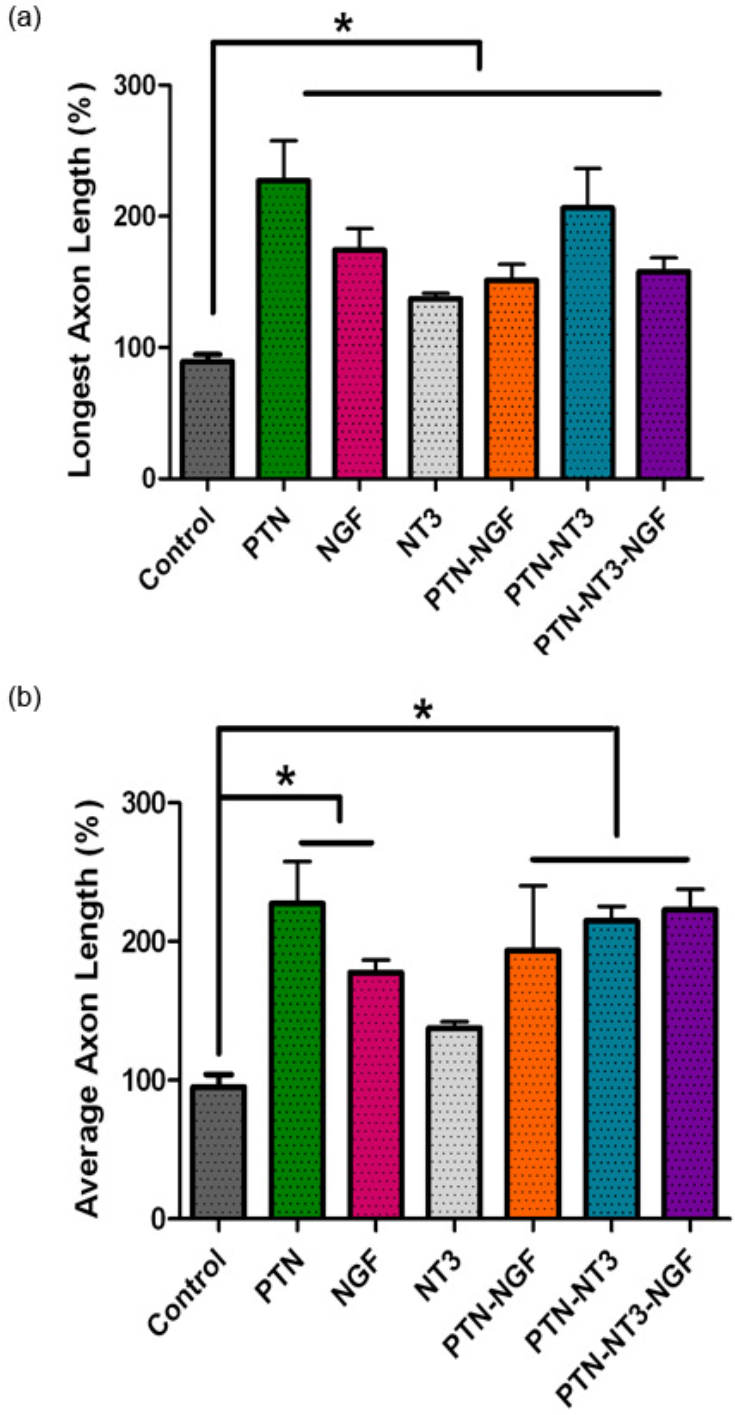

Figure A.4 Quantitative analysis of the (a) longest axonal length and (b) average of the axonal length showed that all the experimental groups had longer axons compared to control ($p<0.05$; $n=4$-6). PTN had the longest axons among the single growth factor experiment. There was not a significant difference between the combinatorial groups.

Combined growth factors had no effect on axon length

The trend that a combination of growth factors is more effective is reversed when the average length of projecting axons are investigated. It was found that NGF alone had the longest axons, followed by BDNF, GDNF, and NT-3. The axonal length was higher in all the experimental groups compared to control (no treatment). Out of the combinatorial groups investigated the group treated with NT-3 had the lowest effect on axonal length.

Discussion

The data suggests that a combination of growth factors is best for encouraging large number of axons to project out of an explant. PTN and NGF groups enticed the longest axons. This was expected for NGF, since NGF is known as sensory neuron growth factor (Jenq & Coggeshall 1985) and DRG primarily consists of sensory neurons. Our results indicating increase of the axonal length and number in the groups treated with PTN was rather unexpected. PTN is mainly studied as a growth factor being expressed in motor neurons after injury (Mi et al 2007). Although PTN combined with NGF did not give the best result it is still outperformed all lone growth factors. This is promising because PTN is able to act on many different cell types including angiogenesis and is preferable to other nerve growth factor because of this characteristic.

One drawback to using combinations of growth factors to improve regeneration of axon is the slow growth rate. As indicated by the second set of data all axons in lone growth factor media grew much faster than the control or the combination. Within the same time frame the axons immersed in the media with a combination of growth factors were as long as or shorter than the single growth factor. This can potentially increase recovery time in an individual, but the potential benefit of much more axons reaching their target far outweighs is a drawback.

This study indicates that PTN is able to increase the number of regenerating axons. Furthermore, PTN's pleiotrophic properties can encourage other cell types to migrate and differentiate during nerve regeneration, whether through a short or long gap bridge. The most

important property of PTN besides axon regeneration is its' ability to encourage angiogenesis (Chen et al 2009; Li et al 2010). Without adequate irrigation a growing axons will not be able to survive.

The possible application of the combinatorial growth factors has not been studied. Here, we investigated the benefits of the combination of growth factors in axonal growth. Furthermore; we showed the effect of PTN on dorsal root ganglion explants and on sensory neurons. A more thorough investigation of PTN in combination with other growth factor is necessary, since it has never been reported as an effective growth factor on sensory neurons. It is not known if PTN has some specific receptors on sensory neurons or its pleiotrophic effects on other cell types manifests itself as longer and more number of axonal growth. This defines the future direction of this study.

APPENDIX B

VEGF RELEASE IN MULTILUMINAL HYDROGELS DIRECTS ANGIOGENESIS FROM ADULT VASCULATURE *IN VITRO*

Introduction

Microchannels guide the angiogenic vascularization of hydrogel scaffolds

Angiogenesis is a process that involves the migration, proliferation, and differentiation of endothelial cells from preexisting vessels (Hirschi et al 2002). It is well established that angiogenic growth factors promote collateral artery development, in which the median range of new vessel growth is less than 180 μm (Asahara et al 1999). It has been proposed that micropatterning of cells within extracellular matrices can be used to provide control over cellular migration and differentiation from pre-established blood vessels (Shen et al 2008). Indeed, elastomeric microchannels have been used as microfluidic templates to pattern polymers, proteins, and cells (Tan & Desai 2003). However, the cellular patterns defined by microfluidic methods often lose integrity upon removal of the stamp due to cell growth and migration over time (Tan & Desai 2003). Recently, endothelization of filamentous polymeric scaffolds has been proposed as a method for the induction of guided angiogenesis (Gafni et al 2006; Italiano Jr et al 2008; Nasseri et al 2003). While this study underlines the benefit of directing vasculogenesis, the proposed method requires that the polymeric fibers degrade prior to the formation of a vascular lumen.

It is known that aortic tissue contains undifferentiated mesenchymal cells that co-express endothelial and myogenic markers. When embedded in three-dimensional collagen gels, these cells form cohesive cellular cords resembling mature vascular structures (Invernici et al 2007; Zengin et al 2006). In constrained collagen hydrogels, endothelial cells elongate and form vascular tubes with thin wall lumens and show prominent actin stress fibers not seen in floating (unconstrained) hydrogels (Sieminski et al 2004). Despite the efficiency of angiogenesis into constrained ECM, the resulting vessels are often disorganized, leaky and hemorrhagic (Yancopoulos et al 2000).

Multiluminal vascular formation from early postnatal aortic explants

Our lab has demonstrated that multiluminal agarose could be used to entice the migration of endothelial cells into the microchannels. Endothelial cells migrate from both neonatal and adult arotic explants into agarose microchannels with luminal conducive matrix molecules. The cells endothelialize the walls of the microchannels creating a hollow tubular structure. The resulting angiogenic growth is highly stereotypic with observed endothelial tube formation uniformly matching the diameter of the microchannels (i.e., 300 µm). These cells were able to proliferate and differentiate inside the lumens.

We have also demonstrated that angiogenesis can be enticed and guided from existing blood vessels into the agarose microchannels. To test this hypothesis, early postnatal (P4-6) aortic explants were placed perpendicular to the agarose microchannels and allowed it to grow for 6-8 days. During this time, the cultures were taken every other day from the incubator to be evaluated and photographed. As expected, vascular cells migrated radially from the ends of the explants and formed tubular-like structures similar to those seen in 2D. In sharp contrast, cells that migrated into the microchannels, instead of forming such small tubular structures, grew along the walls of the microchannels, eventually forming a monolayer cylinder conforming to the size of the lumen. Visualization at several focal planes revealed that the cells that migrated from the aorta endothelialized the microchannels forming a hollow-tube. We confirmed the hollow nature of the vascular-like structure by embedding the multiluminal gel and obtaining sections subsequently stained with hematoxilin-eosin.

Angiogenic factors such as vascular endothelial growth factor (VEGF) and basic fibroblast growth factor (bFGF) has been shown to stimulate sprouting from pre-existing blood vessels (angiogenesis) (Nillesen et al 2007; Tabata et al 2000), to form *in situ* assembly of capillaries (vasculogenesis) from undifferentiated endothelial cells, and to mediate *in vivo* prevascularization (Cao et al 2005). Despite the angiogenic effect of such factors,

comprehensive vascularization of thick tissues *in vitro* cannot be controlled and lack reproducibility (Ko et al 2007).

It is hypothesized that controlled release of VEGF from polymeric, biodegradable microparticles with a simple and reproducible prevascularization method can induce migration of endothelial cells into a transparent biodegradable multiluminal scaffold used for vascularization.

VEGF is known to stimulate proliferation of vascular endothelial cells *in vitro* and *in vivo* after binding to specific tyrosine kinase receptors (VEGFR1 and VEGFR2) (Frelin et al 2000) and neuropilin-1 co-receptors without enzymatic activity (Soker et al 1998a). Neuropilin contributes to the sum of proangiogenic functions mediated by VEGFR2, and it might also participate in endothelial guidance and vascular patterning (Betsholtz et al 2004). While, time-controlled release of VEGF has already been demonstrated as a mechanism to vascularize tissues(Matsusaki et al 2007; Patel et al 2008; Pike et al 2006), the selective and compartmentalized delivery of growth factors within hydrogel microchannels to prevascularize tissue engineered organs has not been previously reported. We demonstrated that VEGF-containing conduits can be preferentially endothelialized by pre-established blood vessels forming hollow vascular-like structures.

Our laboratory developed a rectangular frame (12.5mm X 36mm) designed for casting agarose gels that can successively be loaded with luminar fillers such as extracellular matrix (ECM) molecules or cells. The casting device was made of plastic and used to guide multiple titanium fibers (0.25 mm X 17 mm; SmallParts, Logansport, IN) through perforations at both ends of the device.

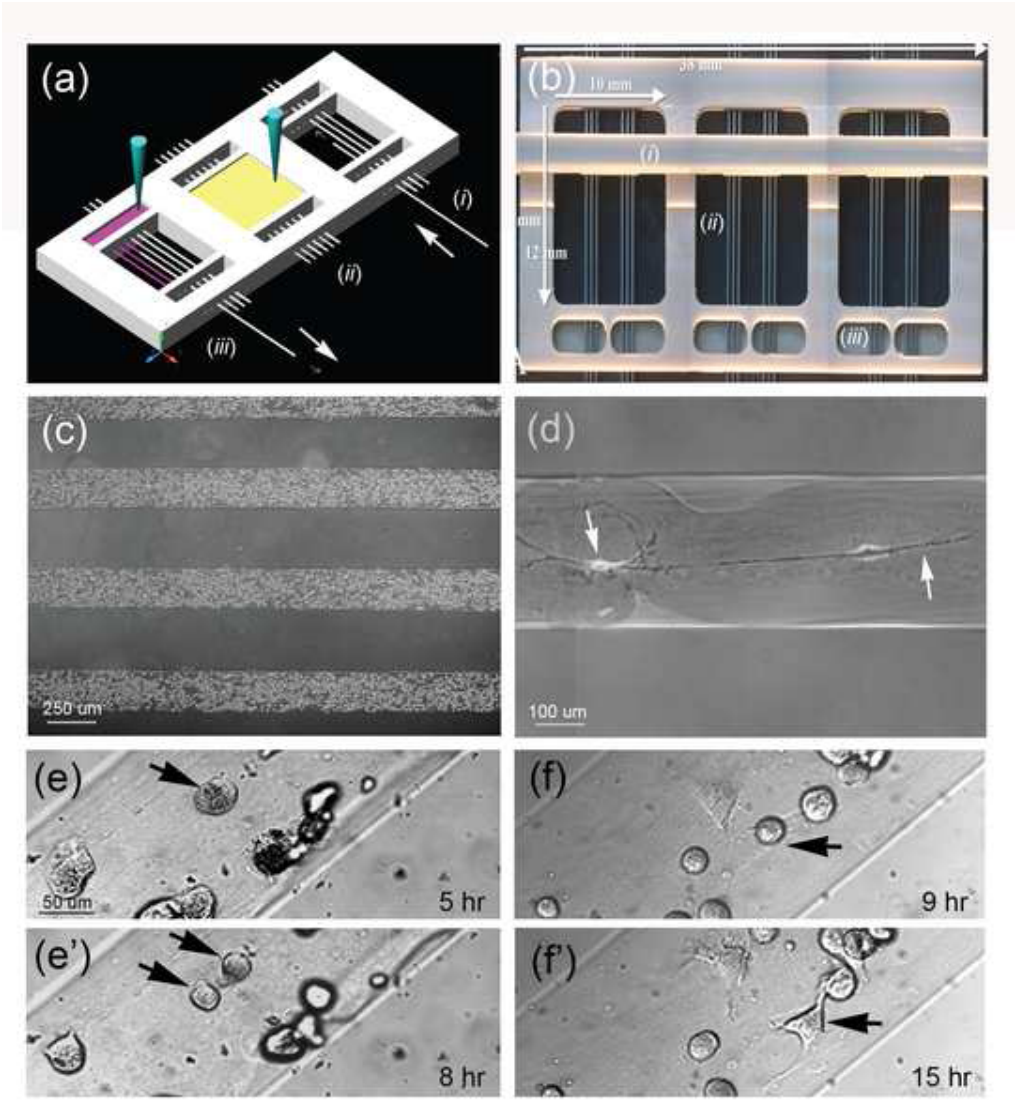

Figure B.1 Multiluminal hydrogels support cell proliferation and differentiation. (a)Schematic of the casting device illustrating the steps in the fabrication of the multiluminal hydrogels: *i)* placement of the fibers into the casting device (left arrow), *ii)*agarose polymerization (yellow), and *iii)* cell seeding and retracting fibers (right arrow).(b) Photograph of the casting device showing: *i)* a comb placed vertically to create a space for aorta explants, *ii)* metal fibers use to cast the microchannels, and *iii)* wells in the scaffold containing the cell suspension. (c) Immediately after seeding, fibroblasts uniformly filled the channels, deployed normal morphology elongated in the channel (d; arrows). Time lapse microscopy demonstrated that cells were able to proliferate (arrows in e and e') and differentiate (arrows in f and f')in the microchannel.

Under sterile conditions, the casting device was placed over a glass slide and a 1.5% ultrapure agarose (Sigma-Aldrich, St. Louis, MO) solution was applied to cover the fibers and allowed to polymerize. Collagen IV (1mg/ml; Chemicon International, Temecula, CA) was paced on the loading well. The negative pressure generated during removal of the titanium fibers from the solidified gel, drew the collagen into the lumen of the casted hydrogel microchannels.

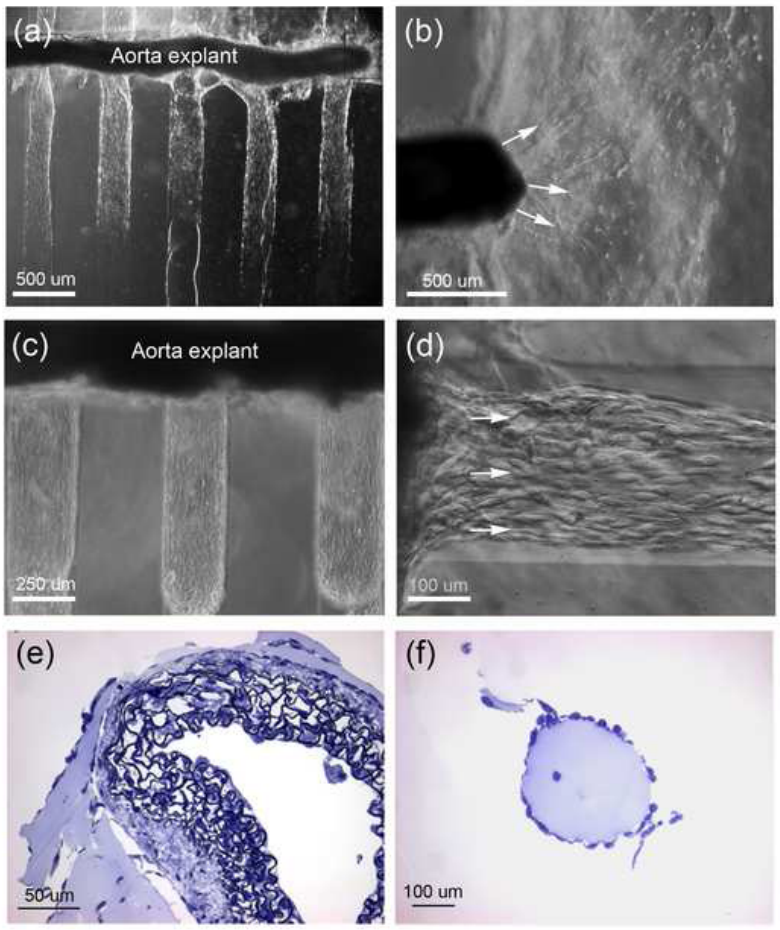

Figure B.2 Guided angiogesis from neonatal aorta explants. Cellular migration from P4-6 aorta explants into the multiluminal hydrogel 8 d after culture (a). Higher magnification of the squared area (a) shows radial migration of the vascular cells from the end of the tissue (b). The aortic cells were observed to migrate, proliferated and eventually formeda monolayer cylindrical structure conforming to the shape and size of the microchannels(c and d). Transverse sections stained with H&E revealed that cells migrating from the aortic explants (e) formed a hollow tube (f).

Whether encapsulated VEGF or BSA in PLGA microparticles would induce vasculogenesis was tested. The cells were incubated in endothelial cell growth media (EGM-2, Lonza, Allendale, NJ) for 4-6 days inside a humidified chamber at 5% CO_2. All the experiments were evaluated by immunocytochemistry at 6-8d of culture.

Material and Methods

Aorta explants

Thoracic aortas were harvested under sterile conditions from deeply anaesthetized neonate (postnatal day 4-6) or adult mice (CharlesRivers, Wilmington, MA) in cold Hank's balanced saline solution (HBSS; Hyclone,Waltham, MA) supplemented with 1% penicillin/streptomycin and cleaned of blood and periadventitial tissue. Five millimeter aorta segments were then embedded in ECM (adults) and placed in a well casted in the agarose gel perpendicular to the microchannels. To accommodate the aorta explants, a detachable 2 mm wide comb device containing perforations aligned with those in the scaffold casting device was manufactured. The fibers were then guided through the perforations in the detachable comb and the casting device, thus holding the comb. Subsequent to agarose polymerization, 17.5 ng / ml of the VEGF microparticles were mixed with ECM and they were pushed inside the lumen when the titanium fibers were removed in all cultures to make the microchannels.

PLGA-VEFG microparticle release

Polylactic-co-glycolic acid (PLGA) microparticles were synthesized using the double emulsion (waterin-oil-in-water) evaporation method. PLGA (Lakeshore Biomaterials, Birmingham, AL) was dissolved in dichloromethane (DCM; Sigma–Aldrich, St. Louis, MO) at a concentration of 200 mg/mL; mixed with aqueous solutions of VEGF (5 mg/mL; Invitrogen, Carlsbad, CA) or BSA (20 mg/mL; Sigma–Aldrich, St. Louis, MO), and sonicated. This solution was then added to polyvinyl alcohol. The mixture was stirred to evaporate the DCM and centrifuged at 4000 rpm for 15 min to pellet the particles. The particles were resuspended in 10

mL PBS and freeze dried for storage. The morphology of the particles was evaluated using a scanning electron microscope (Hitachi S-3000N Variable Pressure SEM), and the size distribution was ascertained with the particle size analyzer (Zeta Pals, Zeta Potential Analyzer).

The loading efficiency of 1 mg of PLGA-VEGF microparticles were calculated to be 66.67 ± 5% by subtracting total amount of applied VEGF from the amount measured by ELISA (Invitrogen, Carlsbad, CA) in the supernatant. VEGF release in PBS was evaluated at 37℃ in a shaker incubator at several time points (1, 2, 4, 8, 24, 38, 96 hrs, and weekly thereafter for 4 weeks). PLGA microparticles-loaded with BSA were used as controls (see General Methods) and their release measured by standard protein assay methods (BCA Assay, Thermo Scientific, Rockford, IL) and 562 nm spectrophotometry.

Staining and visualization

For visualization of vascular formation in the microchannels the gels were fixed in 4% paraformaldehyde (PFA) and processed for immunefluorescence. After rinsing the gels with a blocking solution (0.1% Triton-PBS/ 1% normal serum), the samples were incubated with primary antibodies specific for the CD31/PECAM-1 (1:200; Invitrogen, Carlsbad, CA) was achieved by incubation with Cy2- and Cy3-conjugated secondary antibodies (1:400; R&D Systems, Minneapolis, MN). Counter stains Oregon Green Phalloidin and TO-PRO 3 Iodide (Invitrogen, Carlsbad, CA) were used as cytoskeletal and nuclear labels, respectively. The staining was evaluated using a Zeiss confocal microscope (Zeiss Axioplan 2 LSM 510 META).

Image analysis and quantification

The staining was evaluated and analyzed using regular and fluorescent microscopy and z-stack 3D image reconstruction of the microvascular network in the multi-luminal hydrogels. Quantification of the number of cells and area of tubule formation inside the microchannels in the BSA and VEGF treated groups was achieved using the Axiovision LE software (CarlZeiss, Axiocam, version 4.7.2) and Zeiss LSM Image Browser (version 4.2.0.12).

Time progressive studies

Time-lapse microscopy was performed using a Zeiss Pascal Microscope enclosed in an incubation chamber that maintains the cell culture at 37^{o}C and 5 % CO_2. Images were taken every 10 minutes using DIC for 24 hours to observe cells behavior inside the channels.

Statistical analysis

All data values were expressed as mean ± standard error of the mean. The data was analyzed by parametric student t-test or by non-parametric student-t test followed by Mann Whitney post hoc evaluation using the Prism 4 software (GraphPad Software Inc.). Values with $p \leq 0.05$ were considered to be statistically significant.

Results

VEGF increase angiogenesis into agarose multiluminal scaffolds from postnatal aortic explants

The robust angiogenic growth observed from the neonatal aortic explants was due in part by the VEGF in the media. To determine if angiogenesis could be supported from the young aortic explants in the absence of VEGF, the endothelialization of microchannels in aortic cultures in the presence and absence of VEGF was compared. While VEGF-supplemented P4-6 aortic explants showed a substantial number of cells inside the microchannels (390 ± 57; n= 19), those lacking growth factor support recruited significantly fewer cells (212 ± 48; n= 10). These results suggested to us the possibility of controlling the vascular growth in multiluminal hydrogels by compartmentalizing the delivery VEGF into specific microchannels.

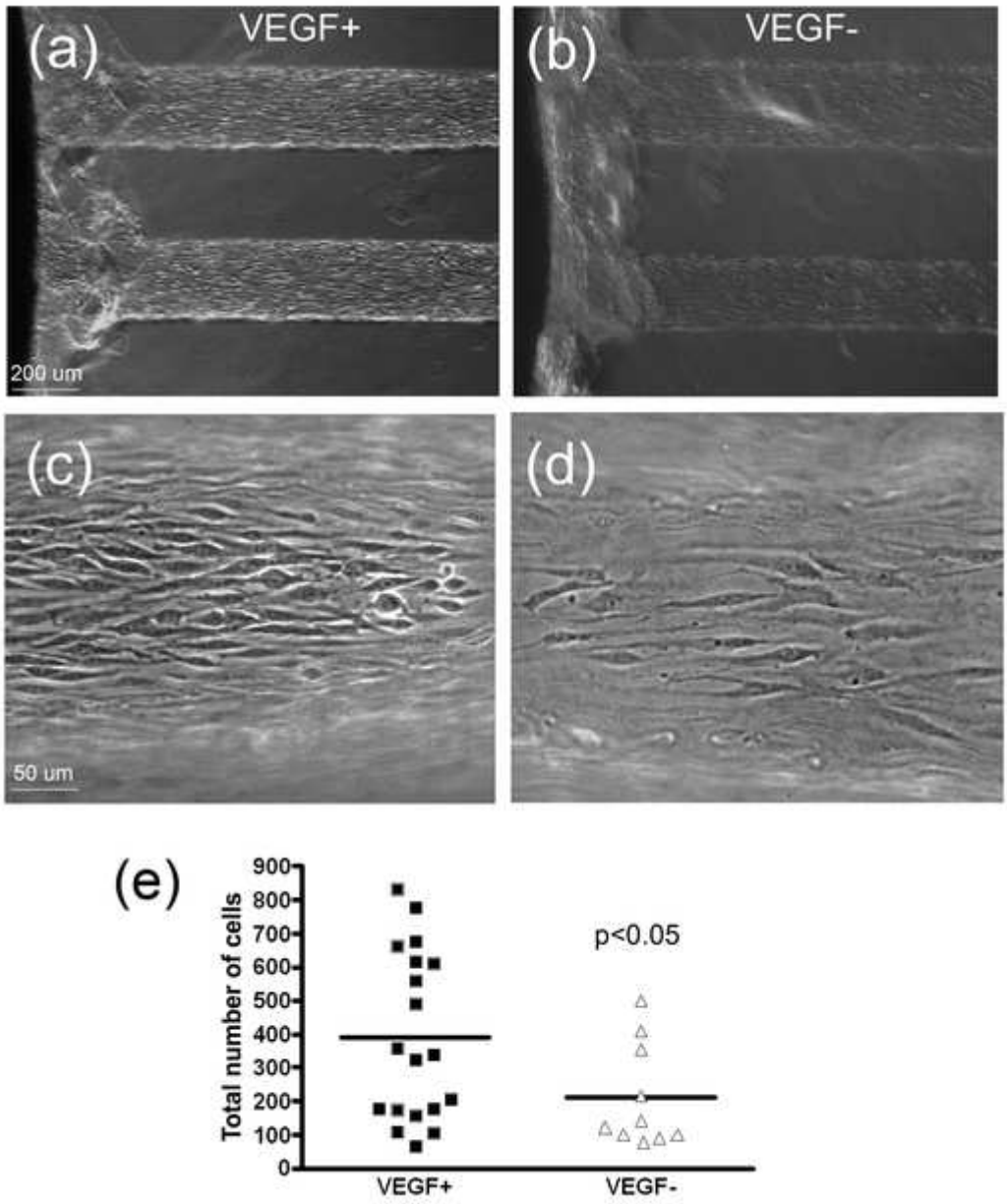

Figure B.3 Enhancement of implant vascularization by VEGF. VEGF-supplemented P4-6 aorta explants contained larger number of cells in the microchannels (a and c) compared to those lacking the growth factor (b and d). Quantitative analysis of individual nuclei (DAPI-positive), confirmed a significant difference ($p < 0.05$) between the total number of cells per microchannel in VEGF+ (n=17) and VEGF- groups (n=8)(e).

Controlled adult angiogenesis by discrete VEFG release

After confirming the enticement of neonatal angiogenesis into multiluminal hydrogel we wonder whether angiogenesis can be a) enticed from adult aorta explants and whether this process can be controlled in individual microchannels. Using aorta explants from 60-90 day mice we were able to demonstrate that, similarly to neonate tissue, angiogenesis can be enticed from adult vasculature.

We then prepared PLGA-VEGF microparticles (0.66 µm mean diameter) and deployed them into selected microchannels to ascertain whether local and controlled release of VEGF can be used to achieve selective growth of endothelial cells. *In-vitro* release kinetic studies with ELISA, revealed a two phase VEGF release pattern from the microparticles; an initial burst phase within the first 3 days, followed by a sustained release over 28 days. To confirm that BSA and VEGF were compartmentalized (i.e., no cross diffusion of fluorescence), PLGA-Cy2-labeled IgG fluorescent microparticles (Cy2), and PLGA-BSA microparticles (negative control) were loaded into adjacent channels, and the diffusion of fluorescence over time (1, 3 and 15 days) was quantified using optical densitometry. Our results demonstrate minimal fluorescence detected in the PLGA-BSA channel over time.

We then investigate whether endothelial cells from adult aorta explants can be differentially guided into microchannels loaded with PLGA-VEGF particles compared to those containing PLGA-BSA. After 15 days in culture, we observed that the number of cells migrating into the microchannels was minimal in those containing BSA microparticles, and that the number was significantly increased in channels in which VEFG was selectively released via microparticles (3.5 ng/day). Quantification of the number of endothelial cells inside the VEGF containing microchannels (258 ± 34) revealed a ten-fold increase ($p= 0.001$) compared to those with BSA eluting microspheres (29 ± 8). The average area of tubule formation in the channels

with VEGF particles (73 ±8 μm^2) was also significantly higher (p = 0.001) than those with BSA (11 ± 4μm^2).

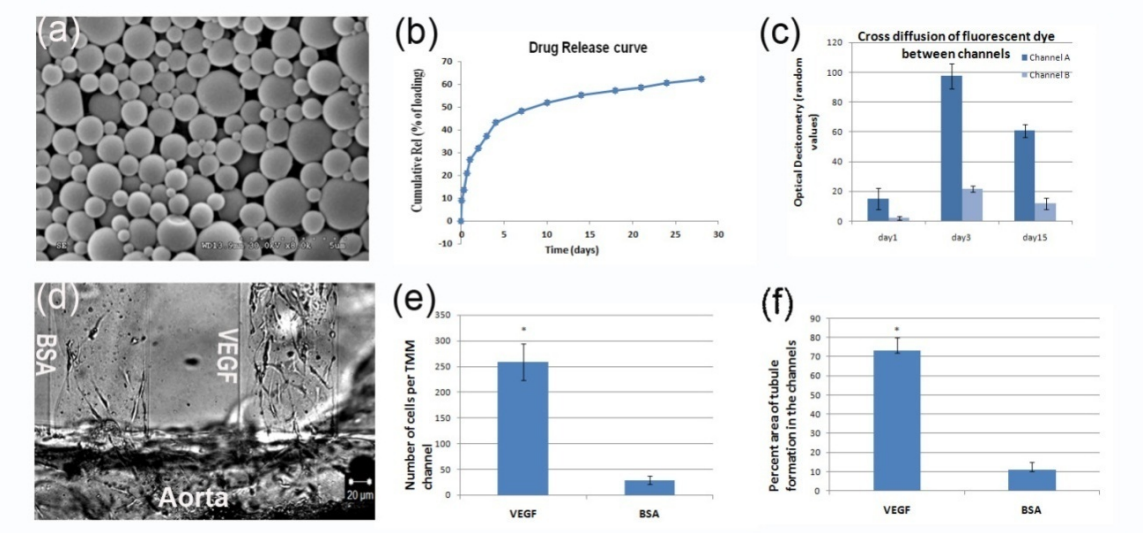

Figure B.4 Controlled release of VEGF induces angiogenesis in adult aortic explants.(a) SEM picture showing morphology of VEGF-encapsulated PLGA microspheres. The particles had a smooth surface and were uniformly dispersed. (b) Continued released of VEGF *In vitro* was confirmed from the PLGA microparticles using ELISA (mean ± SD;n=4). (c) Fluorescent density was measured and compared in different areas over time when one of the channels was loaded with PLGA-Cy2 microspheres and the other one was loaded with PLGA-BSA microspheres. (d) Microchannels with luminal VEGF microspheres specifically increased the number of endothelial cells in those channels compared to those supplemented with BSA as control 7 days after implantation. (e, f)Image analysis quantification showed that number of cells and the distance travelled per microchannel were significantly higher in VEGF treated groups than the control BSA group (n = 8 per group; * = p< 0.001).

Together, this data provides evidence that vascular growth can be enticed and controlled within three-dimensional biodegradable matrices, and supports the notion that angiogenic vascularization from either neonate or adult preexisting blood vessels can be stimulated by intraluminal VEGF. This strategy may offer a viable alternative for the formation of vascular structures within thick bioengineered tissues, prior to grafting.

Discussion

Our lab developed a simple and reproducible vascularization method that integrates a transparent biodegradable multiluminal scaffold for guided endothelial migration stimulated by

intraluminal controlled release of Vascular Endothelial Growth Factor (VEGF). This study demonstrated that VEGF can be loaded in PLGA microparticles and into the lumen of the agarose microchannels, from where it can direct endothelial cell migration.

Selective Angiogenesis within 3D hydrogel scaffolds

Our study demonstrated that VEGF can be used to supplement the luminal collagen matrix in selected microchannels, thus providing a method to induce the migration of angiogenic cells and the formation of new vascular structures selectively.

Since it has been demonstrated that the formation of vascular-like structures *in vitro* can subsequently connect to the host vascular system after implantation (Hochberg et al 2006), methods that allowed selective and guided angiogenesis could be of value in engineering a vascular network within separate compartments of those occupied by other structural cells needed for bioengineered organs. This argument is supported by recent reports demonstrating that prevascularization of a particular artificial skin construct was able to form healthy anastomosis with the host vascular system within four days, whereas *de novo* vascularization of a non-prevascularized graft took as long as 14 days after implantation (Hochberg et al 2006; Priya et al 2008). By extension, the method reported here might be used to decrease the time that is needed to vascularize thick bioengineered organs, as host vessels are not required to grow into the entire implant, but only into its outer regions to meet the preformed vascular network.

Vascularization of hydrogel scaffolds

Improved vascularization of bioengineered tissues is essential to promote implant survival of tissue-engineered organs, such as heart, lungs and liver. Current methods for tissue neovascularization, either through *in situ* assemblies of capillaries from undifferentiated endothelial cells, or through the sprouting of capillaries from pre-existing blood vessels, offer partial or insufficient control of vascular formation within the implant.

The formation of new blood vessels requires the interplay of cells, soluble growth factors, cytokines and extracellular matrix (Au et al 2007; Frelin et al 2000; Rouwkema et al 2008). It is known that endothelial progenitor cells alone do not form viable vascular tissues, but when co-seeded, vascular tubes are able to grow into the porous architecture of PGA-PLLA scaffolds(Echeverria Victoria1 & Hayes1 2008; Wu et al 2004). Despite this ability, the random nature of the scaffold's porosity limits its use. Here, we demonstrated that multi-luminal gelatinous matrices can be used to linearly guide the growth of vascular endothelial cells in specified channels where cell attachment, differentiation, and proliferation inside the channels can be dynamically ascertained *in vitro*.

Engineered organs with relatively thin and/or avascular structures (i.e., skin and cartilage) have been successfully developed for clinical use (Kopp et al 2004; Moon et al 2008; Moon & West 2008; Priya et al 2008; Roberts et al 2008). By extension, larger bioengineered organs such as kidney, liver, heart and lung bear the promise of alleviating the shortage of transplantable organs (Vacanti 2006). However, tissue engineering of thick organs presents critical challenges yet to be resolved, such as their complex tridimensional heterogeneous cellular structure, and the need to establish immediate perfusion by the host vascular network to support implant survival (Ko et al 2007). While recent progress in the development of microvascular networks *in vitro* has demonstrated the possibility of generating prevascularized bioengineered organs (Norotte et al 2009), the infiltration of surrounding vessels and the formation of anastomosis with the host vasculature is known to require days to weeks, leading to ischemia and implant failure (Clark & Clark 1939).

Limitations

It is acknowledged that functional vascularization might not be fully achieved *in vitro* and that the incorporation of fluid biomechanical forces is necessary to fully test this possibility. Future experiments will test whether the vascular structures that are formed *in vitro*, can form

functional blood vessels *in vivo*. Furthermore, although the delivery of angiogenic growth factors generally results in increased angiogenesis, the resulting vessels are often disorganized, leaky and hemorrhagic (Yancopoulos et al 2000). It has been reported that other growth factors are needed for the stabilization of new vessels including platelet-derived growth factor (PDGF) for the recruitment of smooth muscle cells and pericytes, as well as transforming growth factor β and angiopoietin 1, for the production of extracellular matrix and the correct interaction between endothelial cells and mural cells (Hirschi et al 1999).

While this study demonstrates that angiogenesis can be directed within specific hydrogel microchannels, further studies are necessary in order to test whether a combination of various growth factors or temporal exposure to other growth factors would enhance the stabilization of the bioengineered vasculature, and whether formed vasculature can sustain mechanical stimulation regimes, such as cyclical radial distension and/or shear stress, in a bioreactor (Dahl et al 2007; Iwasaki et al 2008; Konig et al 2009).

In contrast to the current technology available, the flexibility in the present design allows for the possibility of culturing multiple cell types in both a temporally and spatially controlled manner. This, in turn, allows the possibility of designing multi-cellular bioartificial organs in which some channels are used to seed specific cell subtypes of a particular organ while others are dedicated for prevascularization. Microchannel vascularization might be particularly suited for peripheral nerve long gap regeneration. Devoting specific channels exclusively to blood vessels via a method analogous to that used in this study, may allow multi-luminal nerve grafts to induce nerve regeneration across longer gaps than previously reported (Bender et al 2004; Chen et al 2006a; Chen et al 2006b; de Ruiter et al 2008). The benefit of using VEGF to entice nerve regeneration has already been demonstrated (Zachary 2005) , but its application in prevascularization of a bioengineered nerve graft is an area requiring further study.

REFERENCES

Adelson PD, Bonaroti EA, Thompson TP, Tran M, Nystrom NA. 2004. End-to-side neurorrhaphies in a rodent model of peripheral nerve injury: a preliminary report of a novel technique. *J Neurosurg* 101:78-84

Airaksinen MS, Titievsky A, Saarma M. 1999. GDNF family neurotrophic factor signaling: four masters, one servant? *Mol Cell Neurosci* 13:313-25

Arvidsson J, Johansson K. 1988. Changes in the central projection pattern of vibrissae innervating primary sensory neurons after peripheral nerve injury in the rat. *Neurosci Lett* 84:120-4

Asahara T, Takahashi T, Masuda H, Kalka C, Chen D, et al. 1999. VEGF contributes to postnatal neovascularization by mobilizing bone marrow-derived endothelial progenitor cells. *Embo J* 18:3964-72

Au P, Tam J, Fukumura D, Jain RK. 2007. Small blood vessel engineering. *Methods Mol Med* 140:183-95

Averill S, McMahon SB, Clary DO, Reichardt LF, Priestley JV. 1995. Immunocytochemical localization of trkA receptors in chemically identified subgroups of adult rat sensory neurons. *Eur J Neurosci* 7:1484-94

Baloh RH, Enomoto H, Johnson EM, Jr., Milbrandt J. 2000. The GDNF family ligands and receptors - implications for neural development. *Curr Opin Neurobiol* 10:103-10

Belmin J, Valensi P. 1996. Diabetic neuropathy in elderly patients. What can be done? *Drugs Aging* 8:416-29

Bender M, Bennett J, Waddell R, Doctor J, Marra K. 2004. Multi-channeled biodegradable polymer/CultiSpher composite nerve guides. *Biomaterials* 25:1269-78

Benvenuto A, Raspopovic S, Hoffmann KP, Carpaneto J, Cavallo G, et al. 2010. Intrafascicular thin-film multichannel electrodes for sensory feedback: Evidences on a human amputee. *Conf Proc IEEE Eng Med Biol Soc* 2010:1800-3

Berke B, Keshishian H. 2011. Cracking the combinatorial semaphorin code. *Neuron* 70:175-7

Betsholtz C, Lindblom P, Bjarnegard M, Enge M, Gerhardt H, Lindahl P. 2004. Role of platelet-derived growth factor in mesangium development and vasculopathies: lessons from platelet-derived growth factor and platelet-derived growth factor receptor mutations in mice. *Current opinion in nephrology and hypertension* 13:45

Biran R, Martin DC, Tresco PA. 2005. Neuronal cell loss accompanies the brain tissue response to chronically implanted silicon microelectrode arrays. *Exp Neurol* 195:115-26

Biran R, Martin DC, Tresco PA. 2007. The brain tissue response to implanted silicon microelectrode arrays is increased when the device is tethered to the skull. *J Biomed Mater Res A* 82:169-78

Bloch B, Normand E, Kovesdi I, Bohlen P. 1992. Expression of the HBNF (heparin-binding neurite-promoting factor) gene in the brain of fetal, neonatal and adult rat: an in situ hybridization study. *Brain Res Dev Brain Res* 70:267-78

Bloch J, Fine EG, Bouche N, Zurn AD, Aebischer P. 2001. Nerve growth factor- and neurotrophin-3-releasing guidance channels promote regeneration of the transected rat dorsal root. *Exp Neurol* 172:425-32

Blondet B, Carpentier G, Lafdil F, Courty J. 2005. Pleiotrophin cellular localization in nerve regeneration after peripheral nerve injury. *J Histochem Cytochem* 53:971-7

Bonhoeffer F, Huf J. 1982. In vitro experiments on axon guidance demonstrating an anterior-posterior gradient on the tectum. *EMBO J* 1:427-31

Boyd JG, Gordon T. 2001. The neurotrophin receptors, trkB and p75, differentially regulate motor axonal regeneration. *J Neurobiol* 49:314-25

Boyd JG, Gordon T. 2002. A dose-dependent facilitation and inhibition of peripheral nerve regeneration by brain-derived neurotrophic factor. *Eur J Neurosci* 15:613-26

Boyd JG, Gordon T. 2003a. Glial cell line-derived neurotrophic factor and brain-derived neurotrophic factor sustain the axonal regeneration of chronically axotomized motoneurons in vivo. *Exp Neurol* 183:610-9

Boyd JG, Gordon T. 2003b. Neurotrophic factors and their receptors in axonal regeneration and functional recovery after peripheral nerve injury. *Mol Neurobiol* 27:277-324

Brill N, Polasek K, Oby E, Ethier C, Miller L, Tyler D. 2009. Nerve cuff stimulation and the effect of fascicular organization for hand grasp in nonhuman primates. *Conf Proc IEEE Eng Med Biol Soc* 2009:1557-60

Brown PB, Koerber HR, Millecchia R. 2004. From innervation density to tactile acuity: 1. Spatial representation. *Brain Res* 1011:14-32

Brushart TM. 1991. Central course of digital axons within the median nerve of Macaca mulatta. *J Comp Neurol* 311:197-209

Brushart TM. 1993. Motor axons preferentially reinnervate motor pathways. *J Neurosci* 13:2730-8

Cajal Ry. 1928. Degeneration and regeneration of the nervous system. *2*

Cao X, Shoichet MS. 2001. Defining the concentration gradient of nerve growth factor for guided neurite outgrowth. *Neuroscience* 103:831-40

Cao X, Shoichet MS. 2003. Investigating the synergistic effect of combined neurotrophic factor concentration gradients to guide axonal growth. *Neuroscience* 122:381-9

Cao Y, Sun Z, Liao L, Meng Y, Han Q, Zhao R. 2005. Human adipose tissue-derived stem cells differentiate into endothelial cells in vitro and improve postnatal neovascularization in vivo. *Biochemical and biophysical research communications* 332:370-9

Castro J, Negredo P, Avendano C. 2008. Fiber composition of the rat sciatic nerve and its modification during regeneration through a sieve electrode. *Brain Res* 1190:65-77

Chaldakov G. 2011. The metabotrophic NGF and BDNF: an emerging concept. *Arch Ital Biol* 149:257-63

Chen H, Campbell RA, Chang Y, Li M, Wang CS, et al. 2009. Pleiotrophin produced by multiple myeloma induces transdifferentiation of monocytes into vascular endothelial cells: a novel mechanism of tumor-induced vasculogenesis. *Blood* 113:1992-2002

Chen M, Zhang F, Lineaweaver W. 2006a. Luminal fillers in nerve conduits for peripheral nerve repair. *Annals of plastic surgery* 57:462

Chen MB, Zhang F, Lineaweaver WC. 2006b. Luminal fillers in nerve conduits for peripheral nerve repair. *Ann Plast Surg* 57:462-71

Cheng M, Cao W, Gao Y, Gong Y, Zhao N, Zhang X. 2003. Studies on nerve cell affinity of biodegradable modified chitosan films. *J Biomater Sci Polym Ed* 14:1155-67

Chung EK, Zhang XJ, Xu HX, Sung JJ, Bian ZX. 2007. Visceral hyperalgesia induced by neonatal maternal separation is associated with nerve growth factor-mediated central neuronal plasticity in rat spinal cord. *Neuroscience* 149:685-95

Clark E, Clark E. 1939. Microscopic observations on the growth of blood capillaries in the living mammal. *American Journal of Anatomy* 64:251-301

Curinga G, Smith GM. 2008. Molecular/genetic manipulation of extrinsic axon guidance factors for CNS repair and regeneration. *Exp Neurol* 209:333-42

Dadon-Nachum M, Melamed E, Offen D. 2011. Stem cells treatment for sciatic nerve injury. *Expert Opin Biol Ther* 11:1591-7

Dahl S, Rhim C, Song Y, Niklason L. 2007. Mechanical properties and compositions of tissue engineered and native arteries. *Annals of biomedical engineering* 35:348-55

Dario P, Garzella P, Toro M, Micera S, Alavi M, et al. 1998. Neural interfaces for regenerated nerve stimulation and recording. *IEEE Trans Rehabil Eng* 6:353-63

Dawood A, Lotfi P, Dash S, Kona S, Nguyen K, Romero-Ortega M. 2011. VEGF Release in Multiluminal Hydrogels Directs Angiogenesis from Adult Vasculature <i>In Vitro</i&gt. *Cardiovascular Engineering and Technology* 2:173-85

Dawood L, Dash, Kona, K. T. Nguyen, Romero-Ortega, . 2011. VEGF Release in Multiluminal Hydrogels Directs Angiogenesis

from Adult Vasculature In Vitro. *Cardiovascular Engineering and Technology*

de Ruiter G, Onyeneho I, Liang E, Moore M, Knight A, et al. 2008. Methods for in vitro characterization of multichannel nerve tubes. *Journal of Biomedical Materials Research Part A* 84:643

Deuchar EM. 1970. Diffusion in embryogenesis. *Nature* 225:671

Dhillon GS, Horch KW. 2005. Direct neural sensory feedback and control of a prosthetic arm. *IEEE Trans Neural Syst Rehabil Eng* 13:468-72

Dhillon GS, Lawrence SM, Hutchinson DT, Horch KW. 2004. Residual function in peripheral nerve stumps of amputees: implications for neural control of artificial limbs. *J Hand Surg Am* 29:605-15; discussion 16-8

Dodla MC, Bellamkonda RV. 2006. Anisotropic scaffolds facilitate enhanced neurite extension in vitro. *J Biomed Mater Res A* 78:213-21

Drgas S, Blaszak MA. Perception of speech in reverberant conditions using AM-FM cochlear implant simulation. *Hear Res* 269:162-8

Echeverria Victoria1 TW, Allyson Skoien1, Casey Lamers1, Ivar Meyvantsson1, Andrew Goulter2, Wayne Bowen2,Steven, Hayes1. 2008. A Heterogeneous Angiogenesis Assay using Primary Cell Co-culture in Microchannels

Edell DJ, Churchill JN, Gourley IM. 1982. Biocompatibility of a silicon based peripheral nerve electrode. *Biomater Med Devices Artif Organs* 10:103-22

Edstrom A, Edbladh M, Ekstrom P. 1992. Adenosine inhibition of the regeneration in vitro of adult frog sciatic sensory axons. *Brain Res* 570:35-41

Ernsberger U. 2008. The role of GDNF family ligand signalling in the differentiation of sympathetic and dorsal root ganglion neurons. *Cell Tissue Res* 333:353-71

Fallaux FJ, van der Eb AJ, Hoeben RC. 1999. Who's afraid of replication-competent adenoviruses? *Gene Ther* 6:709-12

Fitzsimmons NA, Drake W, Hanson TL, Lebedev MA, Nicolelis MA. 2007. Primate reaching cued by multichannel spatiotemporal cortical microstimulation. *J Neurosci* 27:5593-602

Flanagan JG. 2006. Neural map specification by gradients. *Curr Opin Neurobiol* 16:59-66

Franz CK, Rutishauser U, Rafuse VF. 2005. Polysialylated neural cell adhesion molecule is necessary for selective targeting of regenerating motor neurons. *J Neurosci* 25:2081-91

Freier T, Koh HS, Kazazian K, Shoichet MS. 2005. Controlling cell adhesion and degradation of chitosan films by N-acetylation. *Biomaterials* 26:5872-8

Frelin C, Ladoux A, D'Angelo G. 2000. Vascular endothelial growth factors and angiogenesis. *Ann Endocrinol (Paris)* 61:70-4

Friedman WJ, Greene LA. 1999. Neurotrophin signaling via Trks and p75. *Exp Cell Res* 253:131-42

Fu SY, Gordon T. 1997. The cellular and molecular basis of peripheral nerve regeneration. *Mol Neurobiol* 14:67-116

Gafni Y, Zilberman Y, Ophir Z, Abramovitch R, Jaffe M, et al. 2006. Design of a filamentous polymeric scaffold for in vivo guided angiogenesis. *Tissue Eng* 12:3021-34

Gallarda BW, Bonanomi D, Muller D, Brown A, Alaynick WA, et al. 2008. Segregation of axial motor and sensory pathways via heterotypic trans-axonal signaling. *Science* 320:233-6

Garde K. 2008. *Regenerative Peripheral Neurointerfacing of Upper Exterimity Prostheses*. University of Texas at Arlington. 108 pp.
Garde K, Keefer E, Botterman B, Galvan P, Romero MI. 2009. Early interfaced neural activity from chronic amputated nerves. *Front Neuroengineering* 2:5
Gaunt RA, Hokanson JA, Weber DJ. 2009. Microstimulation of primary afferent neurons in the L7 dorsal root ganglia using multielectrode arrays in anesthetized cats: thresholds and recruitment properties. *J Neural Eng* 6:55009
Gavazzi I, Kumar RD, McMahon SB, Cohen J. 1999. Growth responses of different subpopulations of adult sensory neurons to neurotrophic factors in vitro. *Eur J Neurosci* 11:3405-14
Gierer A. 1981. Some physical, mathematical and evolutionary aspects of biological pattern formation. *Philos Trans R Soc Lond B Biol Sci* 295:429-40
Ginsberg HS. 1996. The ups and downs of adenovirus vectors. *Bull N Y Acad Med* 73:53-8
Goldstein ME, House SB, Gainer H. 1991. NF-L and peripherin immunoreactivities define distinct classes of rat sensory ganglion cells. *J Neurosci Res* 30:92-104
Gomez N, Schmidt CE. 2007. Nerve growth factor-immobilized polypyrrole: bioactive electrically conducting polymer for enhanced neurite extension. *J Biomed Mater Res A* 81:135-49
Goodman CS. 1996. Mechanisms and molecules that control growth cone guidance. *Annu Rev Neurosci* 19:341-77
Gotz R, Koster R, Winkler C, Raulf F, Lottspeich F, et al. 1994. Neurotrophin-6 is a new member of the nerve growth factor family. *Nature* 372:266-9
Green RA, Lovell NH, Poole-Warren LA. 2009. Impact of co-incorporating laminin peptide dopants and neurotrophic growth factors on conducting polymer properties. *Acta Biomater*
Grill WM, Norman SE, Bellamkonda RV. 2009. Implanted neural interfaces: biochallenges and engineered solutions. *Annu Rev Biomed Eng* 11:1-24
Haipeng G, Yinghui Z, Jianchun L, Yandao G, Nanming Z, Xiufang Z. 2000. Studies on nerve cell affinity of chitosan-derived materials. *J Biomed Mater Res* 52:285-95
Hale NA, Yang Y, Rajagopalan P. 2010. Cell migration at the interface of a dual chemical-mechanical gradient. *ACS Appl Mater Interfaces* 2:2317-24
Hari A, Djohar B, Skutella T, Montazeri S. 2004. Neurotrophins and extracellular matrix molecules modulate sensory axon outgrowth. *Int J Dev Neurosci* 22:113-7
Harper AA, Lawson SN. 1985. Conduction velocity is related to morphological cell type in rat dorsal root ganglion neurones. *J Physiol* 359:31-46
Henderson CE, Camu W, Mettling C, Gouin A, Poulsen K, et al. 1993. Neurotrophins promote motor neuron survival and are present in embryonic limb bud. *Nature* 363:266-70
Henderson CE, Phillips HS, Pollock RA, Davies AM, Lemeulle C, et al. 1994. GDNF: a potent survival factor for motoneurons present in peripheral nerve and muscle. *Science* 266:1062-4
Hirschi K, Rohovsky S, Beck L, Smith S, D'Amore P. 1999. Endothelial cells modulate the proliferation of mural cell precursors via platelet-derived growth factor-BB and heterotypic cell contact. *Circulation research* 84:298
Hirschi KK, Skalak TC, Peirce SM, Little CD. 2002. Vascular assembly in natural and engineered tissues. *Ann N Y Acad Sci* 961:223-42
Ho C, O'Leary ME. 2011. Single-cell analysis of sodium channel expression in dorsal root ganglion neurons. *Mol Cell Neurosci* 46:159-66
Hochberg LR, Serruya MD, Friehs GM, Mukand JA, Saleh M, et al. 2006. Neuronal ensemble control of prosthetic devices by a human with tetraplegia. *Nature* 442:164-71
Hoke A, Redett R, Hameed H, Jari R, Zhou C, et al. 2006. Schwann cells express motor and sensory phenotypes that regulate axon regeneration. *J Neurosci* 26:9646-55

Hu X, Cai J, Yang J, Smith GM. 2010. Sensory axon targeting is increased by NGF gene therapy within the lesioned adult femoral nerve. *Exp Neurol* 223:153-65

Ilag LL, Lonnerberg P, Persson H, Ibanez CF. 1994. Role of variable beta-hairpin loop in determining biological specificities in neurotrophin family. *J Biol Chem* 269:19941-6

Invernici G, Emanueli C, Madeddu P, Cristini S, Gadau S, et al. 2007. Human fetal aorta contains vascular progenitor cells capable of inducing vasculogenesis, angiogenesis, and myogenesis in vitro and in a murine model of peripheral ischemia. *Am J Pathol* 170:1879-92

Italiano Jr J, Richardson J, Patel-Hett S, Battinelli E, Zaslavsky A, et al. 2008. Angiogenesis is regulated by a novel mechanism: pro-and antiangiogenic proteins are organized into separate platelet {alpha} granules and differentially released. *Blood* 111:1227

Iwasaki K, Kojima K, Kodama S, Paz A, Chambers M, et al. 2008. Bioengineered three-layered robust and elastic artery using hemodynamically-equivalent pulsatile bioreactor. *Circulation* 118:S52

Jelsma TN, Aguayo AJ. 1994. Trophic factors. *Curr Opin Neurobiol* 4:717-25

Jeng CL, Torrillo TM, Rosenblatt MA. 2010. Complications of peripheral nerve blocks. *Br J Anaesth* 105 Suppl 1:i97-107

Jenq CB, Coggeshall RE. 1985. Long-term patterns of axon regeneration in the sciatic nerve and its tributaries. *Brain Res* 345:34-44

Jin L, Jianghai C, Juan L, Hao K. 2009. Pleiotrophin and peripheral nerve injury. *Neurosurg Rev* 32:387-93

Josephson A, Widenfalk J, Trifunovski A, Widmer HR, Olson L, Spenger C. 2001. GDNF and NGF family members and receptors in human fetal and adult spinal cord and dorsal root ganglia. *J Comp Neurol* 440:204-17

Jubran M, Widenfalk J. 2003. Repair of peripheral nerve transections with fibrin sealant containing neurotrophic factors. *Exp Neurol* 181:204-12

Jun SB, Hynd MR, Dowell-Mesfin NM, Al-Kofahi Y, Roysam B, et al. 2008. Modulation of cultured neural networks using neurotrophin release from hydrogel-coated microelectrode arrays. *J Neural Eng* 5:203-13

Juttner R, Rathjen FG. 2005. Molecular analysis of axonal target specificity and synapse formation. *Cell Mol Life Sci* 62:2811-27

Kimpinski K, Campenot RB, Mearow K. 1997. Effects of the neurotrophins nerve growth factor, neurotrophin-3, and brain-derived neurotrophic factor (BDNF) on neurite growth from adult sensory neurons in compartmented cultures. *J Neurobiol* 33:395-410

Klinge PM, Vafa MA, Brinker T, Brandis A, Walter GF, et al. 2001. Immunohistochemical characterization of axonal sprouting and reactive tissue changes after long-term implantation of a polyimide sieve electrode to the transected adult rat sciatic nerve. *Biomaterials* 22:2333-43

Ko HC, Milthorpe BK, McFarland CD. 2007. Engineering thick tissues--the vascularisation problem. *Eur Cell Mater* 14:1-18; discussion -9

Koliatsos VE, Clatterbuck RE, Winslow JW, Cayouette MH, Price DL. 1993. Evidence that brain-derived neurotrophic factor is a trophic factor for motor neurons in vivo. *Neuron* 10:359-67

Kolodkin AL, Tessier-Lavigne M. 2011. Mechanisms and molecules of neuronal wiring: a primer. *Cold Spring Harb Perspect Biol* 3

Kong Q, Majeska RJ, Vazquez M. 2011. Migration of connective tissue-derived cells is mediated by ultra-low concentration gradient fields of EGF. *Exp Cell Res* 317:1491-502

Konig G, McAllister T, Dusserre N, Garrido S, Iyican C, et al. 2009. Mechanical properties of completely autologous human tissue engineered blood vessels compared to human saphenous vein and mammary artery. *Biomaterials* 30:1542-50

Kopp J, Jeschke M, Bach A, Kneser U, Horch R. 2004. Applied tissue engineering in the closure of severe burns and chronic wounds using cultured human autologous keratinocytes in a natural fibrin matrix. *Cell and Tissue Banking* 5:81-7

Ladoux A, Frelin C. 2000. Coordinated Up-regulation by hypoxia of adrenomedullin and one of its putative receptors (RDC-1) in cells of the rat blood-brain barrier. *J Biol Chem* 275:39914-9

Lago N, Udina E, Ramachandran A, Navarro X. 2007. Neurobiological assessment of regenerative electrodes for bidirectional interfacing injured peripheral nerves. *IEEE Trans Biomed Eng* 54:1129-37

Lee S, Carvell GE, Simons DJ. 2008. Motor modulation of afferent somatosensory circuits. *Nat Neurosci* 11:1430-8

Lefurge T, Goodall E, Horch K, Stensaas L, Schoenberg A. 1991. Chronically implanted intrafascicular recording electrodes. *Ann Biomed Eng* 19:197-207

Lehmann HJ. 1953. The epineurium as a diffusion barrier. *Nature* 172:1045-6

Lerma E, Romero M, Gallardo A, Pons C, Munoz J, et al. 2008. Prognostic significance of the Fas-receptor/Fas-ligand system in cervical squamous cell carcinoma. *Virchows Arch* 452:65-74

Leung BK, Biran R, Underwood CJ, Tresco PA. 2008. Characterization of microglial attachment and cytokine release on biomaterials of differing surface chemistry. *Biomaterials* 29:3289-97

Leventhal DK, Durand DM. 2004. Chronic measurement of the stimulation selectivity of the flat interface nerve electrode. *IEEE Trans Biomed Eng* 51:1649-58

Levi-Montalcini R, Angeletti PU. 1963. Essential role of the nerve growth factor in the survival and maintenance of dissociated sensory and sympathetic embryonic nerve cells in vitro. *Dev Biol* 7:653-9

Li F, Tian F, Wang L, Williamson IK, Sharifi BG, Shah PK. 2010. Pleiotrophin (PTN) is expressed in vascularized human atherosclerotic plaques: IFN-{gamma}/JAK/STAT1 signaling is critical for the expression of PTN in macrophages. *FASEB J* 24:810-22

Li J, Shi R. 2007. Fabrication of patterned multi-walled poly-l-lactic acid conduits for nerve regeneration. *J Neurosci Methods* 165:257-64

Lin LR, Huang HP. 1997. Mechanism and computer simulation of a new robot hand for potential use as an artificial hand. *Artif Organs* 21:59-69

Lindsay RM. 1988. Nerve growth factors (NGF, BDNF) enhance axonal regeneration but are not required for survival of adult sensory neurons. *J Neurosci* 8:2394-405

Lopez CA, Fleischman AJ, Roy S, Desai TA. 2006. Evaluation of silicon nanoporous membranes and ECM-based microenvironments on neurosecretory cells. *Biomaterials* 27:3075-83

LoPresti P, Scott SA. 1994. Target specificity and size of avian sensory neurons supported in vitro by nerve growth factor, brain-derived neurotrophic factor, and neurotrophin-3. *J Neurobiol* 25:1613-24

Lowrie MB. 1999. Contralateral effects of peripheral nerve injury. *Trends Neurosci* 22:496-7

Lundberg P, Lerner UH. 2002. Expression and regulatory role of receptors for vasoactive intestinal peptide in bone cells. *Microsc Res Tech* 58:98-103

Madison RD, Robinson GA, Chadaram SR. 2007. The specificity of motor neurone regeneration (preferential reinnervation). *Acta Physiol (Oxf)* 189:201-6

Maeda N, Nishiwaki T, Shintani T, Hamanaka H, Noda M. 1996. 6B4 proteoglycan/phosphacan, an extracellular variant of receptor-like protein-tyrosine phosphatase zeta/RPTPbeta, binds pleiotrophin/heparin-binding growth-associated molecule (HB-GAM). *J Biol Chem* 271:21446-52

Mannard A, Stein RB, Charles D. 1974. Regeneration electrode units: implants for recording from single peripheral nerve fibers in freely moving animals. *Science* 183:547-9

Marasco PD, Schultz AE, Kuiken TA. 2009. Sensory capacity of reinnervated skin after redirection of amputated upper limb nerves to the chest. *Brain* 132:1441-8

Martini R, Schachner M, Brushart TM. 1994. The L2/HNK-1 carbohydrate is preferentially expressed by previously motor axon-associated Schwann cells in reinnervated peripheral nerves. *J Neurosci* 14:7180-91

Martini R, Xin Y, Schmitz B, Schachner M. 1992. The L2/HNK-1 Carbohydrate Epitope is Involved in the Preferential Outgrowth of Motor Neurons on Ventral Roots and Motor Nerves. *Eur J Neurosci* 4:628-39

Masuda T, Yaginuma H, Sakuma C, Ono K. 2009. Netrin-1 signaling for sensory axons: Involvement in sensory axonal development and regeneration. *Cell Adh Migr* 3:171-3

Matrone GC, Cipriani C, Secco EL, Magenes G, Carrozza MC. 2010. Principal components analysis based control of a multi-DoF underactuated prosthetic hand. *J Neuroeng Rehabil* 7:16

Matsusaki M, Sakaguchi H, Serizawa T, Akashi M. 2007. Controlled release of vascular endothelial growth factor from alginate hydrogels nano-coated with polyelectrolyte multilayer films. *Journal of Biomaterials Science, Polymer Edition* 18:775-83

McInnes C, Sykes BD. 1997. Growth factor receptors: structure, mechanism, and drug discovery. *Biopolymers* 43:339-66

Mi R, Chen W, Hoke A. 2007. Pleiotrophin is a neurotrophic factor for spinal motor neurons. *Proc Natl Acad Sci U S A* 104:4664-9

Micera S, Navarro X. 2009. Bidirectional interfaces with the peripheral nervous system. *Int Rev Neurobiol* 86:23-38

Michael GJ, Averill S, Nitkunan A, Rattray M, Bennett DL, et al. 1997. Nerve growth factor treatment increases brain-derived neurotrophic factor selectively in TrkA-expressing dorsal root ganglion cells and in their central terminations within the spinal cord. *J Neurosci* 17:8476-90

Miller LA, Lipschutz RD, Stubblefield KA, Lock BA, Huang H, et al. 2008. Control of a six degree of freedom prosthetic arm after targeted muscle reinnervation surgery. *Arch Phys Med Rehabil* 89:2057-65

Mingyu C, Kai G, Jiamou L, Yandao G, Nanming Z, Xiufang Z. 2004. Surface modification and characterization of chitosan film blended with poly-L-lysine. *J Biomater Appl* 19:59-75

Misko TP, Radeke MJ, Shooter EM. 1987. Nerve growth factor in neuronal development and maintenance. *J Exp Biol* 132:177-90

Mocchetti I, Brown M. 2008. Targeting neurotrophin receptors in the central nervous system. *CNS Neurol Disord Drug Targets* 7:71-82

Moises T, Dreier A, Flohr S, Esser M, Brauers E, et al. 2007. Tracking TrkA's trafficking: NGF receptor trafficking controls NGF receptor signaling. *Mol Neurobiol* 35:151-9

Moon JH, Kwak SS, Park G, Jung HY, Yoon BS, et al. 2008. Isolation and characterization of multipotent human keloid-derived mesenchymal-like stem cells. *Stem Cells Dev* 17:713-24

Moon JJ, West JL. 2008. Vascularization of engineered tissues: approaches to promote angio-genesis in biomaterials. *Curr Top Med Chem* 8:300-10

Morris JH, Hudson AR, Weddell G. 1972. A study of degeneration and regeneration in the divided rat sciatic nerve based on electron microscopy. II. The development of the "regenerating unit". *Z Zellforsch Mikrosk Anat* 124:103-30

Mueller BK. 1999. Growth cone guidance: first steps towards a deeper understanding. *Annu Rev Neurosci* 22:351-88

Muramatsu T. 2002. Midkine and pleiotrophin: two related proteins involved in development, survival, inflammation and tumorigenesis. *J Biochem* 132:359-71

Nagy JI, Hunt SP. 1982. Fluoride-resistant acid phosphatase-containing neurones in dorsal root ganglia are separate from those containing substance P or somatostatin. *Neuroscience* 7:89-97

Nagy JI, Hunt SP. 1983. The termination of primary afferents within the rat dorsal horn: evidence for rearrangement following capsaicin treatment. *J Comp Neurol* 218:145-58

Nasseri B, Pomerantseva I, Kaazempur-Mofrad M, Sutherland F, Perry T, et al. 2003. Dynamic rotational seeding and cell culture system for vascular tube formation. *Tissue Engineering* 9:291-9

Navarro X, Udina E. 2009. Chapter 6: Methods and protocols in peripheral nerve regeneration experimental research: part III-electrophysiological evaluation. *Int Rev Neurobiol* 87:105-26

Nelson KD, Romero A, Waggoner P, Crow B, Borneman A, Smith GM. 2003. Technique paper for wet-spinning poly(L-lactic acid) and poly(DL-lactide-co-glycolide) monofilament fibers. *Tissue Eng* 9:1323-30

Neufeld G, Cohen T, Gengrinovitch S, Poltorak Z. 1999. Vascular endothelial growth factor (VEGF) and its receptors. *FASEB J* 13:9-22

Nillesen S, Geutjes P, Wismans R, Schalkwijk J, Daamen W, van Kuppevelt T. 2007. Increased angiogenesis and blood vessel maturation in acellular collagen–heparin scaffolds containing both FGF2 and VEGF. *Biomaterials* 28:1123-31

Nomi M, Miyake H, Sugita Y, Fujisawa M, Soker S. 2006. Role of growth factors and endothelial cells in therapeutic angiogenesis and tissue engineering. *Curr Stem Cell Res Ther* 1:333-43

Norotte C, Marga F, Niklason L, Forgacs G. 2009. Scaffold-free vascular tissue engineering using bioprinting. *Biomaterials* 30:5910-7

Oakley RA, Lefcort FB, Clary DO, Reichardt LF, Prevette D, et al. 1997. Neurotrophin-3 promotes the differentiation of muscle spindle afferents in the absence of peripheral targets. *J Neurosci* 17:4262-74

Oppenheim RW, Houenou LJ, Johnson JE, Lin LF, Li L, et al. 1995. Developing motor neurons rescued from programmed and axotomy-induced cell death by GDNF. *Nature* 373:344-6

Otr OV, Reinders-Messelink HA, Bongers RM, Bouwsema H, Van Der Sluis CK. 2010. The i-LIMB hand and the DMC plus hand compared: a case report. *Prosthet Orthot Int* 34:216-20

Ozkaynak E, Abello G, Jaegle M, van Berge L, Hamer D, et al. 2010. Adam22 is a major neuronal receptor for Lgi4-mediated Schwann cell signaling. *J Neurosci* 30:3857-64

Panetsos F, Avendano C, Negredo P, Castro J, Bonacasa V. 2008. Neural prostheses: electrophysiological and histological evaluation of central nervous system alterations due to long-term implants of sieve electrodes to peripheral nerves in cats. *IEEE Trans Neural Syst Rehabil Eng* 16:223-32

Patel Z, Ueda H, Yamamoto M, Tabata Y, Mikos A. 2008. In vitro and in vivo release of vascular endothelial growth factor from gelatin microparticles and biodegradable composite scaffolds. *Pharmaceutical Research* 25:2370-8

Phillips CA. 1988. Sensory feedback control of upper- and lower-extremity motor prostheses. *Crit Rev Biomed Eng* 16:105-40

Pike D, Cai S, Pomraning K, Firpo M, Fisher R, et al. 2006. Heparin-regulated release of growth factors in vitro and angiogenic response in vivo to implanted hyaluronan hydrogels containing VEGF and bFGF. *Biomaterials* 27:5242-51

Piltonen M, Planken A, Leskela O, Myohanen TT, Hanninen AL, et al. 2011. Vascular endothelial growth factor C acts as a neurotrophic factor for dopamine neurons in vitro and in vivo. *Neuroscience* 192:550-63

Piotrowicz A, Shoichet MS. 2006. Nerve guidance channels as drug delivery vehicles. *Biomaterials* 27:2018-27

Ponimaskin E, Dityateva G, Ruonala MO, Fukata M, Fukata Y, et al. 2008. Fibroblast growth factor-regulated palmitoylation of the neural cell adhesion molecule determines neuronal morphogenesis. *J Neurosci* 28:8897-907

Porter BE, Weis J, Sanes JR. 1995. A motoneuron-selective stop signal in the synaptic protein S-laminin. *Neuron* 14:549-59

Priya SG, Jungvid H, Kumar A. 2008. Skin tissue engineering for tissue repair and regeneration. *Tissue Eng Part B Rev* 14:105-18

Raivich G, Kreutzberg GW. 1987. Expression of growth factor receptors in injured nervous tissue. I. Axotomy leads to a shift in the cellular distribution of specific beta-nerve growth factor binding in the injured and regenerating PNS. *J Neurocytol* 16:689-700

Rana AQ, Masroor MS. 2011. Hereditary Neuropathy with Liability to Pressure Palsy: A Brief Review with a Case Report. *Int J Neurosci*

Raulo E, Chernousov MA, Carey DJ, Nolo R, Rauvala H. 1994. Isolation of a neuronal cell surface receptor of heparin binding growth-associated molecule (HB-GAM). Identification as N-syndecan (syndecan-3). *J Biol Chem* 269:12999-3004

Redett R, Jari R, Crawford T, Chen YG, Rohde C, Brushart TM. 2005. Peripheral pathways regulate motoneuron collateral dynamics. *J Neurosci* 25:9406-12

Roberts S, Howard D, Buttery L, Shakesheff K. 2008. Clinical applications of musculoskeletal tissue engineering. *British Medical Bulletin*

Robinson GA, Madison RD. 2004. Motor neurons can preferentially reinnervate cutaneous pathways. *Exp Neurol* 190:407-13

Robinson GA, Madison RD. 2005. Manipulations of the mouse femoral nerve influence the accuracy of pathway reinnervation by motor neurons. *Exp Neurol* 192:39-45

Robinson GA, Madison RD. 2006. Developmentally regulated changes in femoral nerve regeneration in the mouse and rat. *Exp Neurol* 197:341-6

Rocha F, Sundback C, Krebs N, Leach J, Mooney D, et al. 2008. The effect of sustained delivery of vascular endothelial growth factor on angiogenesis in tissue-engineered intestine. *Biomaterials* 29:2884-90

Romero MI, Lin L, Lush ME, Lei L, Parada LF, Zhu Y. 2007. Deletion of Nf1 in neurons induces increased axon collateral branching after dorsal root injury. *J Neurosci* 27:2124-34

Romero MI, Rangappa N, Garry MG, Smith GM. 2001. Functional regeneration of chronically injured sensory afferents into adult spinal cord after neurotrophin gene therapy. *J Neurosci* 21:8408-16

Romero MI, Rangappa N, Li L, Lightfoot E, Garry MG, Smith GM. 2000. Extensive sprouting of sensory afferents and hyperalgesia induced by conditional expression of nerve growth factor in the adult spinal cord. *J Neurosci* 20:4435-45

Rosenberg AS, Langee CL, Stevens GL, Morgan MB. 2002. Malignant peripheral nerve sheath tumor with perineurial differentiation: "malignant perineurioma". *J Cutan Pathol* 29:362-7

Rosenzweig ES, Courtine G, Jindrich DL, Brock JH, Ferguson AR, et al. 2010. Extensive spontaneous plasticity of corticospinal projections after primate spinal cord injury. *Nat Neurosci* 13:1505-10

Rotshenker S. 2011. Wallerian degeneration: the innate-immune response to traumatic nerve injury. *J Neuroinflammation* 8:109

Rouwkema J, Rivron NC, van Blitterswijk CA. 2008. Vascularization in tissue engineering. *Trends Biotechnol*

Saarma M, Sariola H. 1999. Other neurotrophic factors: glial cell line-derived neurotrophic factor (GDNF). *Microsc Res Tech* 45:292-302

Sahenk Z, Oblinger J, Edwards C. 2008. Neurotrophin-3 deficient Schwann cells impair nerve regeneration. *Exp Neurol* 212:552-6

Schaack J. 2005. Adenovirus vectors deleted for genes essential for viral DNA replication. *Front Biosci* 10:1146-55

Schmid C, Schwarz V, Hutter H. 2006. AST-1, a novel ETS-box transcription factor, controls axon guidance and pharynx development in C. elegans. *Dev Biol* 293:403-13

Schmidt CE, Leach JB. 2003. Neural tissue engineering: strategies for repair and regeneration. *Annu Rev Biomed Eng* 5:293-347

Seeger MA, Beattie CE. 1999. Attraction versus repulsion: modular receptors make the difference in axon guidance. *Cell* 97:821-4

Segal RA. 2003. Selectivity in neurotrophin signaling: theme and variations. *Annu Rev Neurosci* 26:299-330

Sendtner M, Holtmann B, Kolbeck R, Thoenen H, Barde YA. 1992. Brain-derived neurotrophic factor prevents the death of motoneurons in newborn rats after nerve section. *Nature* 360:757-9

Shen K, Fetter RD, Bargmann CI. 2004. Synaptic specificity is generated by the synaptic guidepost protein SYG-2 and its receptor, SYG-1. *Cell* 116:869-81

Shen YH, Shoichet MS, Radisic M. 2008. Vascular endothelial growth factor immobilized in collagen scaffold promotes penetration and proliferation of endothelial cells. *Acta Biomater* 4:477-89

Shneider NA, Brown MN, Smith CA, Pickel J, Alvarez FJ. 2009. Gamma motor neurons express distinct genetic markers at birth and require muscle spindle-derived GDNF for postnatal survival. *Neural Dev* 4:42

Shweiki D, Itin A, Soffer D, Keshet E. 1992. Vascular endothelial growth factor induced by hypoxia may mediate hypoxia-initiated angiogenesis. *Nature* 359:843-5

Sieminski A, Hebbel R, Gooch K. 2004. The relative magnitudes of endothelial force generation and matrix stiffness modulate capillary morphogenesis in vitro. *Experimental cell research* 297:574-84

Simeral JD, Kim SP, Black MJ, Donoghue JP, Hochberg LR. Neural control of cursor trajectory and click by a human with tetraplegia 1000 days after implant of an intracortical microelectrode array. *J Neural Eng* 8:025027

Sjoberg J, Kanje M. 1990. The initial period of peripheral nerve regeneration and the importance of the local environment for the conditioning lesion effect. *Brain Res* 529:79-84

Sjoberg J, Kanje M, Edstrom A. 1988. Influence of non-neuronal cells on regeneration of the rat sciatic nerve. *Brain Res* 453:221-6

Skaper SD. 2008. The biology of neurotrophins, signalling pathways, and functional peptide mimetics of neurotrophins and their receptors. *CNS Neurol Disord Drug Targets* 7:46-62

Snider WD, Wright DE. 1996. Neurotrophins cause a new sensation. *Neuron* 16:229-32

Soker S, Takashima S, Miao H, Neufeld G, Klagsbrun M. 1998a. Neuropilin-1 is expressed by endothelial and tumor cells as an isoform-specific receptor for vascular endothelial growth factor. *Cell* 92:735-46

Soker S, Takashima S, Miao HQ, Neufeld G, Klagsbrun M. 1998b. Neuropilin-1 is expressed by endothelial and tumor cells as an isoform-specific receptor for vascular endothelial growth factor. *Cell* 92:735-45

Stoica GE, Kuo A, Aigner A, Sunitha I, Souttou B, et al. 2001. Identification of anaplastic lymphoma kinase as a receptor for the growth factor pleiotrophin. *J Biol Chem* 276:16772-9

Sun QL, Wang J, Bookman RJ, Bixby JL. 2000. Growth cone steering by receptor tyrosine phosphatase delta defines a distinct class of guidance cue. *Mol Cell Neurosci* 16:686-95

Sunderland S. 1965. The connective tissues of peripheral nerves. *Brain* 88:841-54

Tabata Y, Miyao M, Ozeki M, Ikada Y. 2000. Controlled release of vascular endothelial growth factor by use of collagen hydrogels. *Journal of Biomaterials Science, Polymer Edition* 11:915-30

Tan W, Desai T. 2003. Microfluidic patterning of cells in extracellular matrix biopolymers: effects of channel size, cell type, and matrix composition on pattern integrity. *Tissue Engineering* 9:255-67

Tang J, Landmesser L, Rutishauser U. 1992. Polysialic acid influences specific pathfinding by avian motoneurons. *Neuron* 8:1031-44

Tannemaat MR, Eggers R, Hendriks WT, de Ruiter GC, van Heerikhuize JJ, et al. 2008. Differential effects of lentiviral vector-mediated overexpression of nerve growth factor and glial cell line-derived neurotrophic factor on regenerating sensory and motor axons in the transected peripheral nerve. *Eur J Neurosci* 28:1467-79

Tansey KE, Seifert JL, Botterman B, Delgado MR, Romero MI. 2011. Peripheral Nerve Repair Through Multi-Luminal Biosynthetic Implants. *Ann Biomed Eng* 39:815-1828

Terenghi G. 1995. Peripheral nerve injury and regeneration. *Histol Histopathol* 10:709-18

Terenghi G. 1999. Peripheral nerve regeneration and neurotrophic factors. *J Anat* 194 (Pt 1):1-14

Tessier-Lavigne M, Goodman CS. 1996. The molecular biology of axon guidance. *Science* 274:1123-33

Toth G, Yang H, Anguelov RA, Vettraino J, Wang Y, Acsadi G. 2002. Gene transfer of glial cell-derived neurotrophic factor and cardiotrophin-1 protects PC12 cells from injury: involvement of the phosphatidylinositol 3-kinase and mitogen-activated protein kinase kinase pathways. *J Neurosci Res* 69:622-32

Tzou CH, Aszmann OC, Frey M. 2011. Bridging peripheral nerve defects using a single-fascicle nerve graft. *Plast Reconstr Surg* 128:861-9

Urfer R, Tsoulfas P, Soppet D, Escandon E, Parada LF, Presta LG. 1994. The binding epitopes of neurotrophin-3 to its receptors trkC and gp75 and the design of a multifunctional human neurotrophin. *EMBO J* 13:5896-909

Vacanti C. 2006. History of tissue engineering and a glimpse into its future. *Tissue Engineering* 12:1137-42

Vanderwinden JM, Mailleux P, Schiffmann SN, Vanderhaeghen JJ. 1992. Cellular distribution of the new growth factor pleiotrophin (HB-GAM) mRNA in developing and adult rat tissues. *Anat Embryol (Berl)* 186:387-406

Velliste M, Perel S, Spalding MC, Whitford AS, Schwartz AB. 2008. Cortical control of a prosthetic arm for self-feeding. *Nature* 453:1098-101

Walker RG, Foster A, Randolph CL, Isaacson LG. 2008. Changes in NGF and NT-3 protein species in the superior cervical ganglion following axotomy of postganglionic axons. *Brain Res*

Walsh FS, Doherty P. 1997. Neural cell adhesion molecules of the immunoglobulin superfamily: role in axon growth and guidance. *Annu Rev Cell Dev Biol* 13:425-56

Weber DJ, Stein RB, Everaert DG, Prochazka A. 2007. Limb-state feedback from ensembles of simultaneously recorded dorsal root ganglion neurons. *J Neural Eng* 4:S168-80

Wenner P, Frank E. 1995. Peripheral target specification of synaptic connectivity of muscle spindle sensory neurons with spinal motoneurons. *J Neurosci* 15:8191-8

Williams JC, Hippensteel JA, Dilgen J, Shain W, Kipke DR. 2007. Complex impedance spectroscopy for monitoring tissue responses to inserted neural implants. *J Neural Eng* 4:410-23

Winter JO, Cogan SF, Rizzo JF, 3rd. 2007. Neurotrophin-eluting hydrogel coatings for neural stimulating electrodes. *J Biomed Mater Res B Appl Biomater* 81:551-63

Wood MD, MacEwan MR, French AR, Moore AM, Hunter DA, et al. 2010. Fibrin matrices with affinity-based delivery systems and neurotrophic factors promote functional nerve regeneration. *Biotechnol Bioeng* 106:970-9

Wu RH, Wang P, Yang L, Li Y, Liu Y, Liu M. 2011. A potential indicator of denervated muscle atrophy: the ratio of myostatin to follistatin in peripheral blood. *Genet Mol Res* 10

Wu X, Rabkin-Aikawa E, Guleserian KJ, Perry TE, Masuda Y, et al. 2004. Tissue-engineered microvessels on three-dimensional biodegradable scaffolds using human endothelial progenitor cells. *Am J Physiol Heart Circ Physiol* 287:H480-7

Yan Q, Elliott J, Snider WD. 1992. Brain-derived neurotrophic factor rescues spinal motor neurons from axotomy-induced cell death. *Nature* 360:753-5

Yan Q, Matheson C, Lopez OT. 1995. In vivo neurotrophic effects of GDNF on neonatal and adult facial motor neurons. *Nature* 373:341-4

Yanagisawa H, Komuta Y, Kawano H, Toyoda M, Sango K. 2010. Pleiotrophin induces neurite outgrowth and up-regulates growth-associated protein (GAP)-43 mRNA through the ALK/GSK3beta/beta-catenin signaling in developing mouse neurons. *Neurosci Res* 66:111-6

Yancopoulos G, Davis S, Gale N, Rudge J, Wiegand S, Holash J. 2000. Vascular-specific growth factors and blood vessel formation. *NATURE-LONDON*-:242-8

Yano H, Chao MV. 2000. Neurotrophin receptor structure and interactions. *Pharm Acta Helv* 74:253-60

Yeh HJ, He YY, Xu J, Hsu CY, Deuel TF. 1998. Upregulation of pleiotrophin gene expression in developing microvasculature, macrophages, and astrocytes after acute ischemic brain injury. *J Neurosci* 18:3699-707

Yu X, Bellamkonda RV. 2003. Tissue-engineered scaffolds are effective alternatives to autografts for bridging peripheral nerve gaps. *Tissue Eng* 9:421-30

Zachary I. 2005. Neuroprotective role of vascular endothelial growth factor: signalling mechanisms, biological function, and therapeutic potential. *Neurosignals* 14:207-21

Zengin E, Chalajour F, Gehling UM, Ito WD, Treede H, et al. 2006. Vascular wall resident progenitor cells: a source for postnatal vasculogenesis. *Development* 133:1543-51

Zhang N, Zhong R, Deuel TF. 1999. Domain structure of pleiotrophin required for transformation. *J Biol Chem* 274:12959-62

Zhang X, Aman K, Hokfelt T. 1995. Secretory pathways of neuropeptides in rat lumbar dorsal root ganglion neurons and effects of peripheral axotomy. *J Comp Neurol* 352:481-500

Zheng JQ, Poo MM, Connor JA. 1996a. Calcium and chemotropic turning of nerve growth cones. *Perspect Dev Neurobiol* 4:205-13

Zheng JQ, Wan JJ, Poo MM. 1996b. Essential role of filopodia in chemotropic turning of nerve growth cone induced by a glutamate gradient. *J Neurosci* 16:1140-9

Zhou FQ, Snider WD. 2006. Intracellular control of developmental and regenerative axon growth. *Philos Trans R Soc Lond B Biol Sci* 361:1575-92

Ziemba KS, Chaudhry N, Rabchevsky AG, Jin Y, Smith GM. 2008. Targeting axon growth from neuronal transplants along preformed guidance pathways in the adult CNS. *J Neurosci* 28:340-8

Zurn AD, Baetge EE, Hammang JP, Tan SA, Aebischer P. 1994. Glial cell line-derived neurotrophic factor (GDNF), a new neurotrophic factor for motoneurones. *Neuroreport* 6:113-8

BIOGRAPHICAL INFORMATION

Parisa Lotfi, raised in IRAN,graduated in 2001 from the BIHE (Baha'i Institute for Higher Education) with a Bachelor in Pharmacy. Her family and in particular her father had a lot of influence on her passion for reading. She had to leave the country due to the severe persecution opposed againsther being a member of the Baha'i Faith. In 2006, she received her M.Sc. in Biomedical Engineering from the University of Texas at Arlington and the University of Texas Southwestern Medical Center in Dallas. Her thesis subject includes investigation of the foreign body response to the stainless steel cortical implants. Shortly after her acquiring her M.Sc, she married "Ron Tingook" whom she referred to as "her eternal companion and friend". Later, she joined "Dr Mario Romero's" lab to study the peripheral nerve regeneration. She investigated the possibility of using chemical cues in enticing specific cell types, particularly different subtypes of axonal fibers. Some chapters of this work have already been published in journals. Final chapter, developing a novel method in delivery of growth factors in a gradient manner, is under review for a patent application.